1956

Discontinuous damping of relay servomechanisms.

Harris, William L. Jr.

Monterey, California : Naval Postgraduate School

DISCONTINUOUS DAMPING OF RELAY SERVOMECHANISMS

William L. Harris, Jr.

2

DISCONTINUOUS DAMPING
OF
RELAY SERVOMECHANISMS

* * * * * *

William L. Harris, Jr.

DISCONTINUOUS DAMPING
OF RELAY SERVOMECHANISMS

by

William Lawrence Harris, Jr.

Lieutenant, United States Navy

Submitted in partial fulfillment
of the requirements
for the degree of
MASTER OF SCIENCE
IN
ELECTRICAL ENGINEERING

United States Naval Postgraduate School
Monterey, California

1956

This work is accepted as fulfilling

the thesis requirements for the degree of

MASTER OF SCIENCE

IN

ELECTRICAL ENGINEERING

from the

United States Naval Postgraduate School

PREFACE

It is the aim of this paper to investigate the use of dynamic braking in the dead zone of a relay servo to improve its performance as a positioning device.

The investigation was performed at the U.S. Naval Postgraduate School at Monterey, California during the period September, 1955 to May, 1956.

The investigation was suggested and supervised by Professor George J. Thaler of the U.S. Naval Postgraduate School. His assistance and encouragement were gratefully appreciated by the author.

TABLE OF CONTENTS

LIST OF ILLUSTRATIONS

TABLE OF SYMBOLS

θ_c	Position of output shaft
θ_R	Position of command shaft
A, B	Constants
a-c	Alternating current
C	Coulomb friction referred to output
D	Correction signal (input to servomotor)
d-c	Direct current
E	Error signal, $E = \theta_R - \theta_c$
E_m	Voltage at which relay opens
E_n	Voltage at which relay closes
f	Viscous friction referred to output
G	Input signal to relay (sometimes identically E)
HP	Horsepower
i	Instantaneous current
J	System inertia referred to output
K_1, K_2	Constants
K_t	Tachometer electromotive force constant
K_T	Motor torque constant
K_v	Motor electromotive force constant
L	Inductance of motor armature
ln	Naperian logarithm
R	Resistance of motor armature
R_B	Resistance for dynamic braking
t	Time
T	Motor torque
T_B	Motor torque during dynamic braking

V	Motor terminal volts
$\dot{(\ )}$	$\frac{d}{dt}$, the time derivative operator
$\ddot{(\ )}$	$\frac{d^2}{dt^2}$, the second derivative with respect to time
$\approx$	Proportional to

CHAPTER I

INTRODUCTION

The relay servo is a compact, rugged and relatively inexpensive device, but is limited in its application by problems of stability, speed of response and steady state accuracy. This paper analyzes the use of dynamic braking in the dead zone of a relay servo to improve all of these factors.

Chapter II presents a historical review of relay servo theory and analysis methods.

Chapter III presents a phase-plane analysis of the theory of certain relay servo systems:

1. the optimum servo with ideal torque motor
2. the optimum servo with practical d-c motor
3. the proposed dynamic braking principle with viscous and and derivative damping present.
4. the dynamic braking principle with viscous, derivative, and Coulomb damping present.

Chapter IV presents experimental verification of the theory of the dynamically-braked relay servo.

The results of this investigation show that the dynamic braking principle effectively improves stability, speed of response, and steady state of accuracy. The experimental tests show that the response is almost exactly as predicted by theory when larger motors are used. For very small motors the Coulomb friction effect is greater than the dynamic braking effect and the proposed method does not seem practical.

CHAPTER II

HISTORICAL REVIEW OF RELAY SERVO THEORY

1. Basic Concepts; Types of Relay Characteristics.

The relay or contactor servomechanism has been widely used for purposes of automatic control. Besides the advantages of permitting lightweight and compact equipment to be used for control purposes there is the distinct advantage of the tremendous power amplification realized when an electric relay or other contactor is employed. Of course, there will be instances where an essentially continuous type servo system is more applicable.

The relay or on-off servomechanism is a type control system wherein some device called a contactor (herein an electric relay) applies a corrective signal to a servomotor in response to an error signal from a device which compares the actual and desired outputs. The peculiar characteristic of the electric relay is its discontinuous action in that it is capable of initiating a specific rate of output correction in either one of two directions or may call for no correction at all (the so-called inactive or dead zone). Thus it is incapable of signalling explicitly for a varying rate of correction as the conditions might dictate.

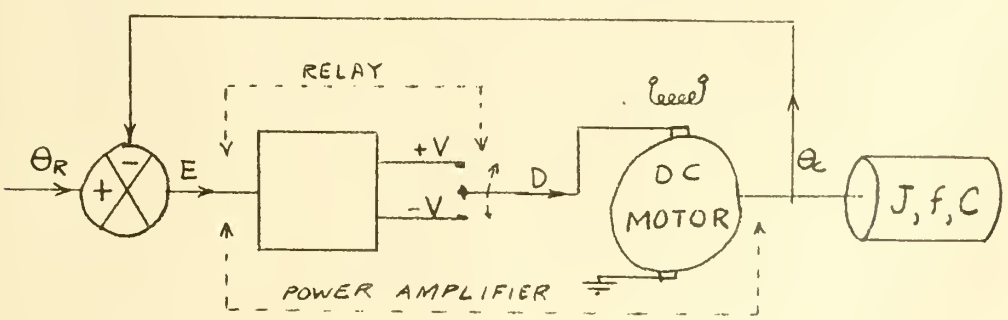

FIG. 1 - BLOCK DIAGRAM OF RELAY SERVO

Figure 1 is a block diagram of the basic single-loop relay servomechanism. The main difference from the continuous servo is illustrated; i.e. the signal to the servomotor is either full positive terminal voltage ($+V$), or full negative terminal voltage ($-V$), or possibly no voltage at all.

The relay is essentially a discontinuous power amplifying device. In response to the control or error signal, E, it produces a correction signal, D. The three most common relay characteristics are illustrated in Figure 2. The more complicated types of relay characteristics will not be discussed; e.g., nonsymmetrical corrective action, multistep relays. The corrective action being controlled by the relays of Figure 2 is designated V, the rated terminal voltage of the servomotor. The sense of V, positive or negative, may be arbitrarily defined.

The characteristic shown in Figure 2(a) is that of a relay which initiates either positive or negative correction, depending on the sense of the error signal. In this case no dead zone is provided and the servomotor has either full positive voltage or full negative voltage applied to its terminals.

In Figure 2(b) a dead zone, $2E_n$, is introduced and the error signal must have a magnitude equal to or greater than E_n before the corrective action is initiated; otherwise no corrective signal is applied. A dead zone may be unavoidable due to physical limitations; a finite dead zone must be introduced if dynamic stability is to be realized. Since the dead zone is the range of permissible error in which no corrective action is initiated, it becomes increasingly more difficult to achieve dynamic stability as the dead zone is narrowed.

Most relays exhibit an effect known as relay-hysteresis. In these relays the error signal necessary to initiate corrective action is

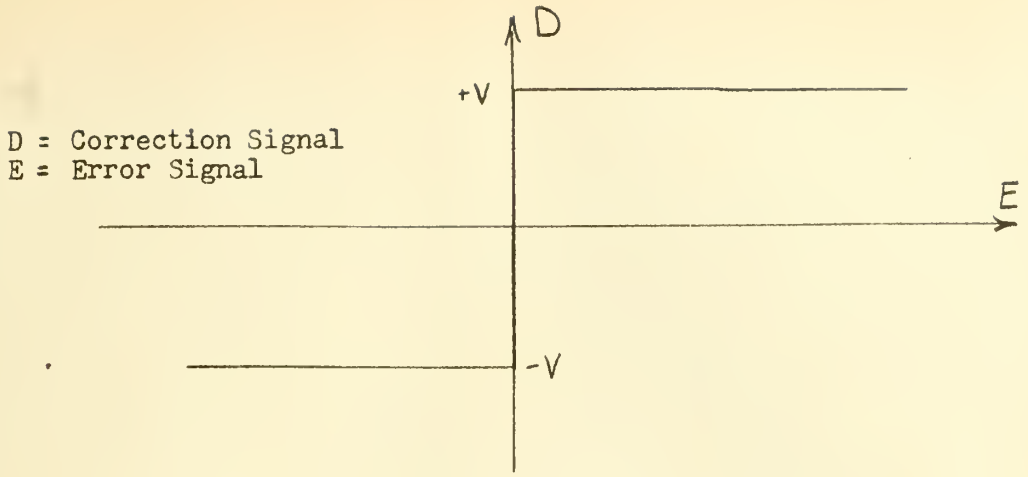

(a) No Dead Zone

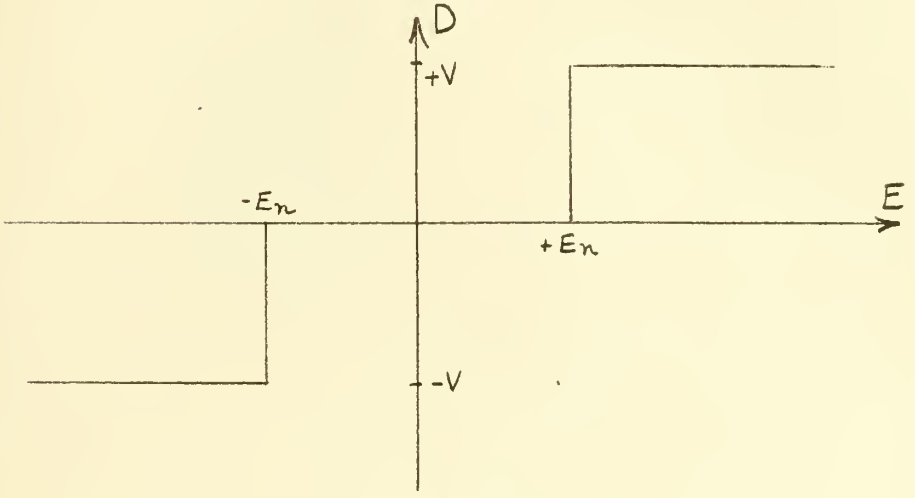

(b) With Dead Zone, 2 E_n, ($E_n = E_m$)

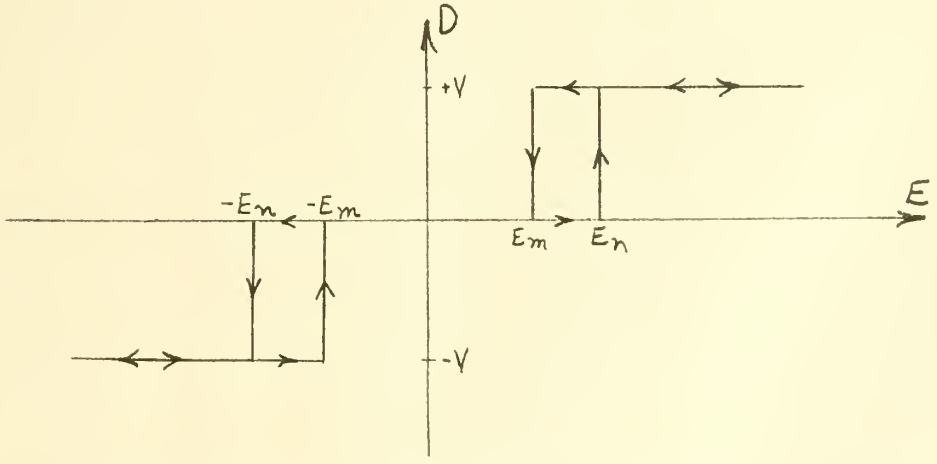

(c) With Dead Zone, $E_n + E_m$; and Hysteresis Zone, $E_n - E_m$

FIGURE 2. TYPICAL RELAY CHARACTERISTICS

greater than that necessary to cut-off corrective action, i.e., the coil current of an electromagnetic relay which is already closed must be reduced to a lesser value than that originally needed to close the relay before the relay will open. The effect of relay-hysteresis on the relay characteristic is shown in Figure 2(c). The hysteresis zone is $E_n - E_m$, and the dead zone is now $E_n + E_m$ in width. Generally the hysteresis effect adversely effects the dynamic stability of the system.

The above discussion on relay characteristics assumed that there was no time lag associated with the relay. Time lag is the delay between the time at which the restoring torque would be applied (or removed) were the relay to act and the resulting torque to build up instantaneously and the time when the torque actually becomes effective. This time lag may be different for the application and the removal of the torque. Part of this time lag is due to inertia effects of the moving parts, which of course cannot move instantaneously with the application of force. In an electrically operated relay there is an additional delay due to the inductance of the coil winding. When voltage is applied to the coil the build-up of current cannot take place instantaneously, and conversely requires a finite time to drop to zero when the voltage is removed.

The effect of time lag in a relay, when used in a relay servomechanism, is to increase the dead zone (reckoned in position dimensions) by an amount depending on the velocity of the output at the time the relay is attempting to actuate. Thus, the effective increase in dead zone is variable, but for systems where the time lag is small, or the output velocity is low, the effect of time lag may be represented by a fixed small increase in dead zone width.

Often the time lag is so small as to have an insignificant effect

upon the servo operation. A relay servo having Coulomb friction is relatively insensitive to small values of time lag, whereas a viscous-friction damped relay servo is quite sensitive to such delay. The effect of time lag is to decrease dynamic stability.

2. Transient Analysis.

There are three basic transient methods of analyzing relay servos; these use the transient response relations derived from the differential equations which describe the system. The "phase-plane" method of approach, where the response determination may be reduced to a simple graphical procedure by eliminating time as a variable, is treated in section 3 of Chapter I. The method suggested by Kahn [1], where a series solution is obtained through the application of the Laplace-transform is briefly treated in sub-section(b) below. The classical differential equation approach, suggested by Hagen [2], is treated in sub-section (a) below.

a. Classical method. The classical step-by-step determination of the response from the system differential equations is treated now. Because of the nonlinearity of the relay, new analytical relations for the response must be derived and plotted for each correction interval. This method is capable of giving results for systems of any order but in actual practice it is found that the labor of computation becomes excessive when the relay servo involves a degree of complexity beyond second order.

As with other transient response methods, the classical approach consists of first composing the various differential equations (with time as independent variable), describing the dynamic characteristics of the system and then combining them to obtain an overall differential

equation which relates wither the system output, θ_C, or system error, $E = \theta_R - \theta_C$, to the system input, θ_R.

Consider a simple relay servo (Fig. 1) with dead zone equal to $2E_n$, no hysteresis effect, no time lag, motor torque built up instantaneously, and only Coulomb friction damping present (other forms of damping are treated in section 5). Coulomb friction, C, is a constant frictional drag which opposes motion but has a magnitude which is independent of velocity. The force required to initiate motion is usually found to be somewhat greater than Coulomb friction and is termed stiction; herein no distinction will be made between the Coulomb friction when output velocity is zero and stiction.

In the general equations, the plus sign will be used preceding the symbol C, for Coulomb friction, but it must be kept in mind that C always takes the sign opposite to that of output velocity, $\dot{\theta}_C$ (the dot represents the time derivative operator). The general equation describing the dynamic characteristics of the servo of Figure 1 is

$$J\ddot{\theta}_c + C = \pm T \tag{1}$$

where the sign of T is generally opposite to that of E, with due regard to dead zone.

For illustration, the transient response to a sudden step input, θ_R, will be considered. Since $E = \theta_R - \theta_C$ and $\theta_R = \theta_{R_o}$ = constant; equation (1) may be written

$$J\ddot{E} + C = \pm T \tag{2}$$

When the step input is applied the initial conditions are

$$t = t_o$$

$$\theta_c = 0 = \dot{\theta}_c$$

$$\theta_R = \theta_{R_0} = E, \quad \theta_{R_0} > |E_1|$$

Figure 3 depicts the system transient response and torque applied for several correction intervals. For the interval from t_0 to t, the system equation is

$$J\ddot{E} = -T + C \tag{3}$$

with the initial conditions as above. At time t_1, when $E = +E_n$ and the relay opens or "drops out", the system conditions are

$$t = t_1$$

$$\theta_c = \theta_{c_1}$$

$$E = \theta_R - \theta_c = +E_n$$

$$\dot{\theta}_c = \dot{\theta}_{c_1}$$

These conditions are the initial conditions for the interval from t_1 to t_2. The procedure is to solve equation (3) with $E = +E_n$, obtaining θ_1 and $\dot{\theta}_1$ which will be used as initial conditions in solving the system equation for the first transit of the dead zone

$$J\ddot{E} = +C \tag{4}$$

Thus each interval must be solved step-by-step applying the terminating conditions of the preceding interval as the initial conditions of the interval under consideration.

Note that with dead zone and Coulomb friction, Figure 3, the system equation takes six distinct forms.

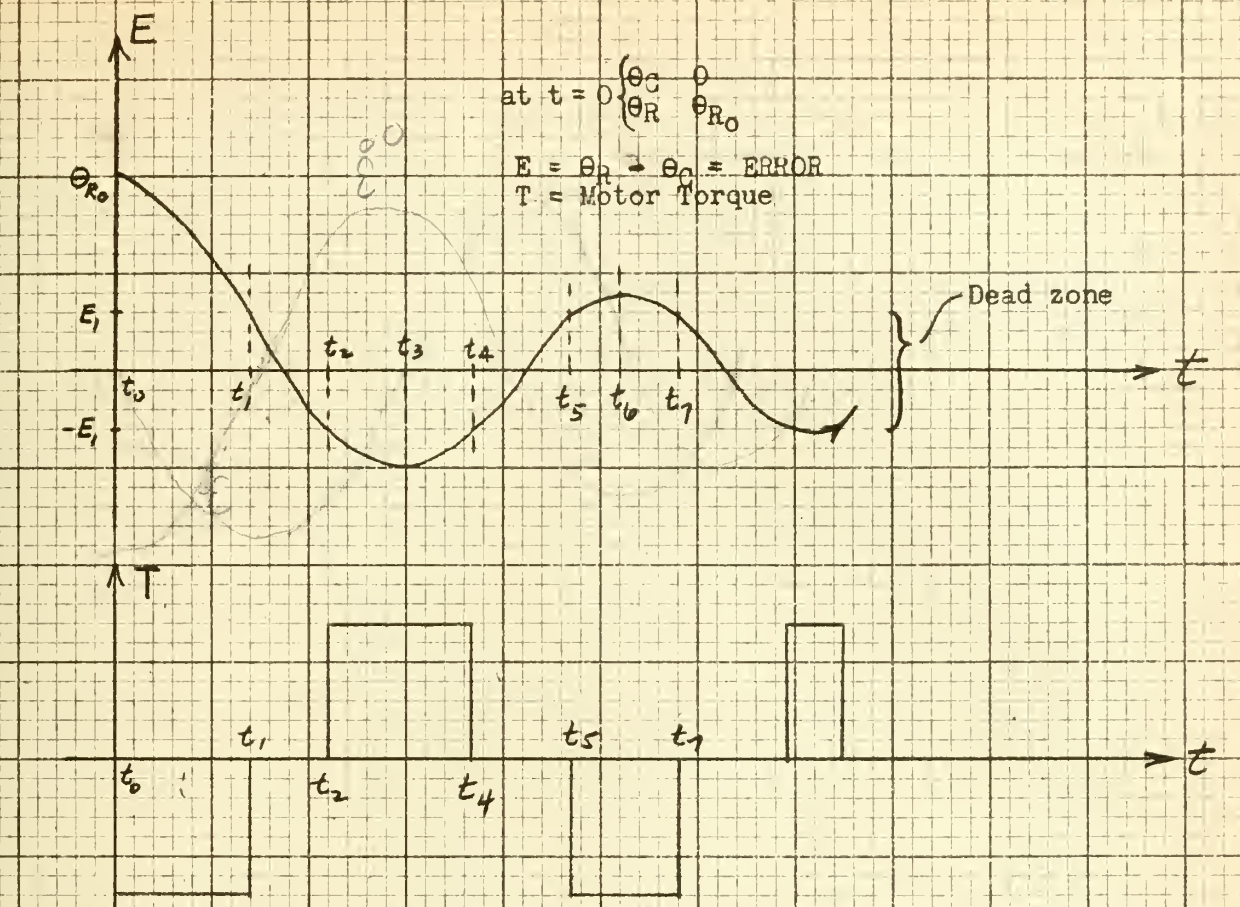

when $t_0 < t < t_1$: $J\ddot{\theta} = -T + C$,
$t_1 < t < t_2$: $= +C$,
$t_2 < t < t_3$: $= +T + C$,
$t_3 < t < t_4$: $= +T - C$,
$t_4 < t < t_5$: $= -C$,
$t_5 < t < t_6$: $= -T - C$,
$t_6 < t < t_7$: $= -T + C$, etc.

FIGURE 3. TRANSIENT RESPONSE OF SECOND ORDER SERVO (WITH COULOMB FRICTION) TO STEP INPUT WHEN RELAY HAS DEAD ZONE.

The classical approach can easily be extended to handle other forms of damping (see section 5), relay hysteresis, time lag, etc. Systems of complexity higher than second order may be handled, but the method becomes increasingly laborious.

b. Kahn's series method. This method of analysis applies the Laplace-transform to the differential equations and obtains a solution in the form of a series of terms. It is necessary to determine the system response to a step-function disturbance initiated by the relay. Each time that a new relay switching operation takes place, it may be taken into account by adding or subtracting this new step-function response, with a translated time axis, from the response relationship already developed by the accumulation of previous switching operations. The process is reduced to a graphical procedure and there appears to be no limit to its application as far as system complexity is concerned.

The problem of determining relative stability is accomplished by eliminating output as a variable and plotting output rate versus time. This method results in a graphical construction which enables the relative stability to be determined without the necessity of computing the actual time response.

3. Phase-Plane Analysis.

The phase-plane method is a method where systems characterized by differential equations of the second order may be solved graphically by plotting the first time derivative of the variable versus the variable itself. The independent variable, time, is thus eliminated as an explicit variable in the problem. As applied to the analysis of relay servos, the advantage lies in the fact that the loci of operating points on such a plot will form certain trajectory shapes; these

contours are merely translated when initial conditions are changed, their general form remaining intact. Graphical solutions are thus greatly simplified. This method is merely a convenient variation of the conventional transient method of analysis.

The solution of a differential equation is usually thought of as another equation relating the function to the independent variable, time in this treatment. However, a curve obtained by plotting this equation is also a solution to the differential equation; and if a curve from whence the variable versus time curve can be obtained is also a solution to the differential equation of the system. The phase-plane curves are plots of variable versus first time derivative of variable, and from these it is possible to obtain the variable versus time curves, if desired.

The phase-plane analysis can be carried out on any piecewise continuous second-order equation which can be manipulated into the form

$$\frac{dy}{dx} = f(y, x) \tag{5}$$

where y and x are functions of time. For an equation of order n, a relationship can be established for a plot in n-dimensional space; this would be a phase-space plot. Phase-space plots are difficult to construct and difficult to interpret, and have not been used to any great extent.

Although the phase-plane method is restricted to systems described by second-order differential equations, the phase-plane analysis of a second-order system containing a specified non-linearity often provides valuable background for analyzing the effect of the non-linearity when

it occurs in a higher order system.

Even after the system equation of a second-order system has been manipulated into the general form of equation (5) above, it cannot be plotted directly on the phase-plane because there are three variables, dy/dx, y, and x. Thus, the general equation must be integrated and then the resulting relationship between y and x may be plotted; four methods of accomplishing this are described by Thaler [3]. The method of isoclines is readily adapted to most linear and non-linear problems and will be illustrated. Once the isoclines are plotted, they permit study of system response to a wide variety of initial conditions, thus allowing trends to be established.

Note that the general equation for the phase-plane relates the slope on the phase-plane, dy/dx, to the coordinate variables, y and x. If a constant value, c^1, is selected for dy/dx, the equation becomes

$$c' = \frac{dy}{dx} = f(y, x) \tag{6}$$

which is the explicit equation of a curve on the phase-plane and has the property that at every point on this curve the phase-plane curve must have a slope c^1, if it crosses this curve. The curve defined by equation (6) is then a locus of constant slope for the phase-plane curve, or an "isocline". If a reasonable number of isoclines are plotted, and if the required slope of the phase-plane curve is clearly designated on each isocline, the phase-plane plot may be drawn in with as much precision as required.

For example, consider the second-order equation

$$a\ddot{E} + b\dot{E} + d = 0 \tag{7}$$

This may be rearranged to give

$$\ddot{E} = \frac{1}{a}\left(-b\dot{E} - d\right) \tag{8}$$

By dividing each side of (8) by $\dot{E}$

$$\frac{\ddot{E}}{\dot{E}} = \frac{\frac{d\dot{E}}{dt}}{\frac{dE}{dt}} = \frac{d\dot{E}}{dE} = \frac{1}{a}\left(-b - \frac{d}{\dot{E}}\right) \tag{9}$$

The equation is now in the form of equation (5), which becomes the equation for the family of isoclines when $d\dot{E}/dE$ is set equal to various constants. In this example, when $d\dot{E}/dE$ is set equal to a constant, the isoclines are straight lines parallel to the E-axis. An approximate graphical construction can be carried out by drawing in the family of isoclines, adding slope markers to each isocline and sketching in the phase-plane curve using the slope markers as a guide. See Figure 4(a) for such a sketch (the starting point is an arbitrary one for the time when $t = o$, $\dot{E} = o$).

A more accurate graphical construction may be accomplished as follows. The isoclines and slope markers are drawn in as before. The phase-plane curve should leave the starting point with the slope designated by the isocline through that point and should cross the next isocline at the slope required by that isocline. If slope markers for the isocline through the starting point and for the next isocline are laid down through the starting point, the point where the phase-plane curve crosses the next isocline lies approximately midway between the intersections of the two slope markers with the second isocline. This procedure is shown in Figure 4(b).

The first phase of the action of the relay servo analyzed in

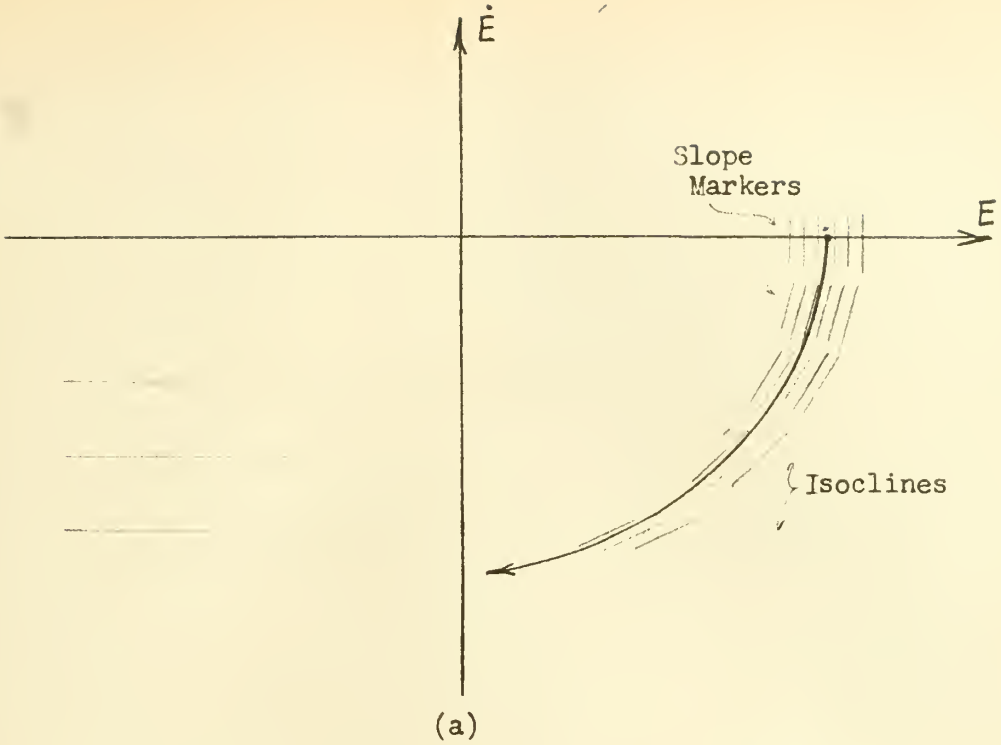

(a)

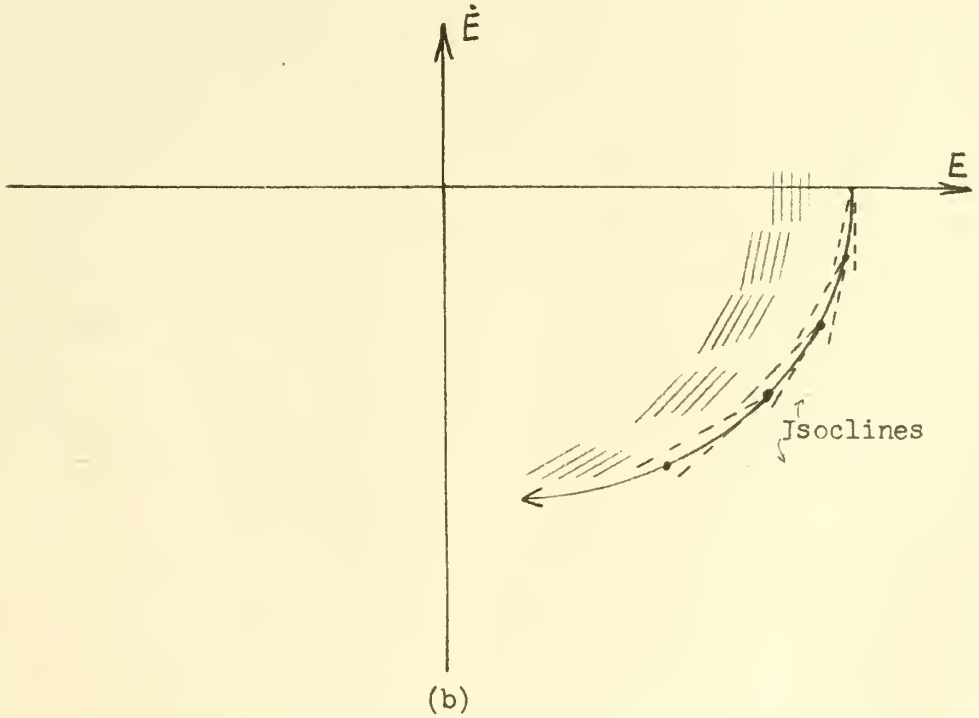

(b)

FIGURE 4. CONSTRUCTION OF PHASE-PLANE PLOT FOR SECOND ORDER LINEAR SYSTEM

section 2 above was described by the equation

$$J\ddot{E} = -T + C \tag{3}$$

By consulting equations (7) and (9), it is seen that equation (3) can be manipulated to

$$\frac{d\dot{E}}{dE} = \frac{1}{J}\left(\frac{-T+C}{\dot{E}}\right) \tag{10}$$

Here, too, the isoclines are straight lines parallel to the E-axis. The manipulation of the remaining five equations describing the action of the servo of section 2 results in equations similar to equation (10). Figure 5(a) is the resulting phase-plane plot of that servo. Note that the two vertical dashed lines are the locus of points of relay action, opening or closing, and therefore are the points of discontinuity of the system equations. Figure 5(b) is a special case, where the relay is assumed to be ideal, i.e., has an infinitisimally small dead zone.

As previously mentioned, the time performance may be derived from the phase-plane plot if desired. Since $\dot{E} = dE/dt$, the basic mathematical relationship between the time response and the phase-plane plot is

$$t = \int \frac{dE}{\dot{E}} \tag{11}$$

Evaluation of this integration by graphical methods gives the time response of the system.

4. Frequency Response Analysis.

The basic disadvantage of the methods of analysis treated above, which are essentially solutions in the time domain, is the great difficulty of analyzing systems which possess more than a few energy-storage

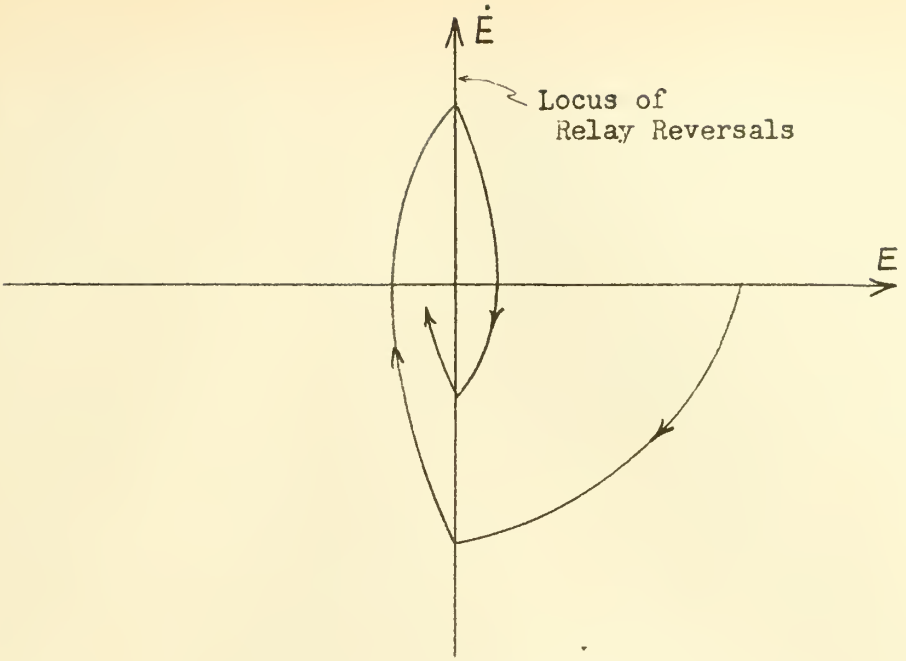

(b) No Dead Zone

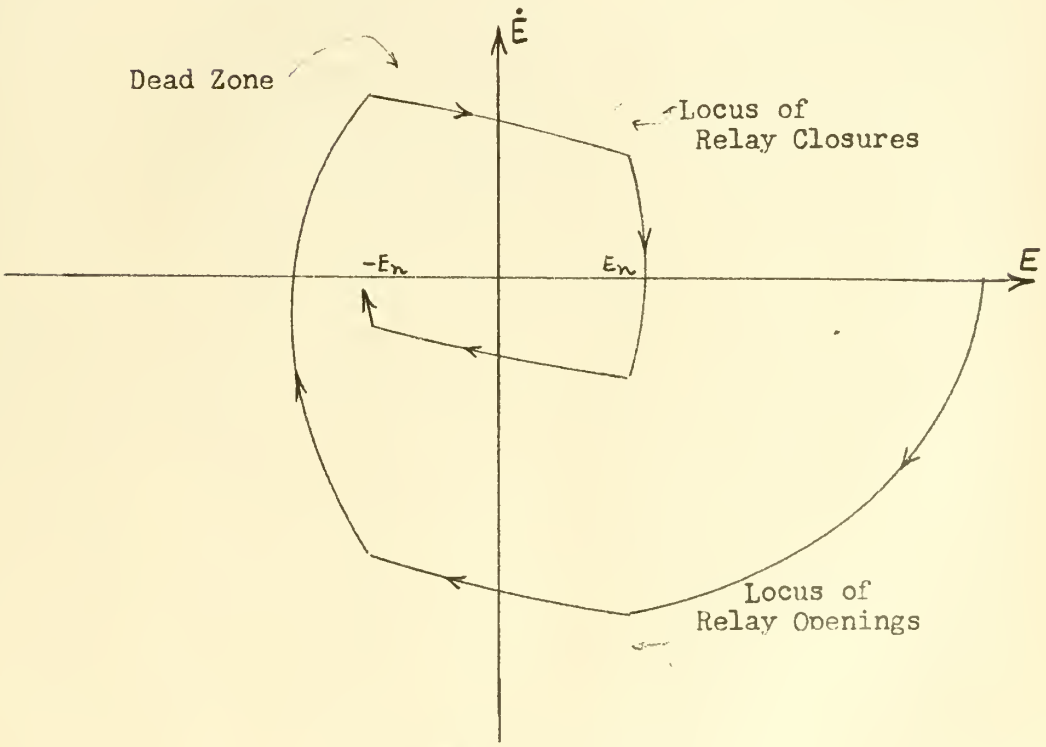

(a) With Dead Zone

FIGURE 5. PHASE-PLANE PLOT OF SIMPLE RELAY SERVO WITH COULOMB FRICTION

elements; e.g., the phase-plane approach is limited to systems describable by second order differential equations. Another disadvantage is that these methods are not easily adaptable to system synthesis. An analysis and synthesis procedure in which the frequency response of the system is employed in a manner analgous to its use with linear continuous servomechanisms has been developed by Kochenburger [4]. This section deals with the frequency response method of analyzing relay servos.

The frequency response or transfer function approach to the analysis of relay servos is essentially the same as for the continuous-type servo. The usual transfer functions of all components except the relay are combined to give a partial system transfer function $KG(j\omega)$. Because of the nonlinearity of the relay response, only an approximate transfer function, KG_R, can be written for the relay. KG_R is an approximation obtained by neglecting all harmonic components higher than the fundamental of the relay's response to a sinusoidal input signal. This approximate transfer function is often termed a describing function. KG_R is found to be a function not of ω but rather of the magnitude of the relay's input signal; thus KG_R must be determined for various error signal magnitudes. A modified version of the Nyquist criteria must be employed to determine system stability.

The transfer functions of the linear components of the servo system are derived in the usual manner by obtaining the complex ratio of the output of each component to its input; combined, these become the partial system transfer function, $KG(j\omega)$, representing the frequency-variant portion of the system (KG_R will be shown to be an amplitude-variant function). The output of the relay to a sinusoidal input is a

series of rectangular pulses of alternating polarity. Figure 6(a) illustrates the response of a simple relay with pull-in and drop-out voltages equal. The approximate transfer function (or describing function) is formed by replacing the rectangular output pulse by only the fundamental component of its Fourier series expansion, Figure 6(b). This is a good engineering approximation for two reasons: 1) for a periodic rectangular wave the amplitude of the fundamental is considerably greater than the amplitude of any of the higher harmonics, and 2) most servomotors are effectively low-pass filters and serve to attenuate the higher harmonics. Note that the approximate transfer function makes the relay appear as only a quasi-linear transfer device in that it operates as a linear device for a given constant amplitude of input signal; i.e., it does not operate as a truly linear device because of the nonlinear relationship between input and output amplitudes. Considering the relay as such a quasi-linear device permits the frequency response method to be used in determining the system stability for a given error signal amplitude.

The determination of the describing function of the relay unit depends upon the relay characteristics. Herein the error signal is assumed to possess no zero-frequency component, i.e., the axis of the sinusoidal error signal coincides with the relay neutral position. For the case where the relay pull-in and drop-out voltages are the same, $E_n = E_m$, as in Figure 6, the relay describing function is

$$KG_R = \frac{\overrightarrow{V_1}}{\overrightarrow{E_1}} = \frac{4V \sin \beta_1}{\pi |E_1|} \angle 0^\circ \qquad (12)$$

where V_1 = amplitude of Fourier fundamental.

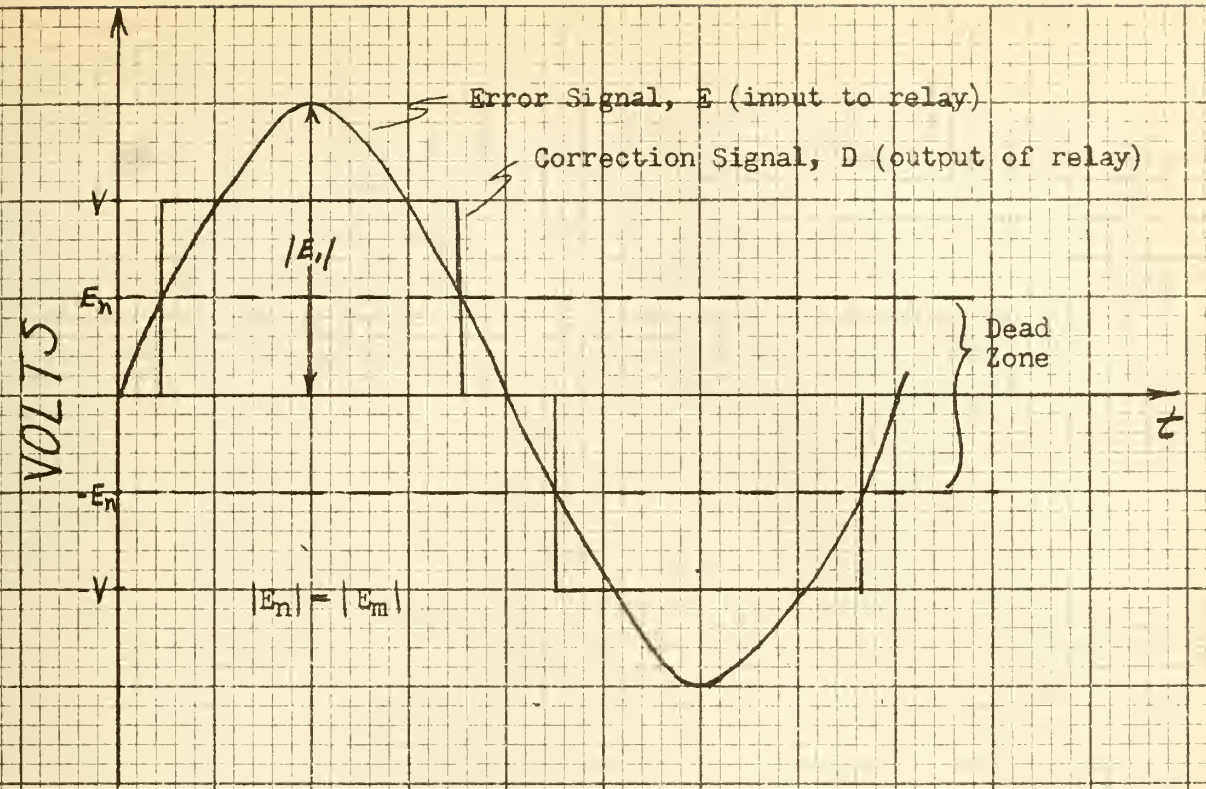

(a)

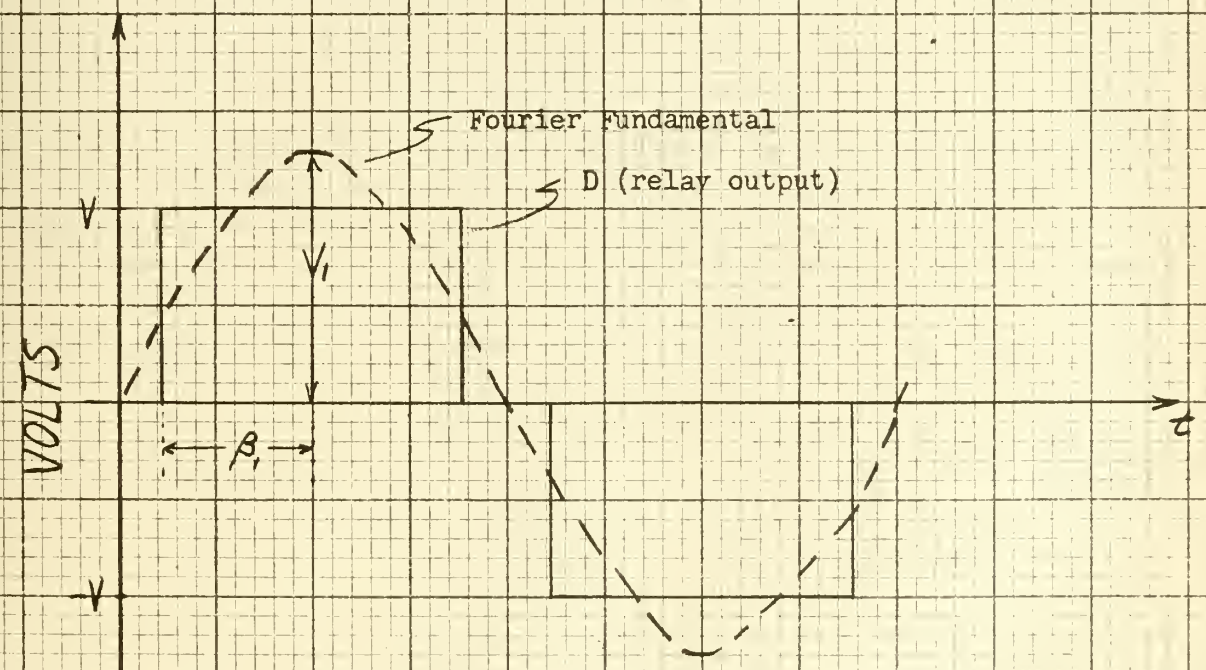

(b)

FIGURE 6. APPROXIMATION OF RELAY OUTPUT TO SINUSOIDAL INPUT

E_1 = amplitude of error signal.

β_1 = one-half duration of relay pulse, in radians.

Note that the above function is valid for only one amplitude of error signal, E_1 in this case. When the amplitude of E is varied the gain constant of the describing function is changed. Figure 7 illustrates how increasing E causes an increase in β. It may be seen, also, that no phase angle is introduced by increasing the error-signal amplitude. For error signal E_2

$$KG_R = \frac{4V \sin \beta_2}{\pi |E_2|} \angle 0^\circ \qquad (13)$$

Thus it is seen that the amplitude of the output fundamental is not proportional to the error amplitude, but varies as the sine of β.

When the pull-in and drop-out characteristics of the relay are not the same, the center line of the relay pulse output lags the centerline of the sinusoidal input and the relay describing function has a constant phase lag associated with it. Figure 8 illustrates this for the positive half of the relay pulse; the negative pulse will be similar. The describing function of the relay unit is now

$$KG_R = \frac{4V \sin \beta}{\pi |E|} \angle \phi \qquad (14)$$

Once the relay portion of the system is expressed as a transfer function, normal graphical means may be employed to represent the locus. Consider the simple relay servo represented by the block diagram in Figure 9 below.

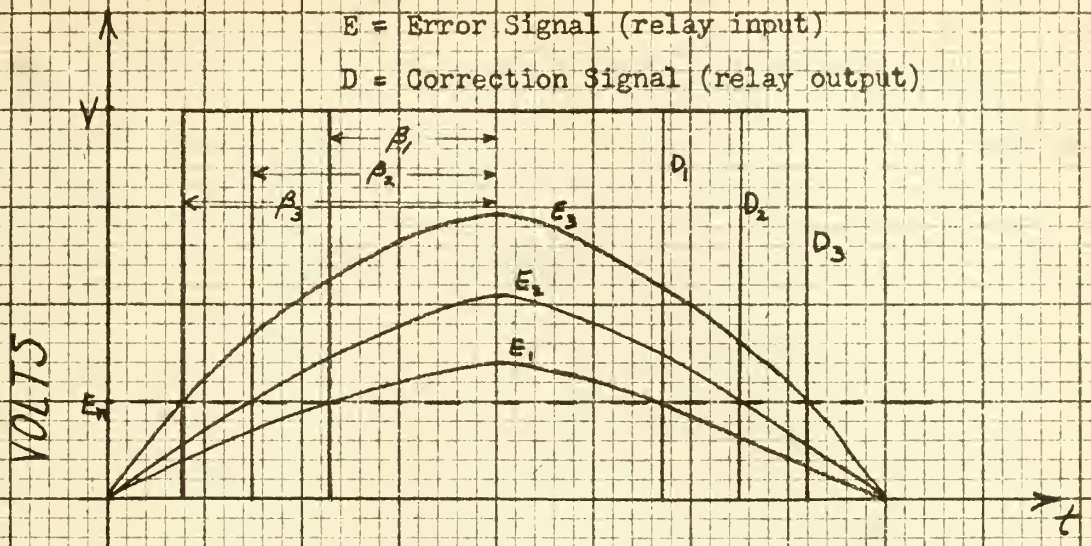

FIGURE 7. EFFECT OF ERROR SIGNAL AMPLITUDE ON RELAY OUTPUT

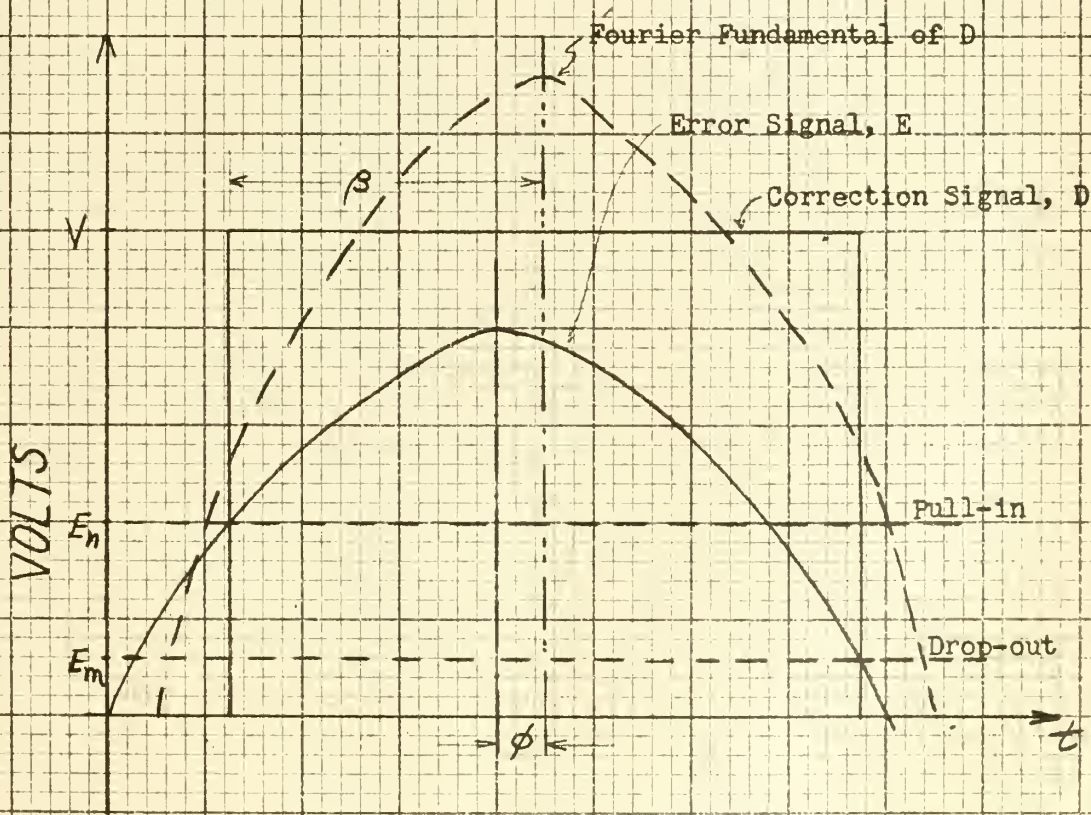

FIGURE 8. EFFECT OF UNEQUAL PULL-IN AND DROP-OUT VALUES

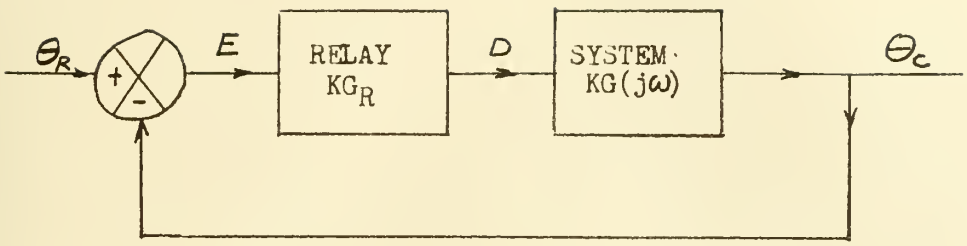

FIGURE 9. BLOCK DIAGRAM OF SIMPLE RELAY SERVO

The transfer function of the system is

$$\frac{\theta_c}{E}(j\omega) = KG_R\, KG(j\omega) \tag{15}$$

where KG_R is a function of the amplitude of the error signal and the relay characteristics and $KG(j\omega)$ is a function of the frequency and the system gain. When the Nyquist stability criterion is employed, the polar locus of equation (15) in the $KG(j\omega)$ plane is one complete curve for any given error signal amplitude. Since this amplitude changes during normal operation, a family of curves is required to determine the degree of stability of the system.

A more convenient means of determining system stability is to plot a locus of stability points, one corresponding to each error signal amplitude. Thus the need for a method lends itself to relay servo design. Instability results when the system transfer function passes through or encloses the $-1 + j0$ point, or mathematically

$$KG(j\omega)\, KG_R \geqslant -1 + j0 \tag{16}$$

If this equation is rewritten, the location of the stability point for each error signal may be defined as

$$\text{Stability Point} = \frac{1\angle 180^\circ}{|KG_R|\angle\phi} = |KG_R^{-1}|\angle 180^\circ - \phi \qquad (17)$$

For the case where pull-in and drop-out voltage are the same, ϕ is equal to zero for all error signal magnitudes and the locus of the stability point is the negative real axis. Figure 10(a) illustrates the determination of system stability for several hypothetical systems employing a relay with zero dead zone. Curve a represents an inherently stable system since the KG ($j\omega$) locus does not enclose any of the stability points. Curve b is inherently unstable since it encloses the entire stability locus. Curve c represents a conditionally stable system since part of the stability locus is enclosed by the KG ($j\omega$) locus. For small disturbances the system is unstable. For large disturbances the system is stable and the oscillatory amplitude decreases down to the steady state amplitude represented by the point K_2G_R. This point also indicates the frequency of the steady state oscillations. Figure 10(b) illustrates the case for systems employing a relay with finite dead zone and equal pull-in and drop-out voltages. Figure 10(c) depicts systems using a relay with unequal pull-in and drop-out voltages.

It has been shown [3, 4] that the transient performance may be accurately estimated from the magnitude loci or M circles provided proper precautions are taken. Also, the approximate frequency response method is adaptable to the design of compensating network which are usually employed to improve system performance.

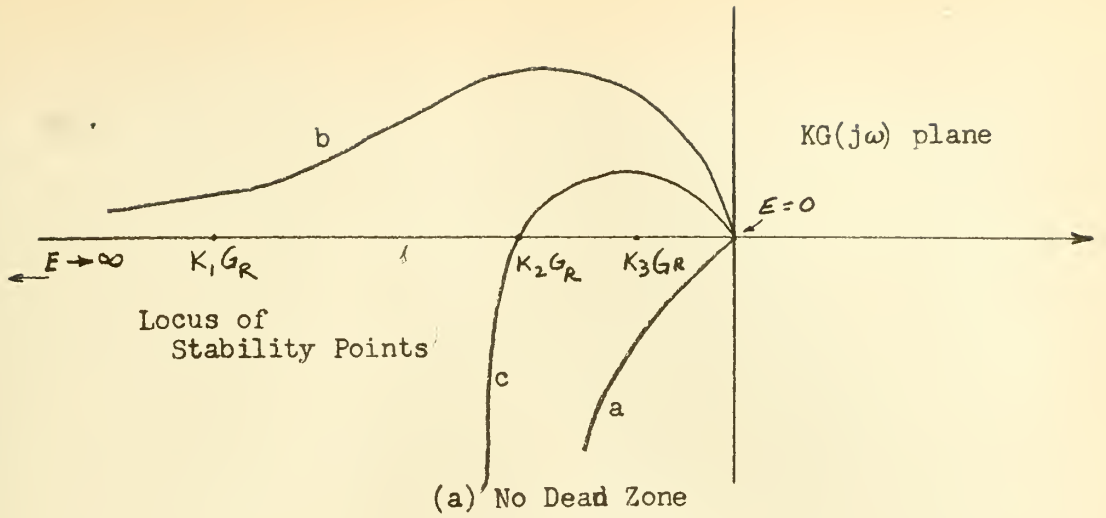

(a) No Dead Zone

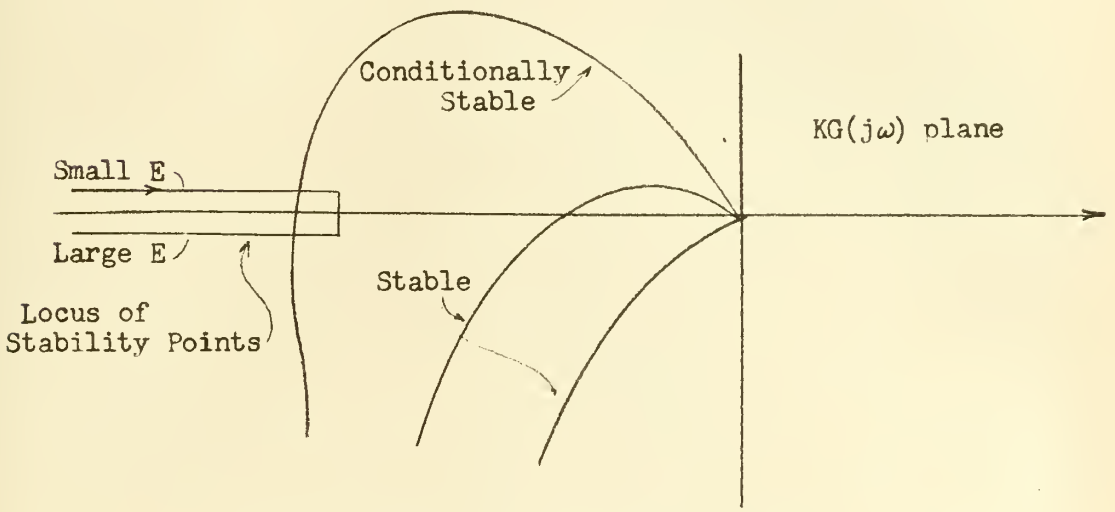

(b) Equal Pull-in and Drop-out Voltages

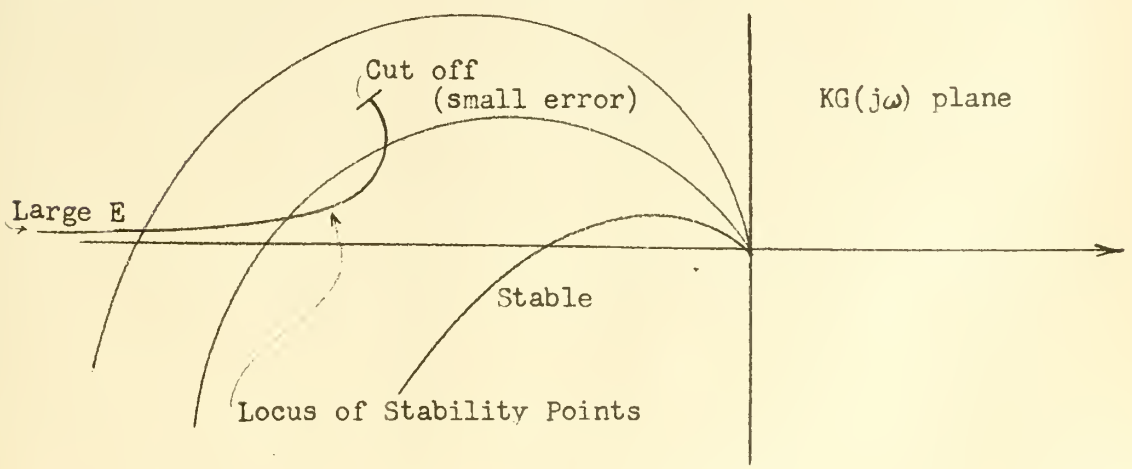

(c) Unequal Pull-in and Drop-out Voltages

FIGURE 10. STABILITY DETERMINATION USING LOCUS OF STABILITY POINTS

The method of describing the non-linear response of relay action by an approximate transfer function should be applicable in the treatment of other non-linear effects such as backlash, Coulomb friction, saturation, etc.

5. Types of Damping.

A practical servomechanism is subject to two principal defects: oscillation, the periodic deviation of output from the desired value; and lag, the average or unidirectional deviation. Through proper design each of these may be reduced to a negligible magnitude. Oscillation would be expected to occur in a servo if definite preventive measures were not employed. Consider a step, or constant, input to a simple servo. If no damping forces were present such a system would oscillate indefinitely at any amplitude at which it began. Damping can reduce these oscillations to a small amplitude or prevent them altogether.

Coulomb friction was explained in subsection 2 above. Also, the method of handling Coulomb friction damping by transient analysis was shown in that section. In subsection 3 Coulomb friction damping was handled by phase-plane analysis. It has been shown [2] that, with a step input, the constant damping of Coulomb friction is preferable to damping dependent upon output velocity from the point of view of reducing the amplitude of oscillation. However, when the input has a constant velocity and the output velocity is unidirectional, Coulomb friction will not damp out oscillations in a relay servo (assuming a finite dead zone). To damp out oscillations under these conditions the frictional force must have a component that varies in magnitude as some positive power of the velocity. It has been shown also that a relay

servo having Coulomb friction is relatively insensitive to small values of relay time lag.

In the remainder of this section several other types of damping will be discussed. The methods of analyzing each type and their effects on relay servo systems will be explained. Viscous damping and error-rate damping are discussed in (a) and (b) below, and are considered to be acting continuously. Discontinuous types of damping are discussed in (c).

a. Viscous damping. Viscous friction, or viscous damping, is caused by a force proportional to the output speed of motion of the system directed opposite to the output speed. Viscous friction includes friction in the servomotor, friction in the load, and in the couplings and gears between the motor and load. Viscous friction can be obtained also through mechanical friction devices such as dashpots, friction disks, and so on, or through electromagnetic friction devices such as an eddy-current damper, consisting of a metal disk rotating in a magnetic field. For the viscous friction described thus far, inherent or applied, note that the torque due to viscous friction must be counterbalanced by the servomotor or the momentum of the system, resulting in a continuous drain of energy.

There are electric motors which have viscous damping characteristics without the objectional power-consumption trait. An example of this is the armature-controlled d-c shunt motor. For a constant applied armature voltage, the shaft torque decreases as the speed increases (counter emf increases, motor current decreases, therefore torque decreases). This is equivalent to a pure torque motor[1] coupled to

1 A pure torque motor is herein defined to be a constant-torque motor, i.e., torque does not depend on speed.

a viscous damper, since the retarding torque of the damper increases linearly with the speed and subtracts from the torque of a pure torque motor to produce an equivalent torque which decreases linearly with speed. Unfortunately, the amount of damping is fixed by motor design and cannot be altered, except by adding resistance in series with the armature thereby decreasing available torque as well as damping. The two phase induction motors used as servomotors generally have a high rotor resistance so that the peak torque occurs at start (stall) rather than near synchronous speed. This gives a torque-speed curve quite similar to that of the armature-controlled d-c motor, and thus the servo induction motor produces equivalent viscous damping. If a wound-rotor motor is available, the damping may be changed by varying rotor resistance, though at the expense of starting torque.

Viscous damping has a stabilizing influence on relay servos, although it causes a dynamic lag error. A servo possessing viscous damping is quite sensitive to relay time lag in comparison to a servo possessing only Coulomb damping.

Herein the symbol f shall denote the viscous friction coefficient, as referred to the output shaft. Thus the retarding viscous friction torque is $f\dot{\theta}$, or $f\dot{E}$ for step input.

Consider now the relay servo diagrammed in Figure 11(a). This is the same servo as in Figure 1, except that viscous damping is present. When the relay has a finite dead zone, with pull-in and drop-out voltages equal, the system equations for a step input are

$$J\ddot{E} + f\dot{E} = -T_j \text{ when } E \geq E_n \tag{18}$$

$$J\ddot{E} + f\dot{E} = +T_j \text{ when } E \leq -E_n \tag{19}$$

Relay Characteristics

when $E \geq E_n$, $D = -V$

when $E \leq -E_n$, $D = +V$

when $-E_n < E < E_n$, $D = 0$

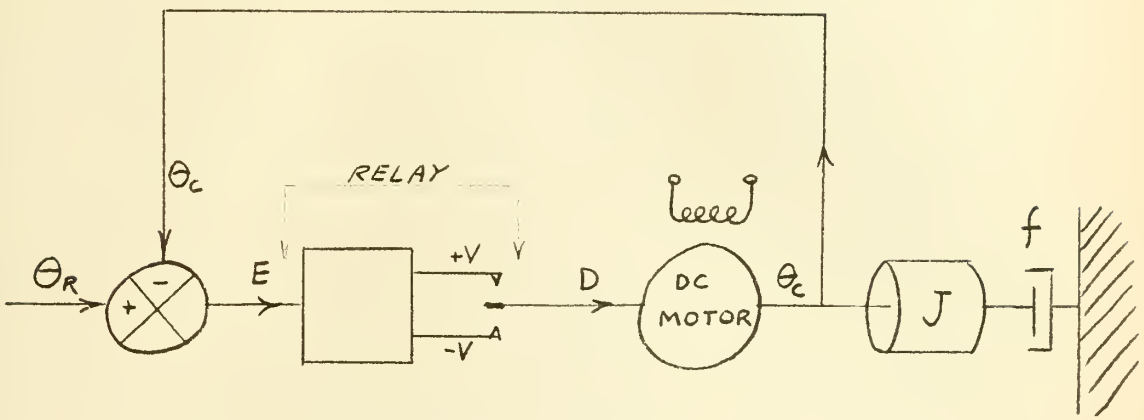

(a) System Diagram

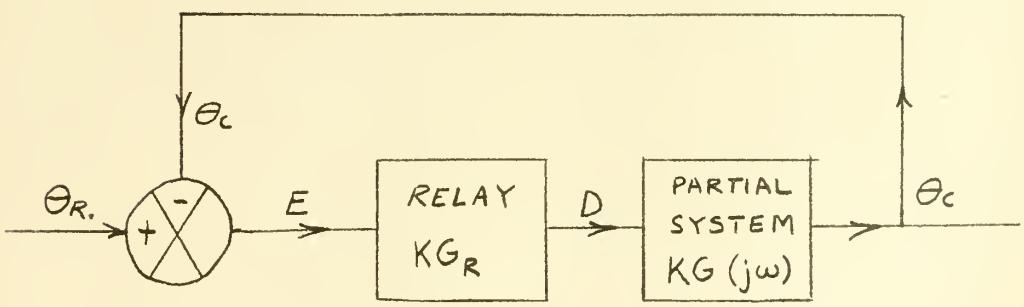

(b) Block Diagram

FIGURE 11. SIMPLE RELAY SERVO WITH VISCOUS DAMPING

$$J\ddot{E} + f\dot{E} = 0 \quad , \text{when } -E_n < E < E_n \tag{20}$$

In section 2(a) above it was shown how the classical method handles the six second order equations which result when Coulomb damping is present. Here there are three second order equations to describe the system and the classical method is applied in a like manner.

Also, the phase-plane method is easily extended to handle the viscous damping case. The first phase of action following a positive step function is described by

$$J\ddot{E} + f\dot{E} = -T \tag{13}$$

Below are the sequence of steps in manipulating this equation into the general form required for use in the phase-plane plot

$$\ddot{E} = \frac{1}{J}\left(-T - f\dot{E}\right) \tag{21}$$

$$\frac{\ddot{E}}{\dot{E}} = \frac{d\dot{E}}{d\dot{E}} = \frac{1}{J}\left(-\frac{T}{\dot{E}} - f\right) \tag{22}$$

The equations of the isoclines result when $d\dot{E}/dE$ is set equal to a series of constants; again the isoclines are straight lines parallel to the E-axis. The phase-plane construction of the three system equations is carried out as outlined in section (3) above. Figure 12 is the phase-plane plot of the response of a relay servo with viscous damping to a positive step function input.

The frequency response method of analyzing the servo with viscous friction is exactly similar to the case outlined in section (4) above; compare Figure 9 with Figure 11(b). The partial system transfer function, $KG(j\omega)$, represents the linear portion of the system and therefore

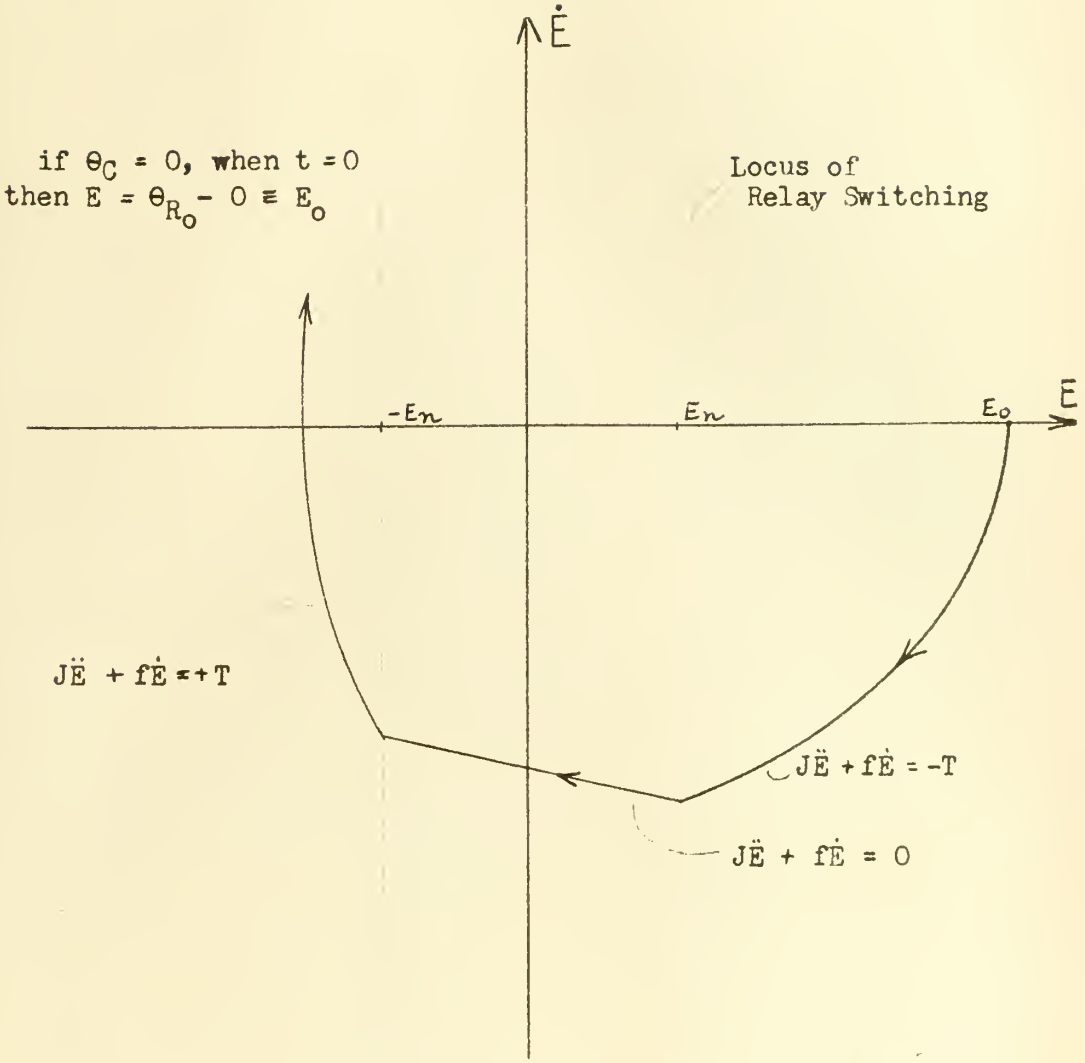

FIGURE 12. PHASE-PLANE PLOT OF A RELAY SERVO WITH VISCOUS DAMPING

now contains the effects of viscous friction. KG_R is the describing function for the relay which allows the non-linear system to be treated as an approximately linear one. The transfer function of the system is

$$\frac{\Theta_c}{E}(j\omega) = KG_R KG(j\omega) \qquad (23)$$

System stability is determined as outlined in section (4).

b. Derivative damping. The form of damping considered in the previous section, viscous damping, consisted of applying to the system a retarding force proportional to the speed of the output member. While such viscous damping effectively reduces transient oscillations it also retards the output and drains energy from the system. In continuous control servos a signal proportional to the first time derivative of output, or of error, is fed to the controller resulting in the advantages, but not the disadvantages of viscous damping. This form of damping is known as derivative damping or derivative compensation.

It should be noted that derivative damping utilizing output-rate, $\dot{\Theta}_c$, and derivative damping utilizing error-rate, $\dot{E}$, are the same only for a step input, $\dot{E} = -\dot{\theta}_c \ (t>0)$. In general, any method which generates the derivative or approximate derivative of output, or of error, will improve the transient response by providing an anticipatory signal. Thus a d-c tachometer might be employed, as in Figure 13, to obtain a signal proportional to output-rate; or an a-c tachometer plus a rectifier might be used. An error-rate signal can be obtained by running the error signal through a differentiating network. Herein the use of the expression "derivative damping" shall refer to damping achieved from either output-rate or error-rate signals since the input signal shall always be a step function. All examples utilizing

Relay Characteristics

when $G \geq E_n$, $D = -V$
when $G \leq -E_n$, $D = +V$
when $-E_n < G < E_n$, $D = 0$

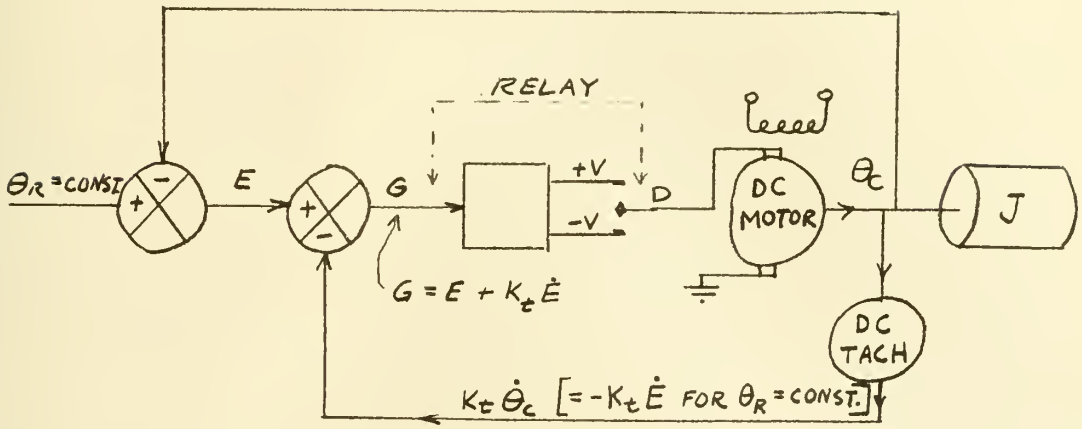

(a) System Diagram

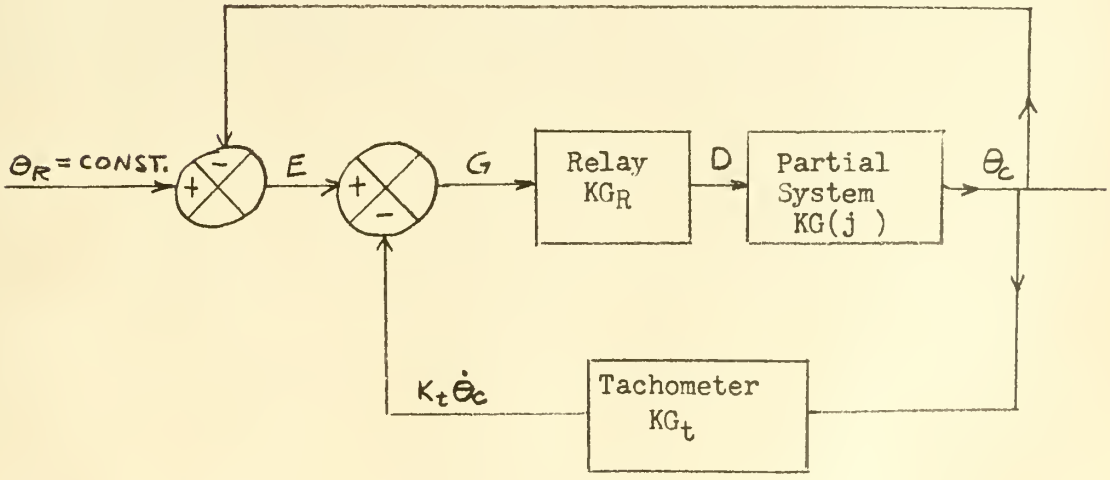

(b) Block Diagram

FIGURE 13. RELAY SERVO WITH DERIVATIVE DAMPING

derivative damping, herein, employ a d-c tachometer to feedback an output-rate signal and therefore the expressions "tach feedback" and "feedback" shall be equivalent to "derivative damping".

In a continuous control servo responding to a step input, the effects of viscous damping and tachometer feedback are identical. If a derivative error signal is used instead of tachometer feedback, the derivative of the step produces an infinite impulse at $t = 0$, which causes an anticipatory acceleration and will usually cause momentary saturation, but for $t > 0$ the damping effect of the error rate signal is also identical with the effect of viscous damping. In the relay servo, however, the effects of derivative and viscous damping are dissimilar, except that each tends to improve transient response. In derivative damping a term describing the derivative signal appears in the equation or statement of the boundary conditions, but does not appear in the equations describing the action of the system. The amount of derivative damping signal employed helps to determine when each of the equations describing the system response becomes effective; i.e., the derivative signal, along with the relay's inherent characteristics, sets the "switching criterion" for the relay.

Figure 13 illustrates a simple positioning relay servo employing derivative damping by feeding back a first derivative of output signal through use of a d-c tachometer geared to the output shaft. The output of the tachometer is a voltage proportional to the angular velocity of the output shaft, or $K_t \dot{\theta}_c$. Since the input, θ_R, is to be a step function, $K_t \dot{\theta}_c = -K_t \dot{E}$, for $t > 0$, the signal going into the relay is now the algebraic sum of the error and the tach feedback signals (for simplicity the amplification of the adding units are assumed to be unity). Thus, if the relay has pull-in and drop-out voltages equal, the

expressions describing the relay switching are

$$\text{when} \quad E + K_t\dot{E} \geqslant E_n \,, \quad D = -V \tag{24}$$

$$\text{when} \quad E + K_t\dot{E} \leqslant -E_n \,, \quad D = +V \tag{25}$$

$$\text{when} \quad -E_n < E + K_t\dot{E} < E_n \,, \quad D = 0 \tag{26}$$

Therefore the system equations are

$$J\ddot{E} = -T \quad \text{, when} \quad E + K_t\dot{E} \geqslant E_n \tag{27}$$

$$J\ddot{E} = +T \quad \text{, when} \quad E + K_t\dot{E} \leqslant -E_n \tag{28}$$

$$J\ddot{E} = 0 \quad \text{, when} \quad -E_n < E + K_t\dot{E} < E_n \tag{29}$$

The above equations are for negative feedback as shown in Figure 13, i.e., the signal to the relay, G, is the difference of the error and tach feedback signals. It will be clear from the phase-plane plot that negative feedback causes the relay to actuate before it normally would, i.e., anticipate.

The classical transient response method of analysis can be used to analyze the derivative damped servo of Figure 13(a) in a manner similar to that outlined in section 2(a) above. The three system equations and accompanying boundary conditions, equations (24) through (29), would be solved step-by-step as previously explained.

The application of the phase-plane method to this example is similar to the Coulomb friction damped illustration of section (3), with three rather than seven system equations to manipulate and plot. An interesting deviation from the Coulomb and viscous friction damped examples is the effect that derivative damping has on the locus of relay

reversals. Consider the first interval of servo action following a positive position command, θ_{R_0}, applied to the input shaft of the servo in Figure 13. Providing the resulting error is greater than or equal to the relay pull-in voltage, the servomotor will develop positive torque, T, to diminish the error. During this first interval, then, the system equation is

$$J\ddot{E} = -T \tag{27}$$

Equation (31) is the manipulated form suitable for plotting in the phase-plane.

$$\ddot{E} = -\frac{T}{J} \tag{30}$$

$$\frac{\ddot{E}}{\dot{E}} = \frac{d\dot{E}}{dE} = -\frac{1}{J}\left(\frac{T}{\dot{E}}\right) \tag{31}$$

However, the loci of relay reversals are no longer the pair of vertical lines, $E = \pm E_n$, found in the previous examples (Figure 5). The loci of relay reverslas are rotated in a counterclockwise manner, by negative derivative damping, and are now described by the equations

$$E + K_t\dot{E} = \pm E_n \tag{32}$$

Figure 14(a) illustrates the rotation of the loci of relay reversals and shows the response of the servo to a specific step input. Figure 14(b) illustrates the action of the same servo system with an ideal relay installed (the ideal relay has a zero width dead zone).

If viscous friction damping were added to the relay servo of Figure 13, the system equations would become

$$J\ddot{E} + f\dot{E} = -T \quad \text{, when } E + K_t\dot{E} \geq E_n \tag{33}$$

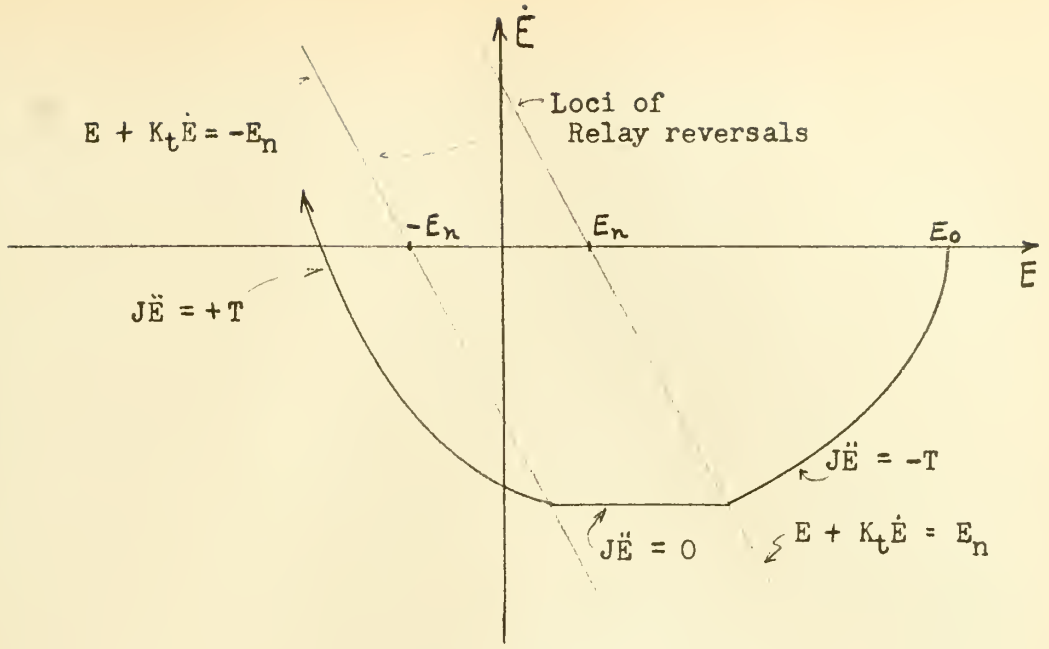

(a) With Dead Zone

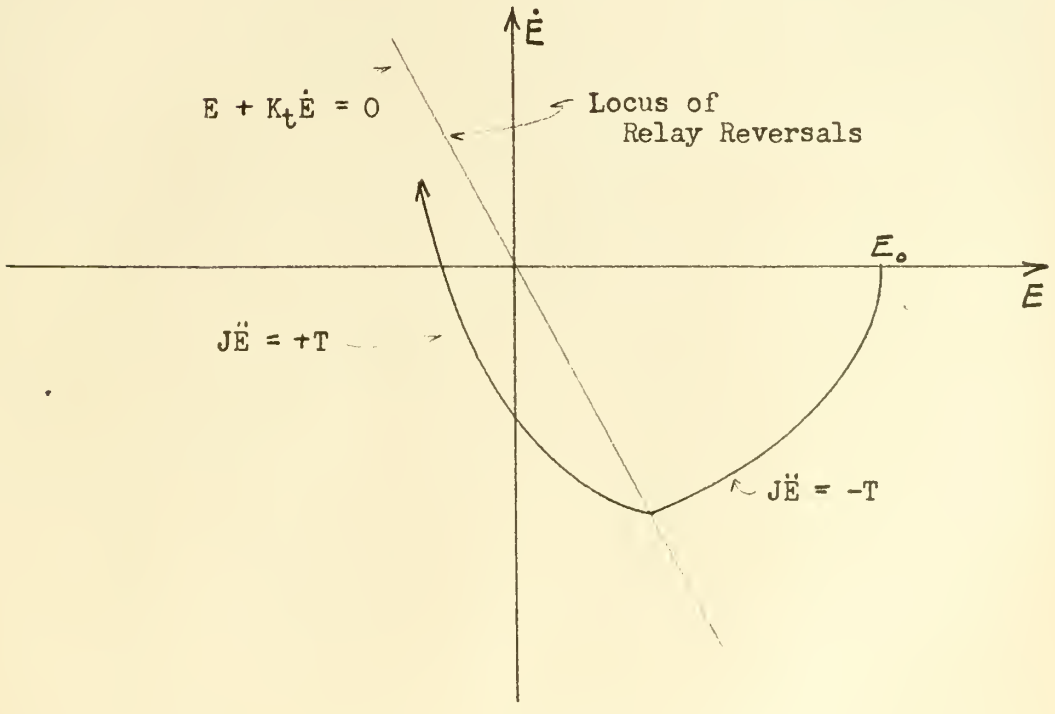

(b) No Dead Zone

FIGURE 14. PHASE-PLANE PLOT OF A RELAY SERVO WITH DERIVATIVE DAMPING ONLY

$$J\ddot{E} + f\dot{E} = +T \text{, when } E + K_t\dot{E} \leq -E_n \tag{34}$$

$$J\ddot{E} + f\dot{E} = 0 \text{ , when } -E_n < E + K_t\dot{E} < E_n \tag{35}$$

The first interval of relay action following the positive step function command, θ_{R_o}, is described by equation (33), which for phase-plane plotting manipulates into

$$\frac{d\dot{E}}{dE} = -\frac{1}{J}\left(\frac{T}{\dot{E}} + f\right) \tag{36}$$

Note that equation (36) is exactly the same as equation (22), which defines the initial action of a relay servo possessing viscous damping only. Thus it is evident that the addition of derivative damping to a relay servo effects only the instant of relay switching. Negative derivative damping causes the relay to operate early and thus provide retarding torque before the error reaches zero (see Figure 14(b)). Figure 15 is the phase-plane plot of a relay servo with dead zone and combined viscous and derivative damping when a specific step input is applied to the input shaft.

The <u>frequency response method</u> of analysis outlined in section (4) above could be extended to handle the relay servo with derivative damping. When the relay is represented by the describing function, KG_R, the block diagram of Figure 12(b) results. The transfer function of the system is equation (38) below

$$\frac{\theta_c}{G}(j\omega) = KG_R\,KG(j\omega) \tag{37}$$

$$\frac{\theta_c}{E}(j\omega) = \frac{KG_R\,KG(j\omega)}{1 + KG_t\,KG_R\,KG(j\omega)} \tag{38}$$

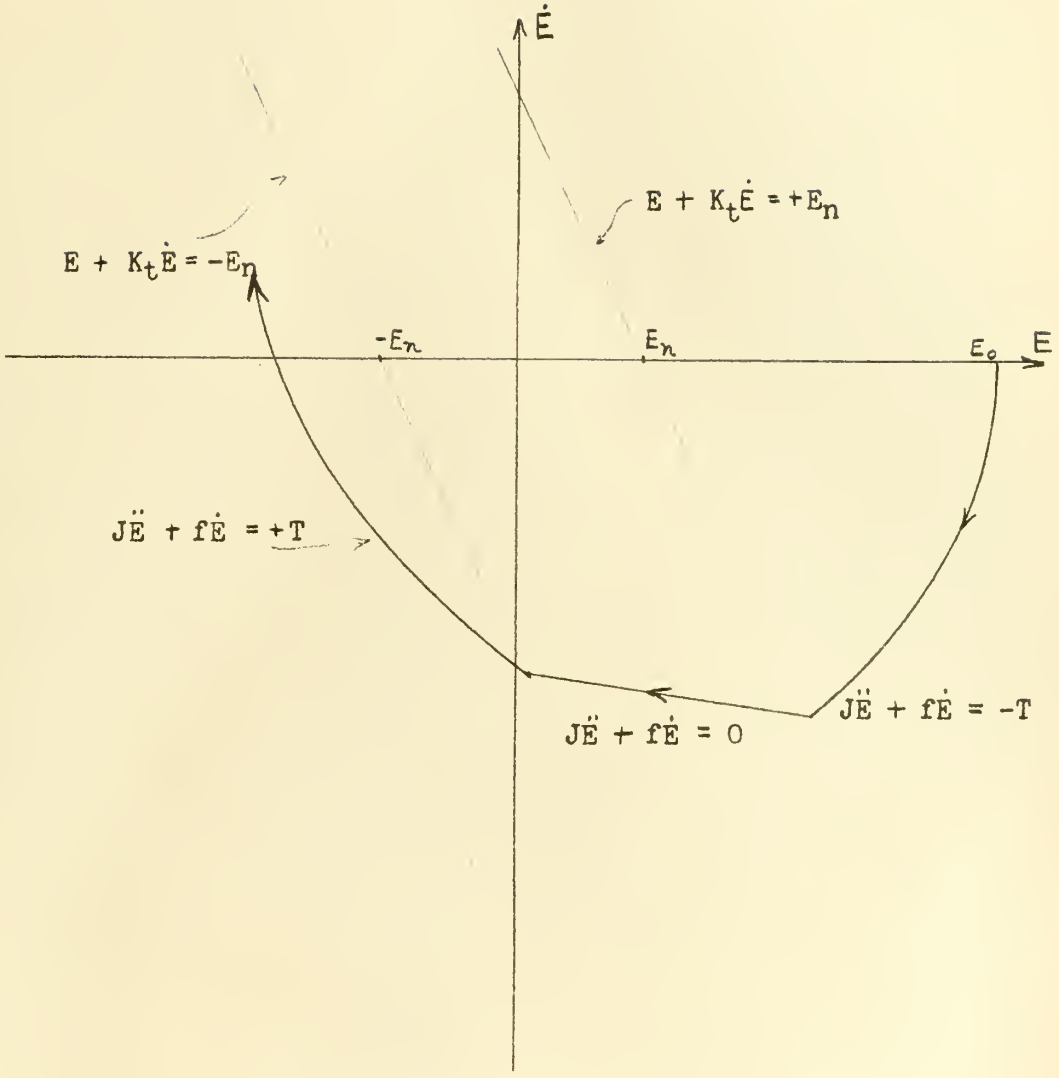

FIGURE 15. PHASE-PLANE PLOT OF RELAY SERVO WITH VISCOUS DAMPING AND DERIVATIVE DAMPING

c. Discontinuous damping. The retarding torques caused by Coulomb friction and by inherent viscous friction are applied continuously whether the servo is accelerating, decelerating or coasting through the dead zone. Derivative damping affects the relay switching rather than the system torque and is usually applied continuously. In systems where viscous dampers have been added it might be desirable to apply the additional damping only when the system is decelerating, since additional damping during acceleration only tends to slow down the servo's response. This is one example of discontinuous damping.

In Figure 14(a) it is observed that the relay servo possessing neither Coulomb nor viscous friction merely coasts through the dead zone with no deceleration. However, Coulomb damping, Figure 5(a), and viscous damping, Figures 12 and 15, cause a deceleration during the transit of the dead zone. When there is deceleration in the dead zone, the dead zone contributes a stabilizing effect on the servo response. It therefore becomes desirable to overcome the tendency of coasting through the dead zone by applying some form of damping in that zone. One method might be to employ a friction brake or clutch to the output shaft during the dead zone. The brake could be held away from the shaft by a solenoid energized by the motor voltage, V. This form of braking action is most practical when the output is at a relatively low power level. When there is no brake slippage (and no time delay), the output shaft can be stopped precisely at the time of relay drop-out; see Figure 16. Theoretically the dead zone could be narrowed to zero width, thus eliminating static error.

Dynamic braking may also be used for discontinuous damping. The concept of dynamic braking within the dead zone is explored in Chapter II

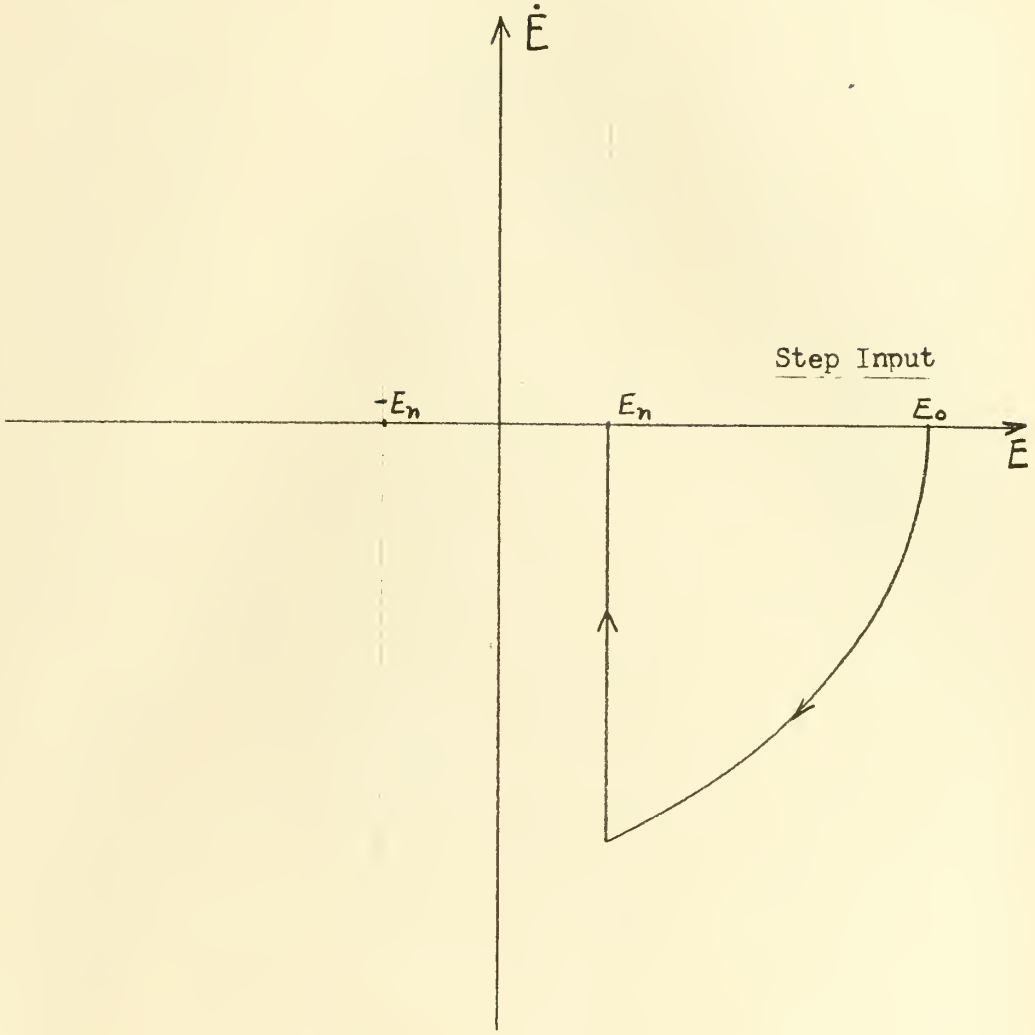

FIGURE 16. PHASE-PLANE PLOT OF RELAY SERVO WITH MECHANICAL BRAKING APPLIED IN THE DEAD ZONE

along with the principle of the optimum servo which employs an anticipator device to reverse the motor torque at precisely the correct time to bring the system to a stop at the desired position.

CHAPTER III

PHASE-PLANE ANALYSIS OF RELAY SERVOS

The phase-plane method of analyzing second-order relay servos was discussed in section 3 of Chapter I and the analysis of a simple relay servo with Coulomb damping and relay dead zone was illustrated. In section 5 the analysis of the same servo possessing viscous damping, derivative damping and combined viscous and derivative damping was illustrated using the phase-plane technique. This chapter will supplement the explanation and illustrations of the use of the phase-plane method given in sections 3 and 5 above. The mathematics of the optimum servo will be presented and illustrated by use of the phase-plane method. Then the concept of utilizing dynamic braking in the relay dead zone will be introduced and analyzed with phase-plane illustrations.

1. The Optimum System.

McDonald [5] and Hopkin [6] have proposed a relay servo system which employs maximum torque, $\pm T$, at all times but is switched at precisely the right moment to make zero error and zero error-rate be reached at the same instant. Thus, for a step input and no frictional torque, this system employs maximum accelerating torque until the error is half its original value and maximum decelerating torque until the error is reduced to zero. This system realizes the minimum possible response time, with the specified maximum torque and pure inertia load, and has been termed the "optimum" system. As will be shown, the instant of relay switching is determined by a comparison of the error and the square of the error-rate. Therefore the locus of switching points on

the phase-plane is not linear, as in the derivative damped servos previously analyzed, but is nonlinear. The device or network which fabricates this nonlinear locus has been termed the "anticipator", and thus this servo system is known also as the anticipator servo and the predictor servo.

The mathematical derivation of the locus of switching points will be carried out, first with an ideal torque motor in the system and then with a practical d-c motor. In the remainder of this section the assumptions are: step inputs, ideal relay, and no time delays.

a. Pure torque motor. Consider now the optimum servo employing a pure torque motor, Figure 17. Since an ideal relay is employed, the relay characteristics are as follows: if relay input, G, is positive, then the correction signal, D, is - V and motor torque is -T; if G is negative, D = + V, and motor torque is + T. Thus the response of the system to a step input is determined from the equation

$$J\ddot{E} = \pm T \tag{39}$$

The steps below will establish the inputs to and the output from the nonlinear anticipator unit which are necessary to achieve the optimum response of the servo. With the output shaft stationary, assume a positive step input is applied at time t = 0. The system equation is then

$$J\ddot{E} = -T \tag{40}$$

Integrating $\dot{E} = C_1 - \frac{T}{J}t$

and since $\dot{E}(0) = 0$

then $C_1 = 0$

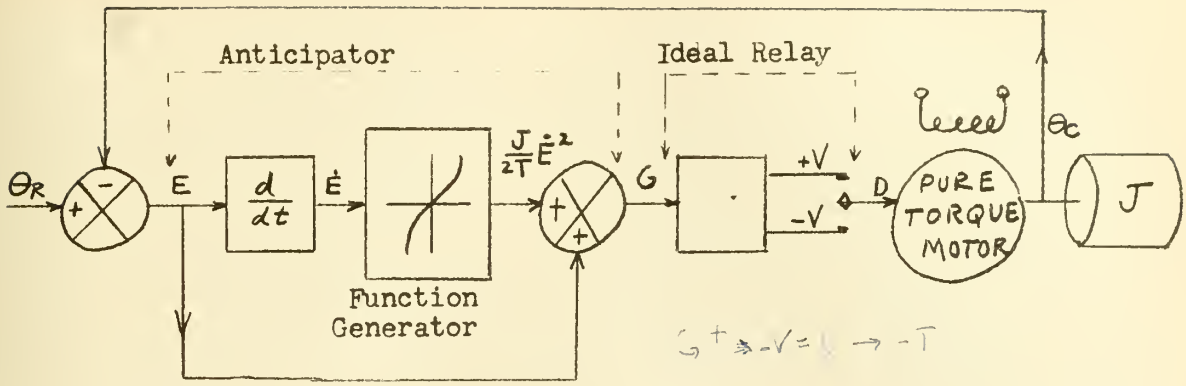

FIGURE 17. BLOCK DIAGRAM OF OPTIMUM SERVO SYSTEM

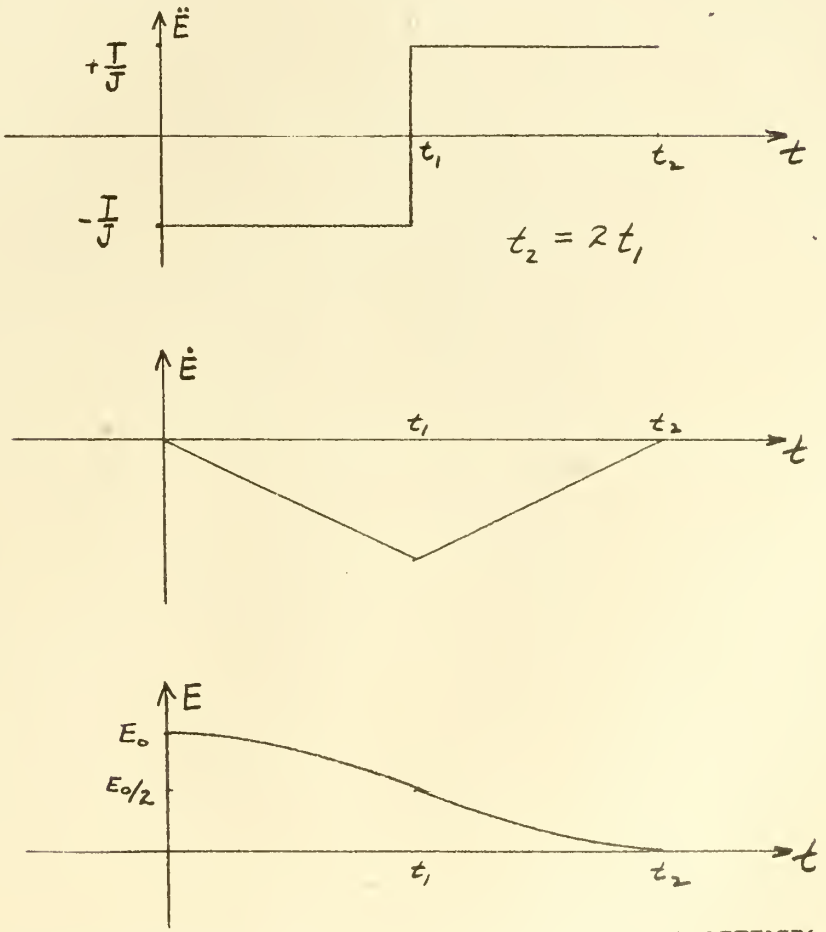

FIGURE 18. ERROR, ERROR-RATE, AND RATE OF ERROR-RATE FOR OPTIMUM SERVO SYSTEM

and $$\dot{E} = -\frac{T}{J}t \qquad (41)$$

Integrating (41) $$E = C_2 - \frac{T}{2J}t^2$$

and since $$E(0) = E_0$$

then $$C_2 = E_0$$

and $$E = E_0 - \frac{T}{2J}t^2 \qquad (42)$$

Equations (41) and (42) are the parametric equations of motion describing, in the phase-plane, the acceleration interval; eliminating the parameter t gives

$$E = E_0 - \frac{T}{2J}\dot{E}^2, \quad 0 \leq t \leq t_1 \qquad (43)$$

At time t_1 the error is reduced to half its original value and the anticipator causes the sense of the torque to reverse, Figure 18. The equation for the deceleration interval is thus

$$J\ddot{E} = +T \qquad (44)$$

Integrating $$\dot{E} = C_3 + \frac{T}{J}t$$

and from (41) $$\dot{E}(t_1) = -\frac{T}{J}t_1$$

then $$C_3 = -2\frac{T}{J}t_1$$

and $$\dot{E} = -\frac{T}{J}(2t_1 - t)$$

but since, response time $= t_2 = 2t_1$

then $$\dot{E} = -\frac{T}{J}(t_2 - t) \qquad (45)$$

Integrating (45) $$E = C_4 + \frac{T}{2J}(t_2 - t)^2$$

and since $$E(t_2) = 0$$

then $$C_4 = 0$$

and $$E = \frac{T}{2J}(t_2 - t)^2 \qquad (46)$$

Equations (45) and (46) are the parametric equations of motion describing the deceleration interval; eliminating the parameter gives

$$E = \frac{J}{2T}\dot{E}^2, \quad t_1 \leq t \leq t_2 \qquad (47)$$

To determine the time of switching,

since $$E(t_1) = \frac{E_o}{2}$$

then from (42) $$t_1 = \sqrt{\frac{J}{T}E_o} \qquad (48)$$

Thus the time of switching varies directly as the square roots of J/T and Eo, the torque-to-inertia ratio and the initial error respectively.

Since $t_2 = 2t_1$,

the response time $= t_2 = 2\sqrt{\frac{J}{T}E_o}$ (49)

Curve 1 of Figure 19 illustrates the phase-plane plot of the system's response to the step input, Eo. Curves 2, 3 and 4 represent the response to inputs of lesser magnitude. Note that the locus of torque reversals is also the path along which the system moves to the origin (a similar locus occurs in the second quadrant). Thus the system equations in the fourth quadrant are

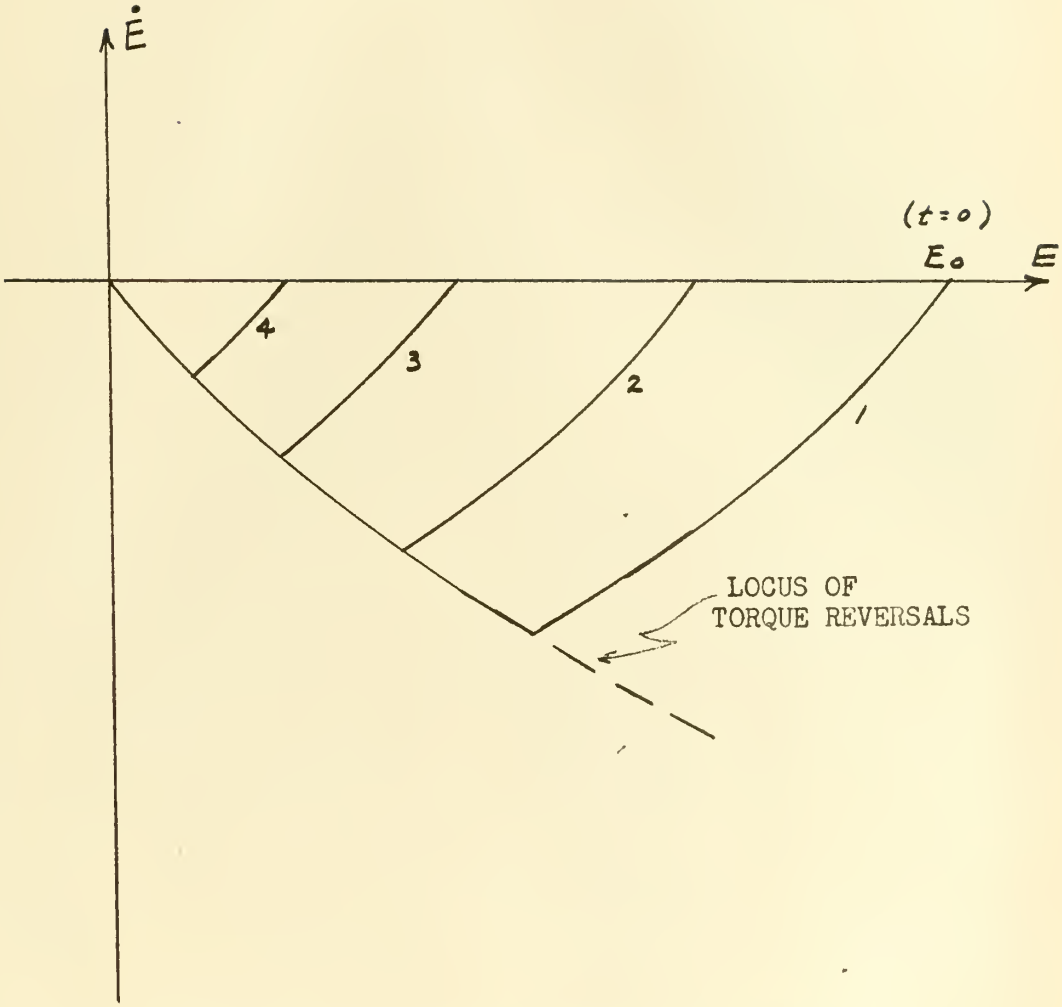

FIGURE 19. PHASE PLANE PLOT OF RESPONSE OF OPTIMUM SYSTEM TO SEVERAL STEP INPUTS (IDEAL TORQUE MOTOR).

when $E - \frac{J}{2T}\dot{E}^2 > 0$, $J\ddot{E} = -T$ or $E = E_0 - \frac{J}{2T}\dot{E}^2$ (50)

when $E - \frac{J}{2T}\dot{E}^2 < 0$, $J\ddot{E} = +T$ or $E = \frac{J}{2T}\dot{E}^2$ (51)

Thus the role of the anticipator is to compare error to the square of error-rate. Hopkin [6] described two methods to achieve the proper switching. One method is to compare two voltages, one proportional to the error and the other proportional to a nonlinear function of the error-rate, the latter voltage being generated by biased-diode networks. The second method is to reproduce the phase-plane plot on the face of a cathode-ray tube in which the horizontal and vertical deflections of the beam depend directly on error and error-rate. An opaque mask covers the region on one side of the torque reversal curve and a photocell determines from the location of the spot whether positive or negative torque is required.

Stout [7] has presented the analysis of some "nearly optimum" systems which take into account the effects of viscous and Coulomb friction. Although the path of deceleration is still along the locus of torque-reversals, the switching no longer occurs when the error is reduced to one-half. Kazda [8] analyzed the effects on the optimum system of certain switching errors.

b. Practical d-c motor. Consider now the use of a practical d-c shunt motor in place of the ideal torque motor. When the shunt field is held constant

$$T = K_T i \tag{52}$$

Where K_T is the motor torque constant; and where i is the armature

current, which can be determined from the following d-c motor relationship

$$V = iR + L\frac{di}{dt} + K_v\frac{d\theta_c}{dt} \tag{53}$$

where R and L refer to motor armature resistance and inductance respectively, and K_v is the counter electromotive force constant. From (53), assuming a step input at t = 0, and assuming that L di/dt is negligible

$$i = \frac{V + K_v\dot{E}}{R} \tag{54}$$

and thus

$$\pm T = \pm\frac{K_T}{R}\left(V + K_v\dot{E}\right) \tag{55}$$

The steps below will establish the inputs to and the outputs from the nonlinear anticipator unit which are necessary to achieve optimum response for a servo using a practical d-c motor. One further assumption is that the step inputs are not large enough to cause saturation to be reached. The system equation for the acceleration interval is

$$J\ddot{E} = -T = -\frac{K_T}{R}\left(V + K_v\dot{E}\right) \tag{56}$$

or

$$\ddot{E} + \frac{K_T K_v}{JR}\dot{E} = -\frac{K_T V}{JR} \tag{57}$$

Define

$$A \equiv \frac{K_T K_v}{JR}, \qquad B \equiv \frac{K_T V}{JR}$$

then (57) becomes

$$\ddot{E} + A\dot{E} = -B \tag{58}$$

Using Laplace transform theory, with s the complex variable:

transforming (58) $\left[s^2E(s) - sE(0^+) - \dot{E}(0^+)\right] + \left[sAE(s) - AE(0^+)\right] = -\frac{B}{s}$

but $E(0^+) = E_0$ and $\dot{E}(0^+) = 0$

therefore $s^2E(s) - sE_0 + sAE(s) - AE_0 = -\frac{B}{s}$

or $E(s) = \frac{-B}{s^2(s+A)} + \frac{E_0}{s}$

therefore $E = -\frac{B}{A^2}\left(e^{-At} + At - 1\right) + E_0$ (59)

from (59) $\dot{E} = -\frac{B}{A}\left(-e^{-At} + 1\right)$ (60)

Equations (59) and (60) are the parametric equations describing the acceleration interval in the phase-plane; they are valid until the instant of switching, t_1. Since, from (60)

$$t = -\frac{1}{A}\ln\left(1 + \frac{A}{B}\dot{E}\right), \quad 0 \leq t \leq t_1 \tag{61}$$

the parameter, t, can be eliminated from (59) and (60) giving

$$E = E_0 - \frac{\dot{E}}{A} + \frac{B}{A^2}\ln\left(1 + \frac{A}{B}\dot{E}\right), \quad 0 \leq t \leq t_1 \tag{62}$$

The equation for the deceleration interval is

$$J\ddot{E} = +T = \frac{K_T}{R}\left(V + K_V\dot{E}\right) \tag{63}$$

or $$\ddot{E} - A\dot{E} = B \tag{64}$$

The general solution of equation (64) is

$$E = C_1e^{At} + C_2 - \frac{B}{A}t$$

and $$\dot{E} = AC_1 e^{At} - \frac{B}{A}$$

Since the final conditions are

$$E(t_2) = \dot{E}(t_2) = 0$$

then $$C_1 = \frac{B}{A^2} e^{-At_2}, \quad C_2 = -\frac{B}{A^2}(-At_2 + 1)$$

therefore $$E = \frac{B}{A^2} e^{-A(t_2 - t)} + \frac{B}{A}(t_2 - t) - \frac{B}{A^2} \tag{65}$$

$$\dot{E} = -\frac{B}{A}\left[-e^{-A(t_2 - t)} + 1\right] \tag{66}$$

Equations (65) and (66) are the parametric equations describing the deceleration interval in the phase-plane, and are valid when $t_1 \leq t \leq t_2$. Since, from (66)

$$(t_2 - t) = -\frac{1}{A} \ln\left(1 + \frac{A}{B}\dot{E}\right), \quad t_1 \leq t \leq t_2 \tag{67}$$

the parameter, t can be eliminated from (65) and (66) giving

$$E = \frac{\dot{E}}{A} - \frac{B}{A^2} \ln\left(1 + \frac{A}{B}\dot{E}\right), \quad t_1 \leq t \leq t_2 \tag{68}$$

So far no criteria have been put on the switching time t_1. Assume, as before, that

$$E(t_1) = \frac{E_0}{2} \quad \text{and} \quad t_1 = \frac{t_2}{2} \tag{69}$$

When these two conditions are placed upon equations (59) and (60), the results are identical to equations (65) and (66) with the same conditions. Thus the switching should occur when the error is reduced by half as assumed. Figure 20 indicates the system's response in the

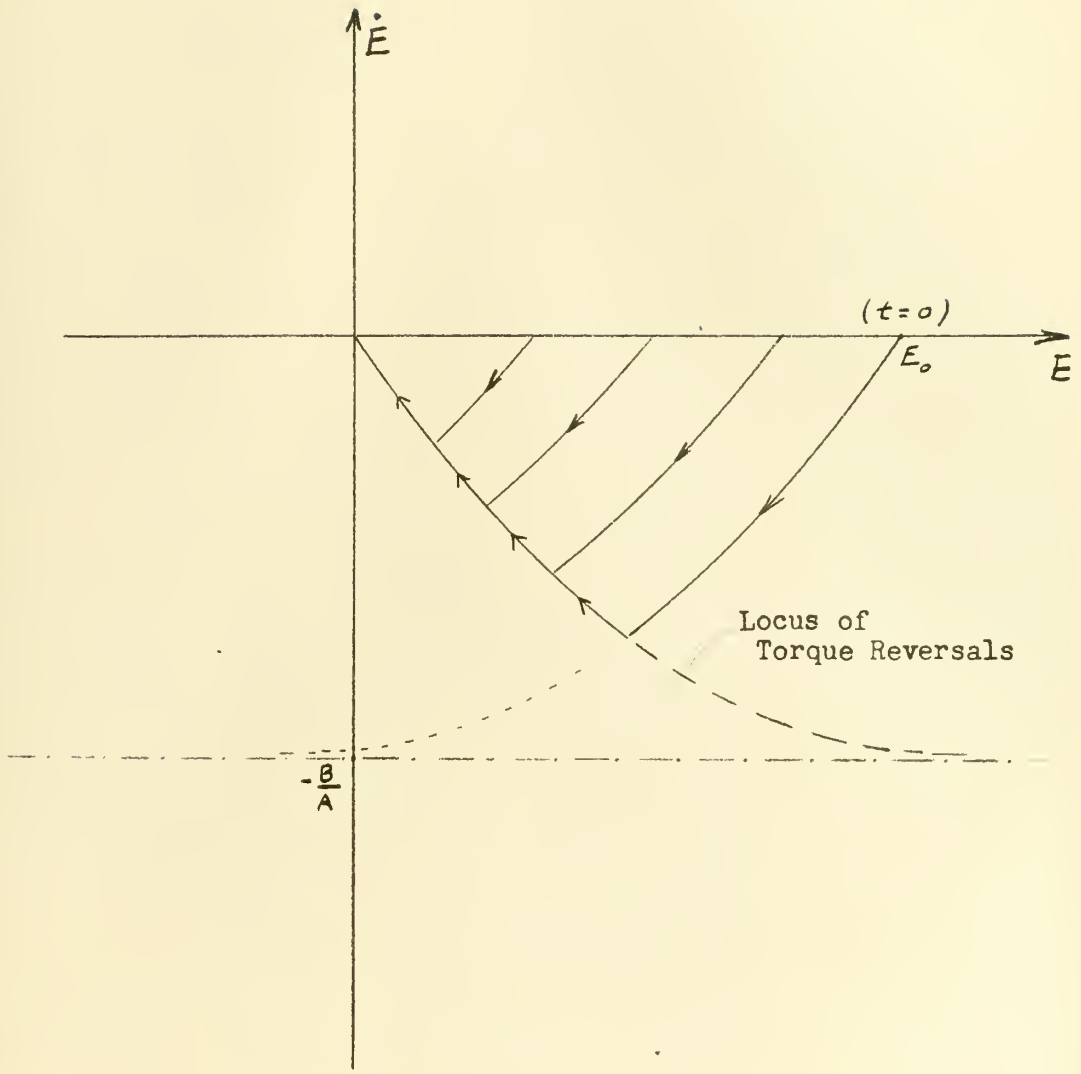

FIGURE 20. PHASE-PLANE PLOT OF RESPONSE OF OPTIMUM SYSTEM TO SEVERAL STEP INPUTS (PRACTICAL D-C MOTOR)

phase-plane to several step inputs. As in Figure 19 the locus of torque reversals is also the path along which the system moves to the origin (a similar locus appears in the second quadrant). In the fourth quadrant the system equations are

when $$E - \frac{JR\dot{E}}{K_T K_v} + \frac{JRV}{K_T K_v^2} \ln\left(1 + \frac{K_v}{V}\dot{E}\right) > 0 \qquad (70)$$

then $$J\ddot{E} = -T \quad \text{or} \quad E = E_0 - \frac{JR\dot{E}}{K_T K_v} + \frac{JRV}{K_T K_v^2} \ln\left(1 + \frac{K_v}{V}\dot{E}\right) \qquad (71)$$

and when $$E - \frac{JR\dot{E}}{K_T K_v} + \frac{JRV}{K_T K_v^2} \ln\left(1 + \frac{K_v}{V}\dot{E}\right) < 0 \qquad (72)$$

then $$J\ddot{E} = +T \quad \text{or} \quad E = +\frac{JR\dot{E}}{K_T K_v} - \frac{JRV}{K_T K_v^2} \ln\left(1 + \frac{K_v}{V}\dot{E}\right) \qquad (73)$$

The role of the anticipator device would be to compare error to a nonlinear function of error-rate as defined by equations (70) and (72). Such a device would be more difficult to fabricate than the anticipator unit required for the ideal torque motor case.

An expression from which the switching time, t_1, can be ascertained is obtained by applying the switching conditions, (69), to equation (59). The expression is

$$\left(\frac{K_T K_v}{JR} t_1\right) + e^{-\left(\frac{K_T K_v}{JR} t_1\right)} = 1 + \frac{K_T K_v}{2JRV} E_0 \qquad (74)$$

Equation (74) is a transcendental equation defining t_1 implicitly in terms of Eo. The switching time, t_1, cannot be expressed explicitly in terms of common functions. However, for any value of Eo, t_1 may be determined by use of a plot on rectangular coordinates, or by use of a table of exponential functions since equation (74) is of the form

$$\alpha + e^{-\alpha} = 1 + C_1 E_0$$

Determining t_1 determines the response time, t_2, since $t_2 = 2t_1$.

2. Dynamic Braking in the Dead Zone.

The optimum servo described above achieved braking action be reversing the motor torque. If the correct instant of torque reversal was chosen the system reached zero error and zero velocity at the same instant, therefore no overshoot. Since the switching was instantaneous an ideal relay was assumed; i.e., no dead zone. Thus the motor employed in the optimum system either had full positive terminal volts or full negative terminal volts applied to it. The system to be suggested in this section employs a practical relay with a finite dead zone. It will be shown how this dead zone can be used to enhance stability rather than limit it. It will be shown that, when derivative damping is properly employed, the system response to an arbitrary step input need not overshoot; and it will be shown that the dead zone may be narrowed down so that a high degree of static accuracy may be realized.

It is proposed that a resistor, R_B, be made to appear across the motor terminals during the transit of the dead zone, resulting in dynamic braking due to generator action. Figure 21(a) is a schematic diagram of one method of achieving this on a simple servo system. In this illustration, and in the remainder of this paper, the dynamic braking resistor, R_B, is connected across the motor terminals at all times. A system could easily be designed so that R_B appeared across the terminals only when the relay was open. The former method imposes an additional drain on the power supply and requires a relay whose

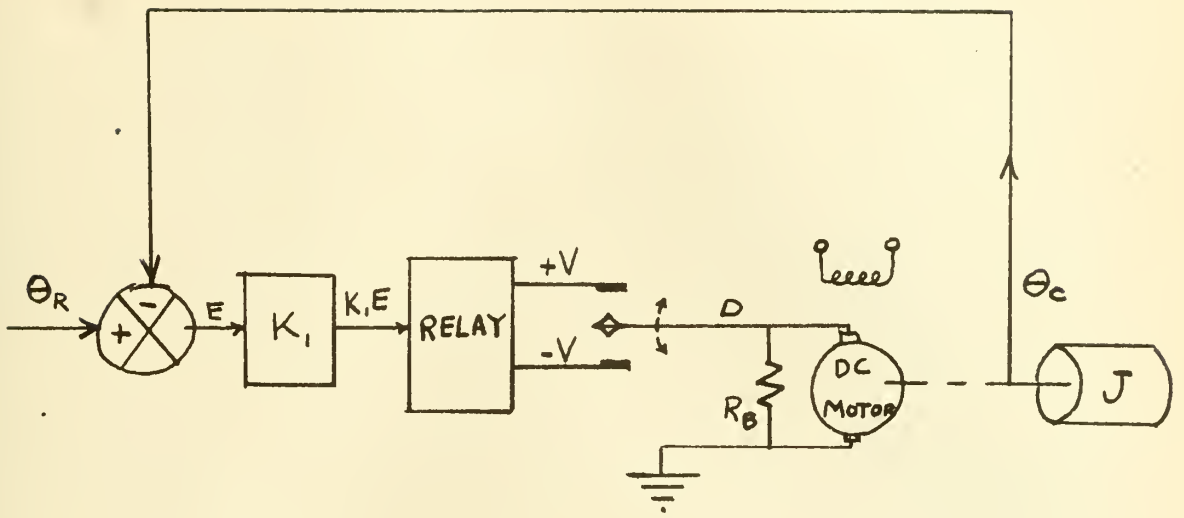

(a) NO DERIVATIVE DAMPING

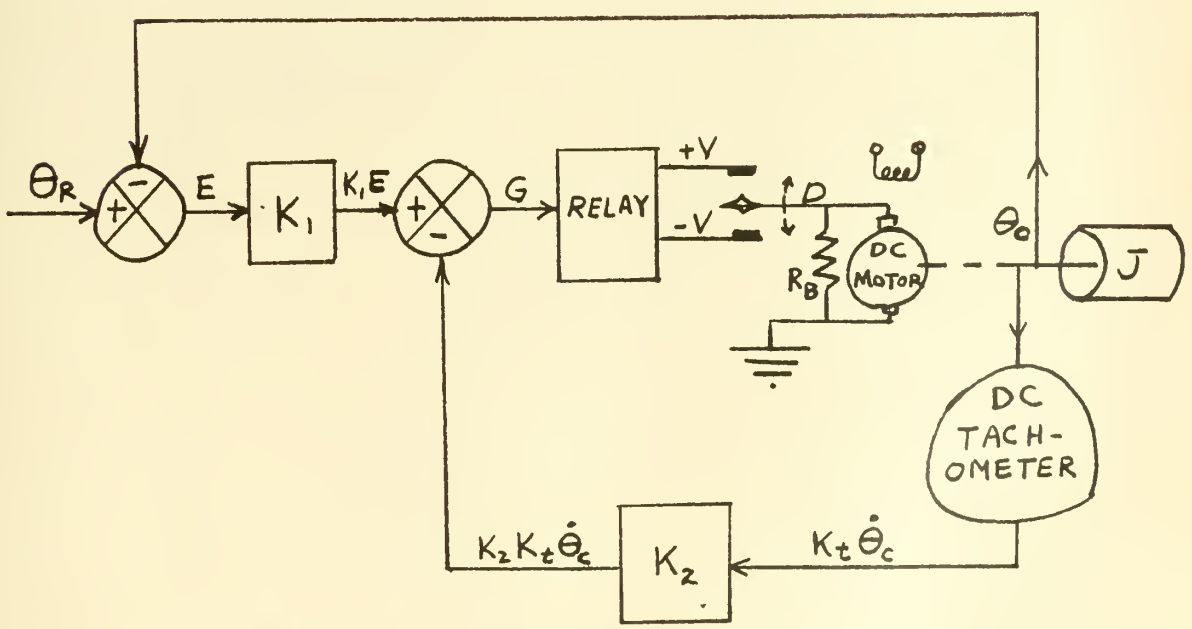

(b) WITH DERIVATIVE DAMPING

FIGURE 21. SCHEMATIC DIAGRAM OF SIMPLE RELAY SERVO WITH DYNAMIC BRAKING.

contacts are adequate for the additional current flow. The proposed system should be designed with as little viscous and Coulomb friction as possible, so that there is minimum opposition to motion during the acceleration period. Thus, when the relay is closed the damping forces are due to the motor's counter electromotive force and any inherent damping force in the system, such as mechanical friction, windage, and so on. When the relay opens generator action drives current through R_B, resulting in dynamic braking which will tend to stabilize the system.

The effect of dynamic braking on a simple relay servo system will be analyzed below, using the phase-plane method. First, a servo system with viscous damping will be analyzed and then one with Coulomb friction. In each case the effects of derivative damping and unsymmetrical relay characteristics will be considered.

a. Dynamic braking plus viscous friction. Consider now the servo illustrated in Figure 21(a) with a finite amount of inherent viscous friction. As before, consider that the output shaft is at an arbitrary zero position when t= 0, so that a positive step input, θ_{R_o}, is identically the initial error E_o. At time t = 0 the step input is applied, the relay closes, and the following equations apply during the acceleration interval(inductance of motor is considered negligible):

$$J\ddot{E} + f\dot{E} = -T = -K_T i \tag{75}$$

$$V = iR + K_v\dot{\theta}_c = iR - K_v\dot{E} \tag{76}$$

Combining (75) and (76) $$J\ddot{E} + \left(f + \frac{K_v K_T}{R}\right)\dot{E} = -\frac{K_T V}{R} \tag{77}$$

Manipulating (77) into the form applicable to the phase-plane

$$\frac{\ddot{E}}{\dot{E}} = \frac{d\dot{E}}{dE} = \left(-\frac{f}{J} - \frac{K_T K_v}{JR}\right) - \frac{K_T V}{JR\dot{E}} \tag{78}$$

For the relay with equal pull-in and drop-out voltages and with no derivative damping, the relay opens when the error is E_n and the following equations describe the system

$$J\ddot{E} + f\dot{E} - T_B = 0 \tag{79}$$

$$T_B = K_T i_B \tag{80}$$

$$0 = i_B(R + R_B) - K_v\dot{E} \tag{81}$$

where T_B is the braking torque due to generator action, and

i_B is the armature current during dynamic braking.

Combining (79), (80) and (81) $$J\ddot{E} + \left[f + \frac{K_T K_v}{(R + R_B)}\right]\dot{E} = 0 \tag{82}$$

Manipulating (82) $$\frac{\ddot{E}}{\dot{E}} = \frac{d\dot{E}}{dE} = -\left[\frac{f}{J} + \frac{K_T K_v}{J(R + R_B)}\right] \tag{83}$$

Equation (83) shows that, in the phase-plane plot, the trajectory of the servo in the dead zone is a straight line of negative slope fixed by the system parameters (including R_B). Note that when $R_B = \infty$, i.e., no dynamic braking, the entire damping action in the dead zone is due to viscous friction; this special case was illustrated in Figure 12. For finite dead zone widths the system with only inherent viscous damping would be oscillatory in the steady state, Figure 22(a). From equation (83) it is seen that the effect of adding the dynamic braking resistor is to increase the viscous damping during dead zone transit, resulting in a greater decrease in output velocity. Such a system

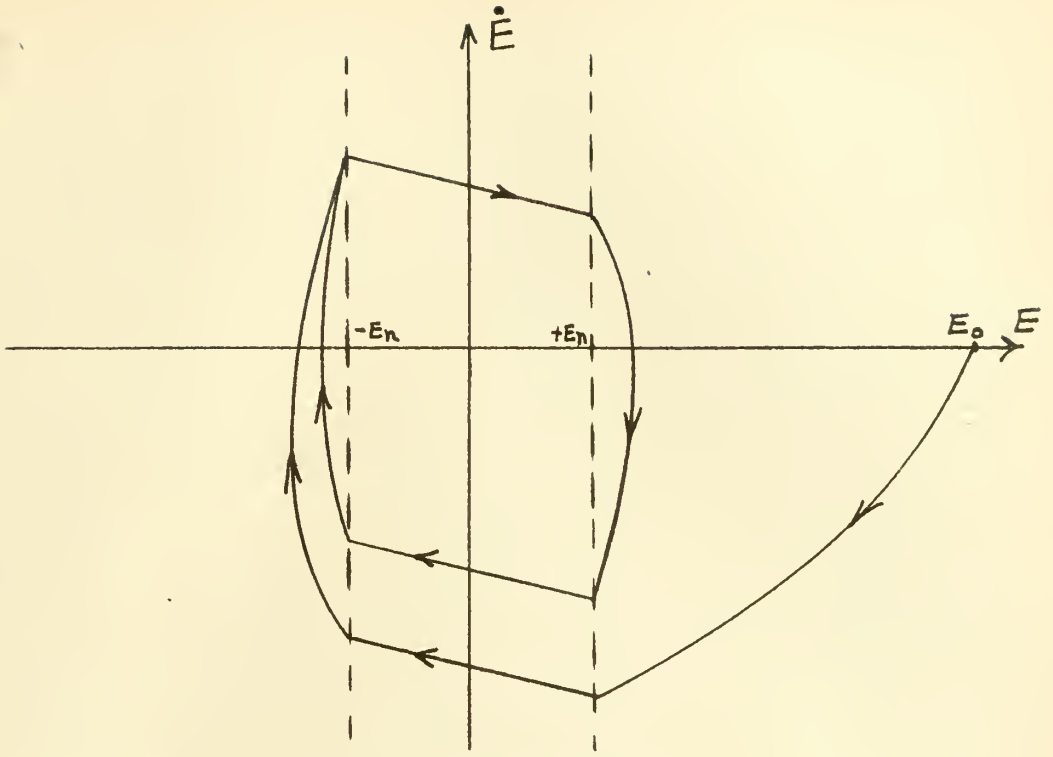

(a) ONLY VISCOUS DAMPING IN DEAD ZONE

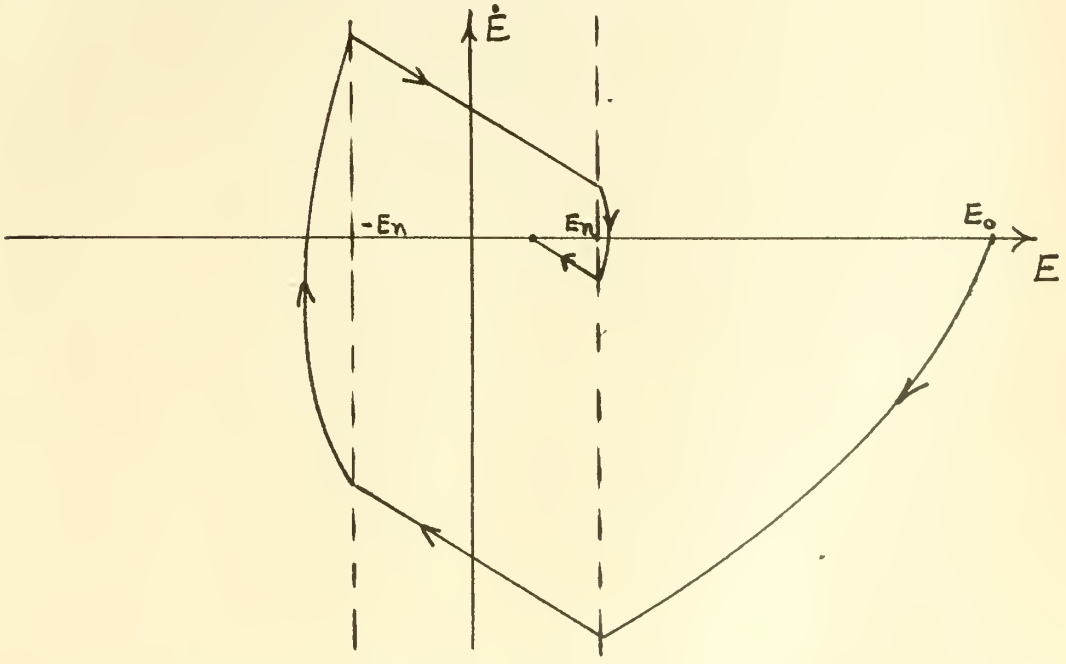

(b) DYNAMIC BRAKING AND VISCOUS DAMPING IN DEAD ZONE

FIGURE 22. PHASE PLANE PLOT OF RELAY SERVO WITH VISCOUS DAMPING AND DYNAMIC BRAKING IN DEAD ZONE.

would probably come to rest in the dead zone after several overshoots, depending on the size of R_B and the width of the dead zone; see Figure 22(b).

In Chapter I, section 5(b), it was shown how the use of negative derivative damping (or tachometer feedback) causes the loci of relay reversals to be rotated in a counterclockwise manner. Figure 21(b) illustrates a simple relay servo with dynamic braking in the dead zone and utilizing derivative damping. Noting that both the error signal and the feedback signal pass through an amplifier, the equations of the loci of relay reversals are, for a step input,

$$K_1 E + K_2 K_t \dot{E} = \pm E_m \tag{84}$$

Equation (84) assumes equal relay pull-in and drop-out voltages. Figure 23(a) illustrates how the use of negative derivative damping can greatly enhance the system's stability and limit the number of overshoots.

From equation (84) it is seen that the slope of the relay switching locus is

$$\frac{d\dot{E}}{dE} = -\frac{K_1}{K_2 K_t} \tag{85}$$

By changing the ratio of K_1/K_2 the locus can be made to rotate to any desired slope. Equation (83) indicates the slope of the phase-plane trajectory in the dead zone. By adjusting K_1, K_2, or R_B the slope of relay switching and the system's dead zone trajectory can be made equal:

$$\frac{K_1}{K_2 K_t} = \frac{f}{J} + \frac{K_T K_U}{J(R + R_B)} \tag{86}$$

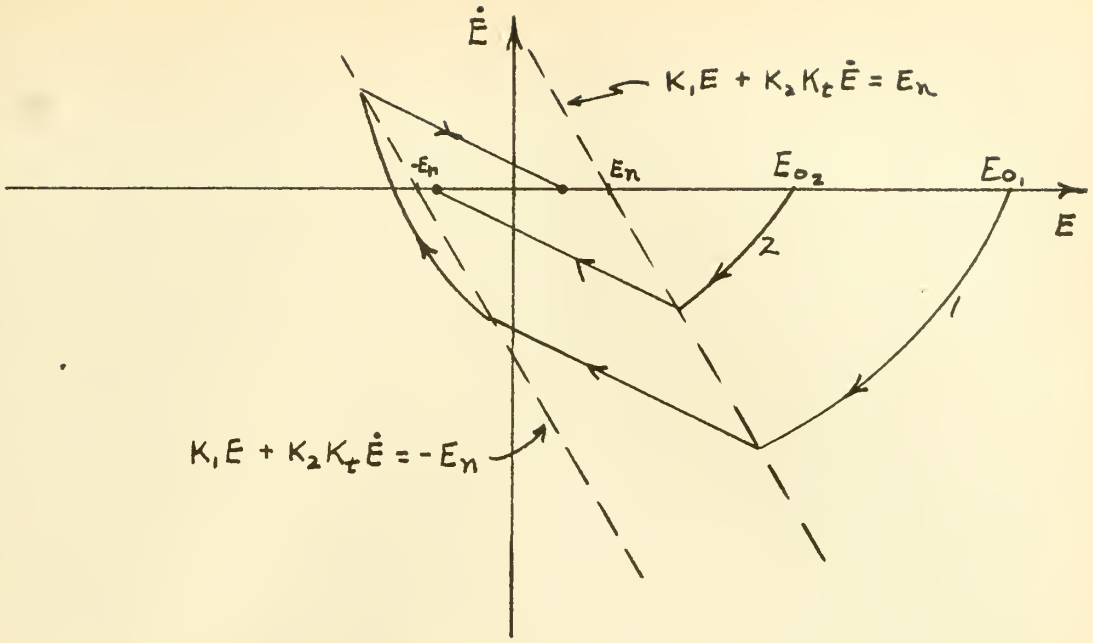

(a) LESS THAN OPTIMUM DERIVATIVE DAMPING

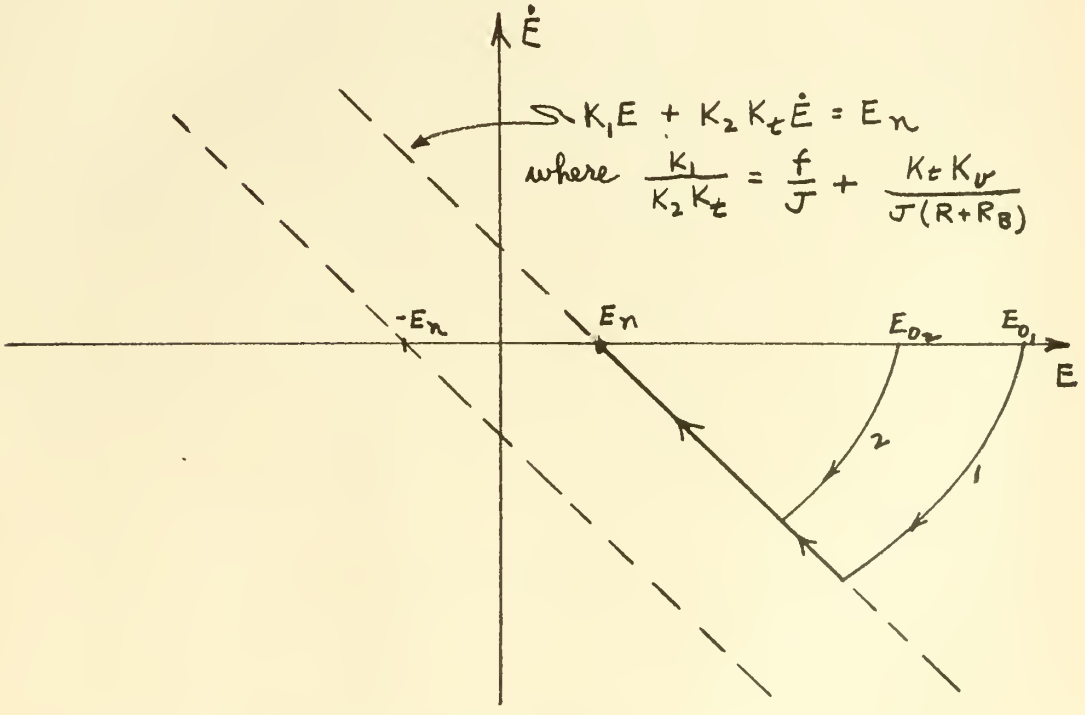

(b) OPTIMUM DERIVATIVE DAMPING

FIGURE 23. PHASE PLANE PLOT OF RELAY SERVO WITH VISCOUS & DERIVATIVE DAMPING AND DYNAMIC BRAKING IN THE DEAD ZONE.

When equation (86) is valid, it is seen that the phase-plane trajectory runs along the switching locus as illustrated in Figure 23(b). Thus the proper amount of derivative damping, for a given R_B, results in a nearly optimum servo system in the sense that full accelerating torque is applied until the error and error-rate reach a predetermined value, then the relay opens and the system is braked, dynamically, to a stop with no overshoot. From Figure 23(b) it is seen that the trajectory stays on the edge of the dead zone, and therefore the dead zone may be reduced to zero width without affecting the dynamic performance, thereby reducing the static error to zero (assuming there is neither Coulomb nor sticking friction). The time of response of such a system would be comparable to, but slightly more than, the optimum system employing a practical d-c motor, section 1(b).

Figure 24 illustrates a system employing a relay with unequal pull-in and drop-out voltages. Figure 24(a) illustrates the response when the optimum amount of derivative damping is realized. Figure 24(b) illustrates the interesting case where too much derivative damping is employed resulting in a series of step corrections in the same direction. If too much derivative damping were employed in the system with a relay possessing equal pull-in and drop-out voltages an infinite number of such steps would result, theoretically (instantaneous switching has been assumed).

b. Dynamic braking plus Coulomb friction. The effect of Coulomb damping on a relay servo utilizing dynamic braking in the dead zone will now be considered. For simplicity, viscous friction, f, will be considered negligible since the effect of dynamic braking is the same as that of viscous damping.

Consider first the effect in the dead zone of Coulomb friction, C,

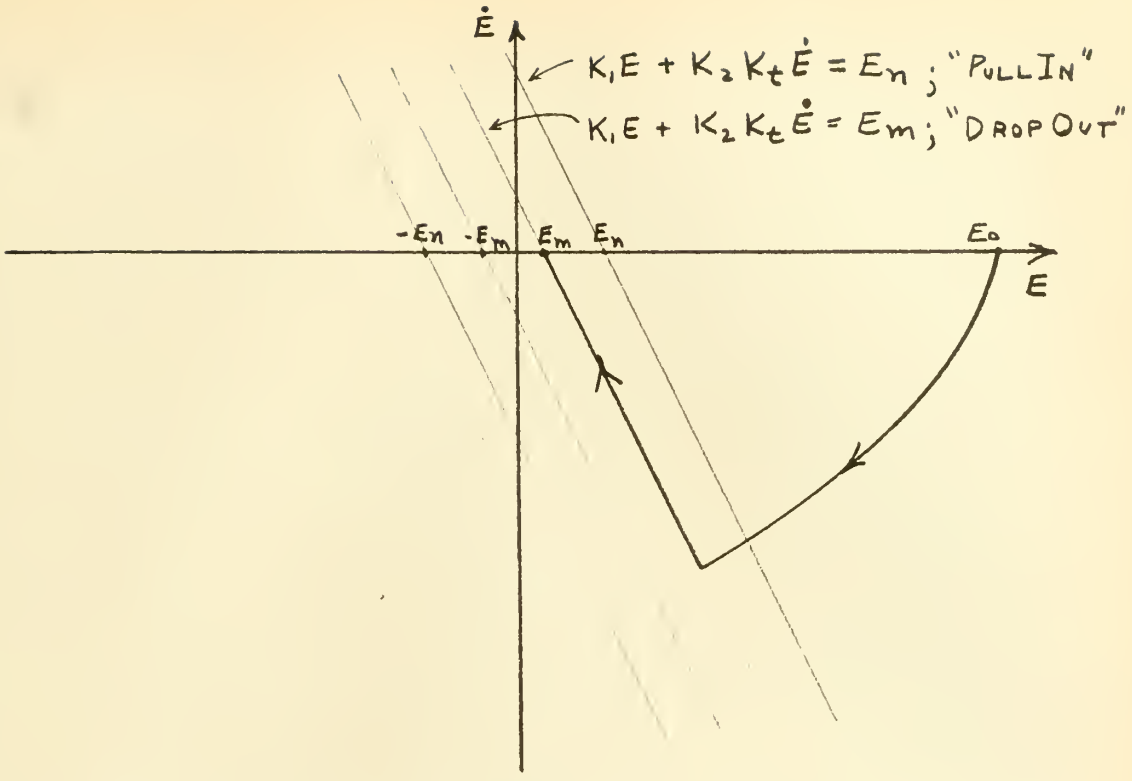

(a) OPTIMUM DERIVATIVE DAMPING

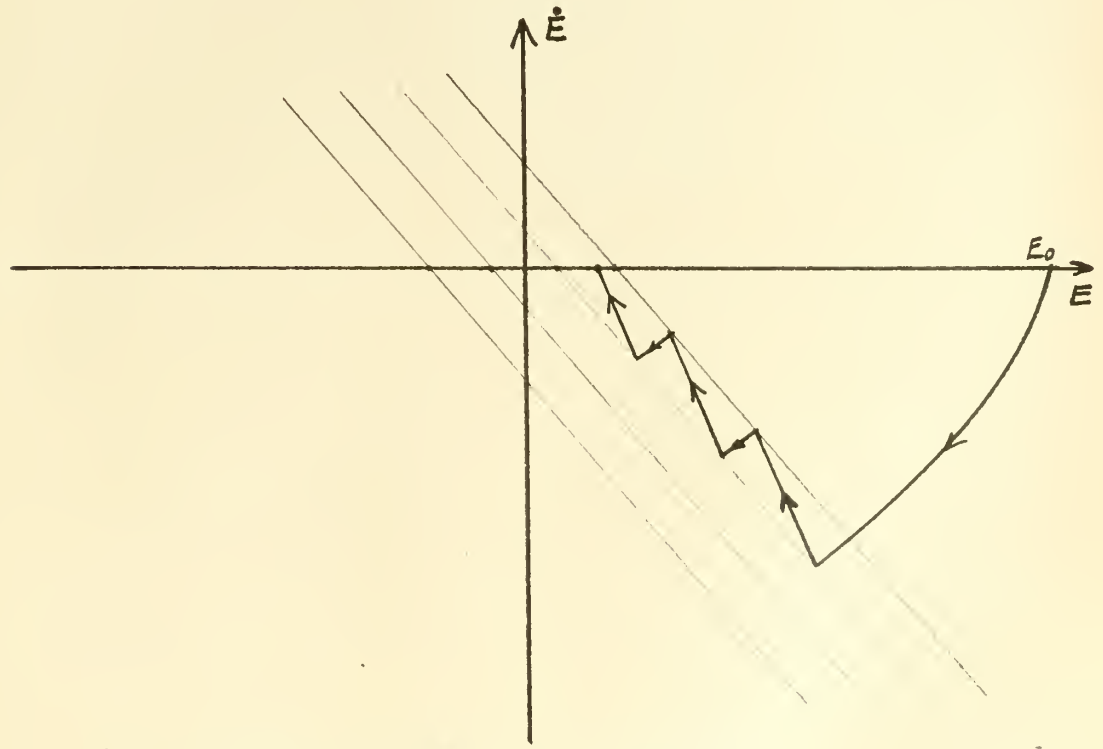

(b) MORE THAN OPTIMUM DERIVATIVE DAMPING

FIGURE 24. PHASE PLANE PLOT OF RELAY SERVO WITH VISCOUS & DERIVATIVE DAMPING AND DYNAMIC BRAKING IN DEAD ZONE; RELAY PULL-IN AND DROP-OUT VOLTAGES DIFFERENT.

when dynamic braking is not employed, i.e., $R_B = \infty$. The describing equation is

$$J\ddot{E} + C = 0 \tag{87}$$

Manipulating (87) $$\frac{\ddot{E}}{\dot{E}} = \frac{d\dot{E}}{dE} = -\frac{C/J}{\dot{E}} \tag{88}$$

Equation (88) indicates that the isoclines are straight lines parallel to the E-axis. It is seen also that the slope markers are vertical when $\dot{E} = 0$, and approach the horizontal as the magnitude of $\dot{E}$ becomes large with respect to the C/J ratio. Figure 25(a) is a representative sketch of the system's trajectories in the dead zone. Figure 25(b) illustrates the effect of adding derivative damping to this case. It is readily seen that the Coulomb damping becomes more effective as the magnitude of $\dot{E}$ decreases to zero. It may also be seen that no single value of derivative damping can give deadbeat [1] performance for various sizes of initial error, unless the dead zone is quite large.

Consider now the effect of both Coulomb damping and dynamic braking in the dead zone. The describing equations are

$$J\ddot{E} + C - T_B = 0 \tag{89}$$

$$T_B = K_T i_B \tag{80}$$

$$0 = i_B(R + R_B) - K_V \dot{E} \tag{81}$$

Combining (80), (81), and (89) $$J\ddot{E} + C - \frac{K_T K_V}{(R+R_B)}\dot{E} = 0 \tag{90}$$

1 Herein "to deadbeat" shall mean to reduce an error to within dead zone limits without overshoot.

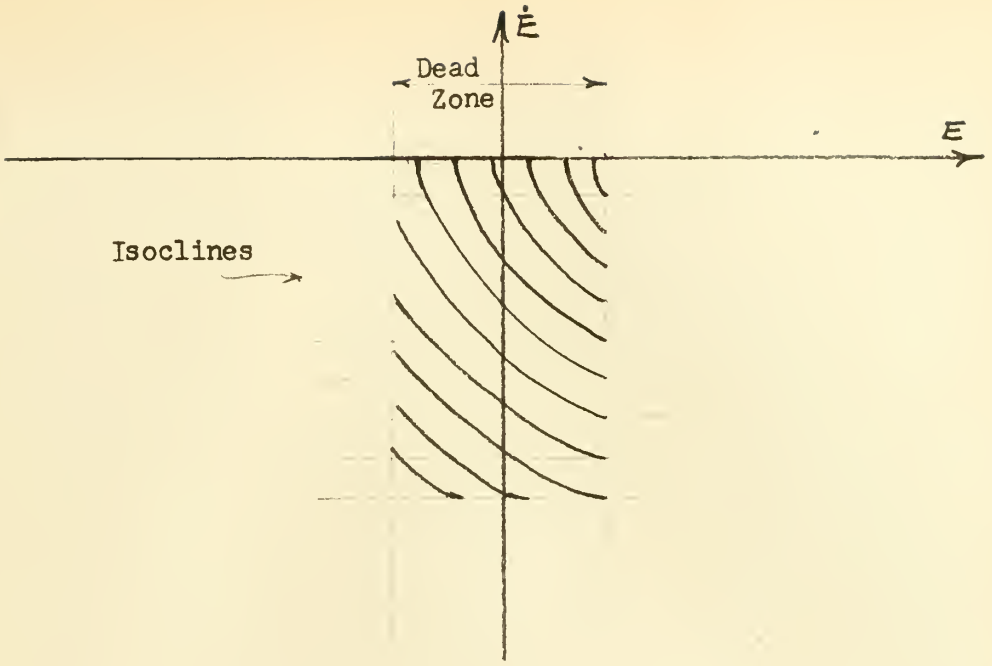

(a) NO DERIVATIVE DAMPING

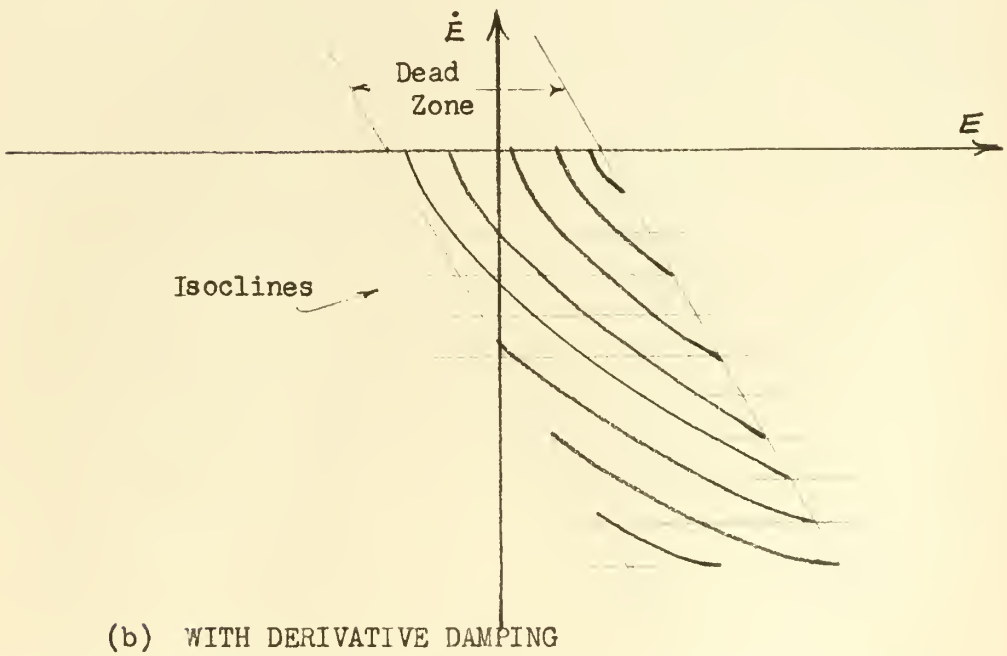

(b) WITH DERIVATIVE DAMPING

FIGURE 25. PHASE PLANE PLOT OF RELAY SERVO RESPONSE IN DEAD ZONE WITH COULOMB DAMPING.

Manipulating (90) $$\frac{\ddot{E}}{\dot{E}} = \frac{d\dot{E}}{dE} = -\frac{C/J}{\dot{E}} - \frac{K_T K_V}{J(R+R_B)} \qquad (91)$$

It is seen from equation (91) that the effect of using the dynamic braking resistor, R_B, is to add viscous damping in the dead zone (the same as in section 2(a) above). Again the isoclines are straight lines; and as $\dot{E}$ approaches zero the slope approaches infinity. However, when $\dot{E}$ becomes very large the slope does not approach zero as in the Coulomb damping only case above, but approaches a fixed negative slope dictated by R_B and the system parameters. Thus, three cases may be defined for a given machine:

(1) When C/J is very small; there is deceleration due to pure viscous damping until $\dot{E}$ is almost zero when a Coulomb damping effect occurs causing the phase-plane trajectory to swing to the vertical.

(2) When $\frac{C/J}{\dot{E}} \gg \frac{K_T K_V}{J(R+R_B)}$; deceleration due to almost pure Coulomb damping.

(3) Intermediate to (1) and (2); deceleration due to dynamic braking when $\dot{E}$ is large, and due to Coulomb damping when $\dot{E}$ becomes small.

Figure 26 illustrates these three cases for a specific position error, Eo.

From Figure 26 it may be seen that, when any amount of Coulomb friction is present, there is no possibility of attaining deadbeat performance with a zero width dead zone as suggested in 2(a) above. When case (1) exists, however, a fairly small dead zone can produce deadbeat performance, Figure 27(a). When a relay having different pull-in and

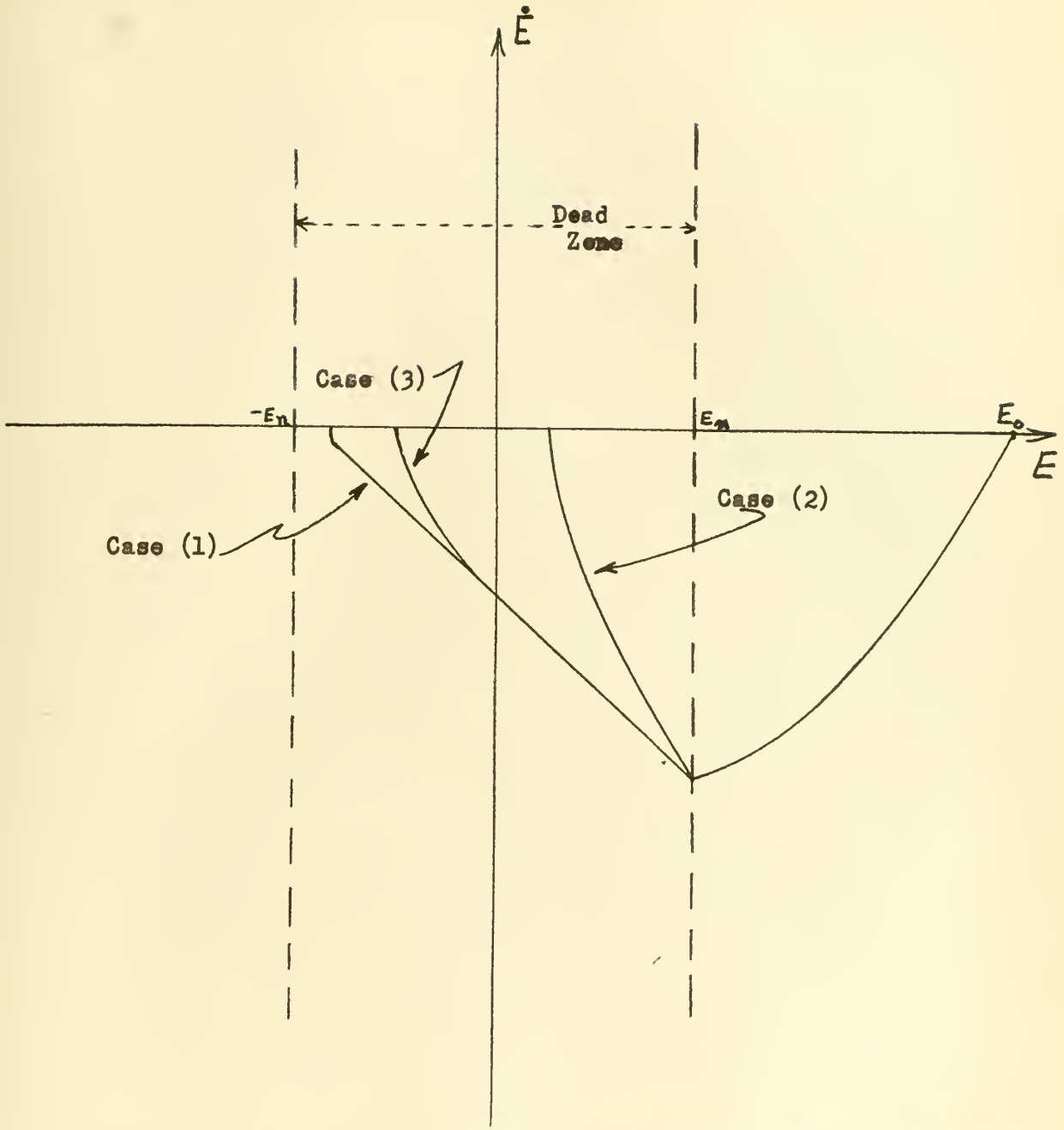

FIGURE 26 PHASE PLANE PLOT OF RELAY SERVO WITH DYNAMIC BRAKING AND COULOMB DAMPING.

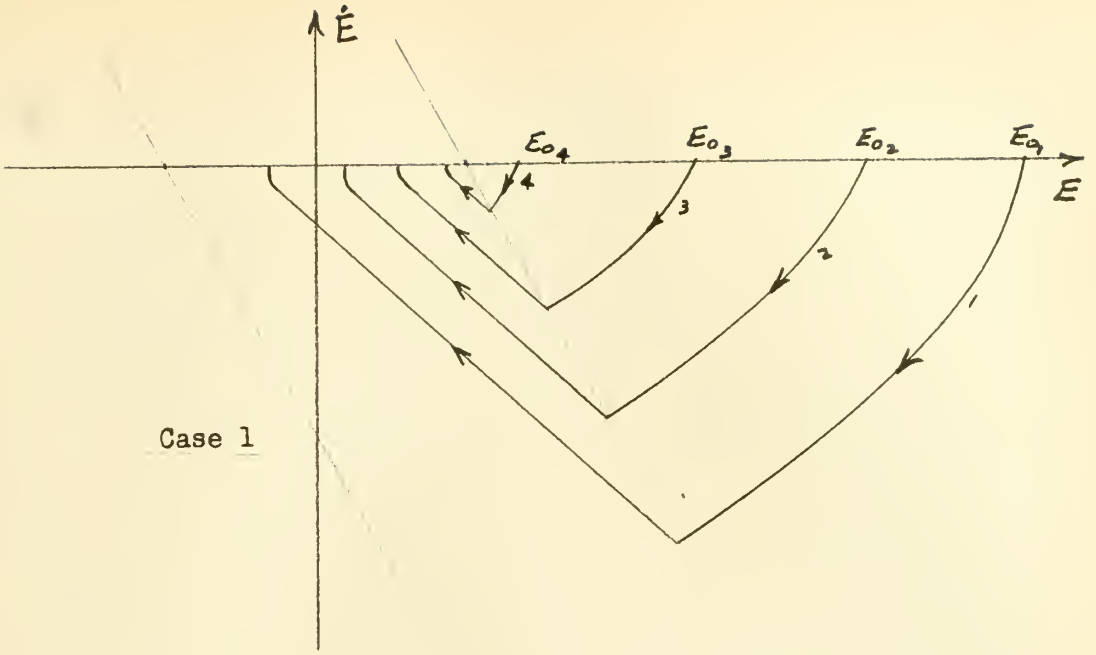

(a) PULL -IN AND DROP-OUT VOLTAGES EQUAL

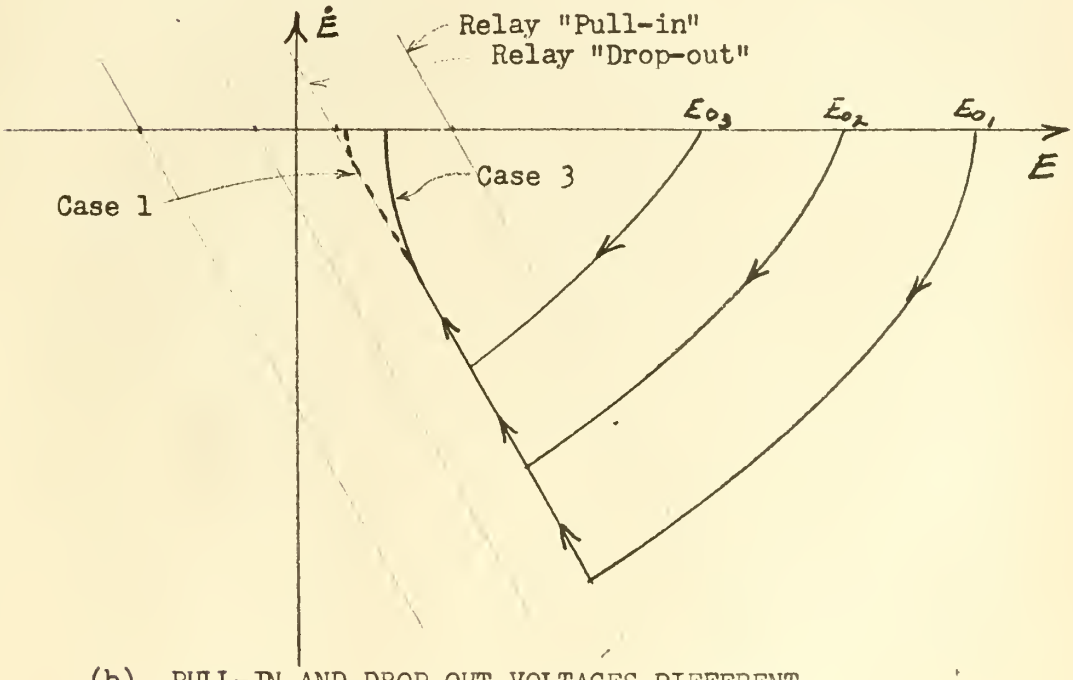

(b) PULL-IN AND DROP-OUT VOLTAGES DIFFERENT

FIGURE 27. PHASE PLANE PLOT OF RELAY SERVO WITH COULOMB & DERIVATIVE DAMPING, AND DYNAMIC BRAKING IN DEAD ZONE.

drop-out voltages is employed, both case (1) and case (3) (depending on magnitude of C and magnitudes of relay switching voltages) can produce deadbeat performance, Figure 27(b). However, the more the case (3) servo system departs from the case (1), the wider the dead zone must be, decreasing the static accuracy.

CHAPTER IV

EXPERIMENTAL RESULTS

In order to verify the theory and to demonstrate the practicality of employing dynamic braking to deadbeat relay servos, tests were conducted on two laboratory set-ups. Both set-ups were similar to the servo illustrated in Figure 21(b). In the first set-up a 1/125 HP Elinco servomotor was used as the driving unit. It was found that the Coulomb damping far surpassed the effect of dynamic braking no matter how small R_B was made; the response with dynamic braking employed was slightly faster than the response when only derivative damping was employed.

In search of a d-c motor with a small Coulomb damping effect, retardation tests were conducted on a 1/8 HP and a 1 HP motor. The 1 HP motor proved to be satisfactory and it replaced the 1/125 HP motor in the lab set-up. Tests using this set-up conclusively verified the theory and illustrated the feasibility of the proposed system. By use of dynamic braking the servo system could be made deadbeat, with a small static error and a very fast response, whereas it was absolutely unstable when only derivative damping was employed.

1. The 1/125 HP Servo System.

Figure 28 is a schematic diagram of the relay servo system employing the 1/125 HP servomotor. Data on the various components appear in Appendix A.

Referring to Figure 2(c), the characteristics of the Sigma relay were as follows

$$E_n = \pm 6.20 \text{ volts}$$
$$E_m = \pm 1.36 \text{ volts}$$

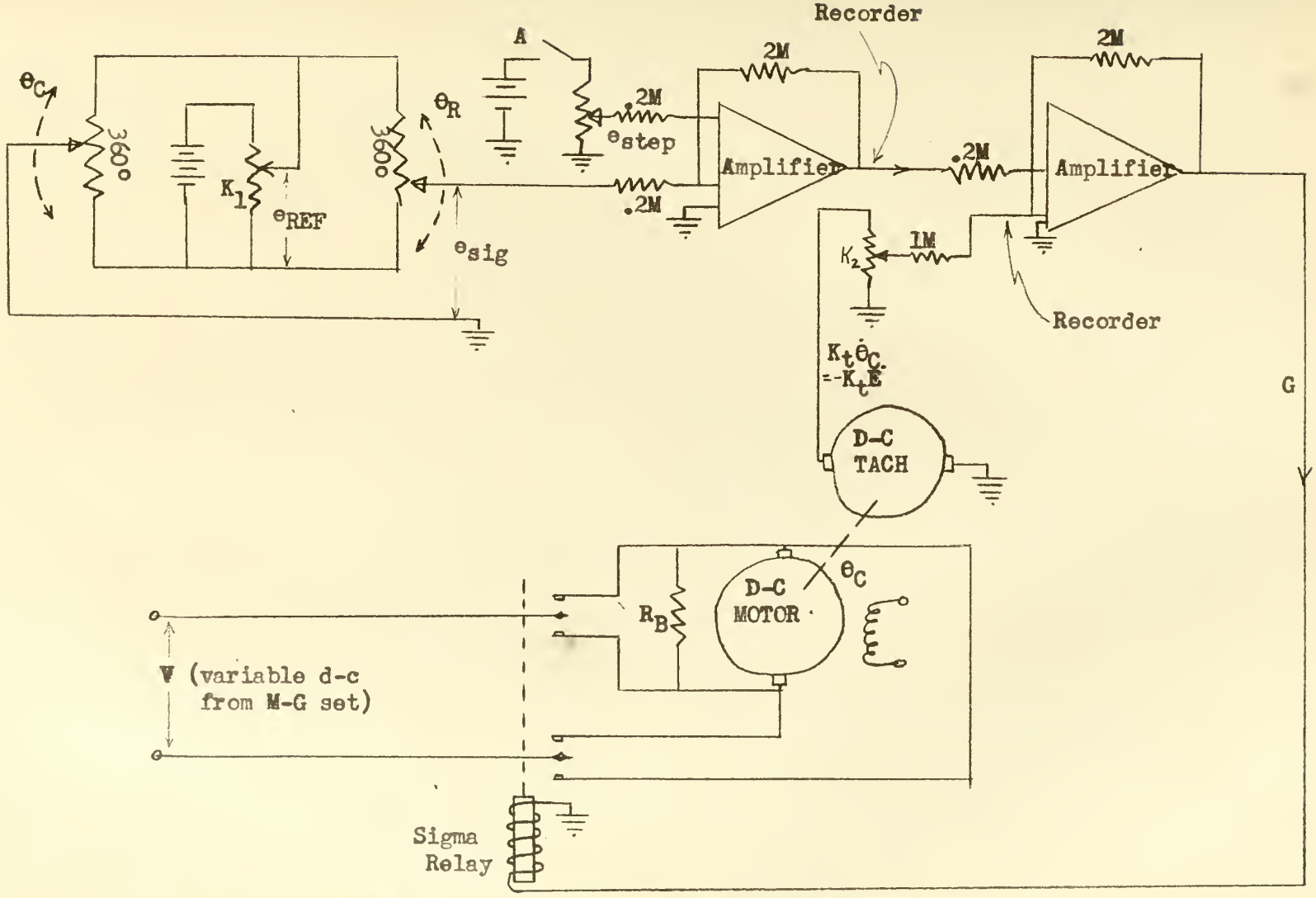

FIGURE 28. SCHEMATIC DIAGRAM OF THE 1/125 HP RELAY SERVO SYSTEM

The width of the dead zone was varied by changing the reference voltage across the output (and input) potentiometers. For a sample calculation of dead zone width refer to Appendix B.

Note that the Boeing d-c amplifiers served as both amplifier and adder.

To obtain a step input error, a separate step of voltage was sent to the first amplifier rather than offsetting the input shaft. This was done in order that the Brush recorder pen would already be indicating the step of error at time t = 0, thus eliminating any error in the data due to the recorder pen inertia. Thus when switch A was closed the system would drive the output shaft to the position which cancelled out the apparent error. So that the error could be recorded separately, two adder-amplifiers were required as shown in Figure 28.

Data for the test runs conducted on this set-up appear in Appendix C.

Figure 29 illustrates the response to a 25 degree step error when no dynamic braking is employed in the dead zone compared to the response when dynamic braking is employed. No tach feedback was used. Note the following:

(a) The no dynamic braking run is oscillatory.

(b) Dead zone trajectory is curved in both cases, but approaches the vertical faster for the dynamic braking case; thus this servo set-up is a good example of case 2 of Figure 26.

(c) The point of relay opening is not at E_m due to relay time lag.

Figure 30 illustrates the transient response of the two test runs of Figure 29, as recorded by the Brush recorder.

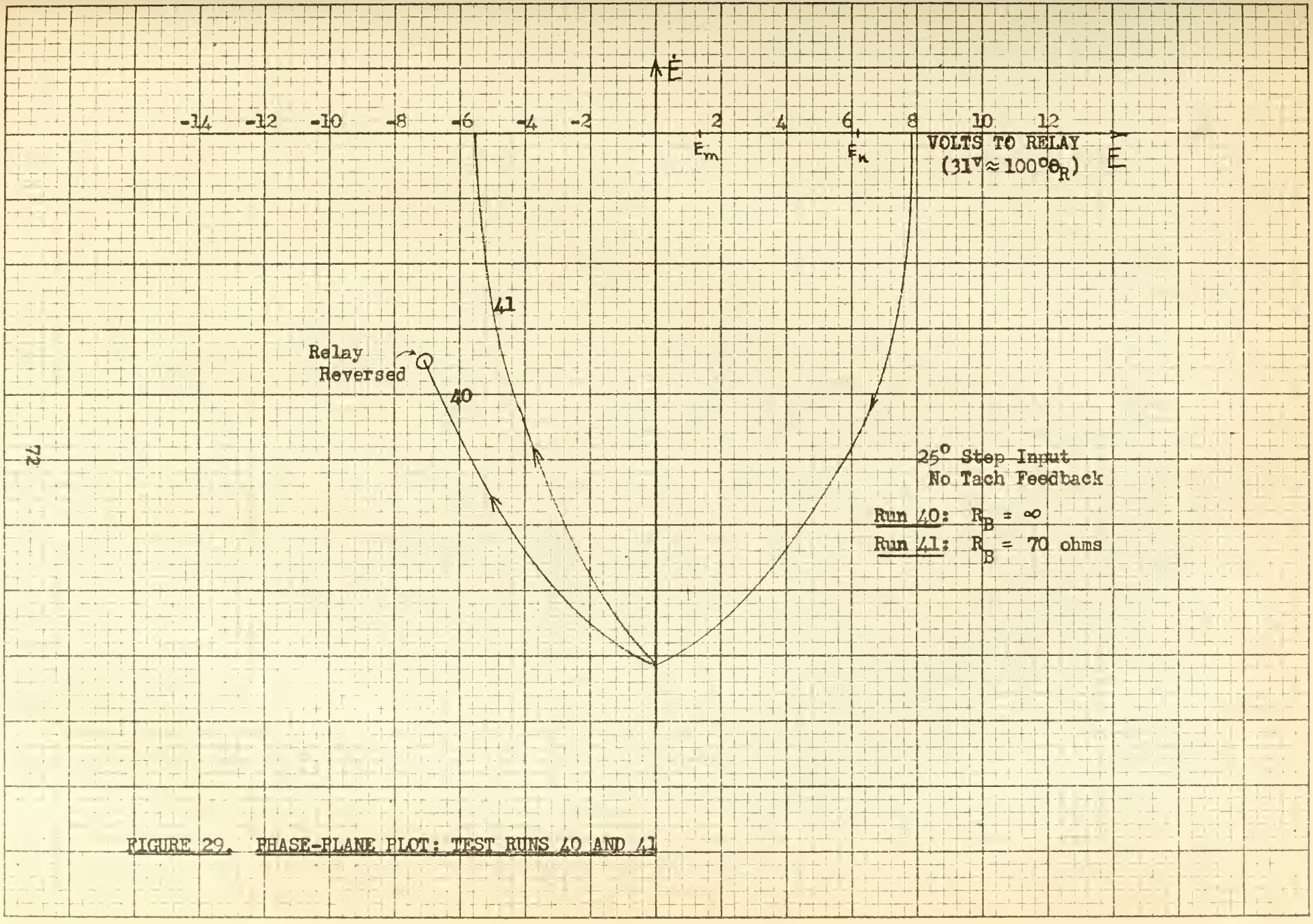

FIGURE 29. PHASE-PLANE PLOT: TEST RUNS 40 AND 41

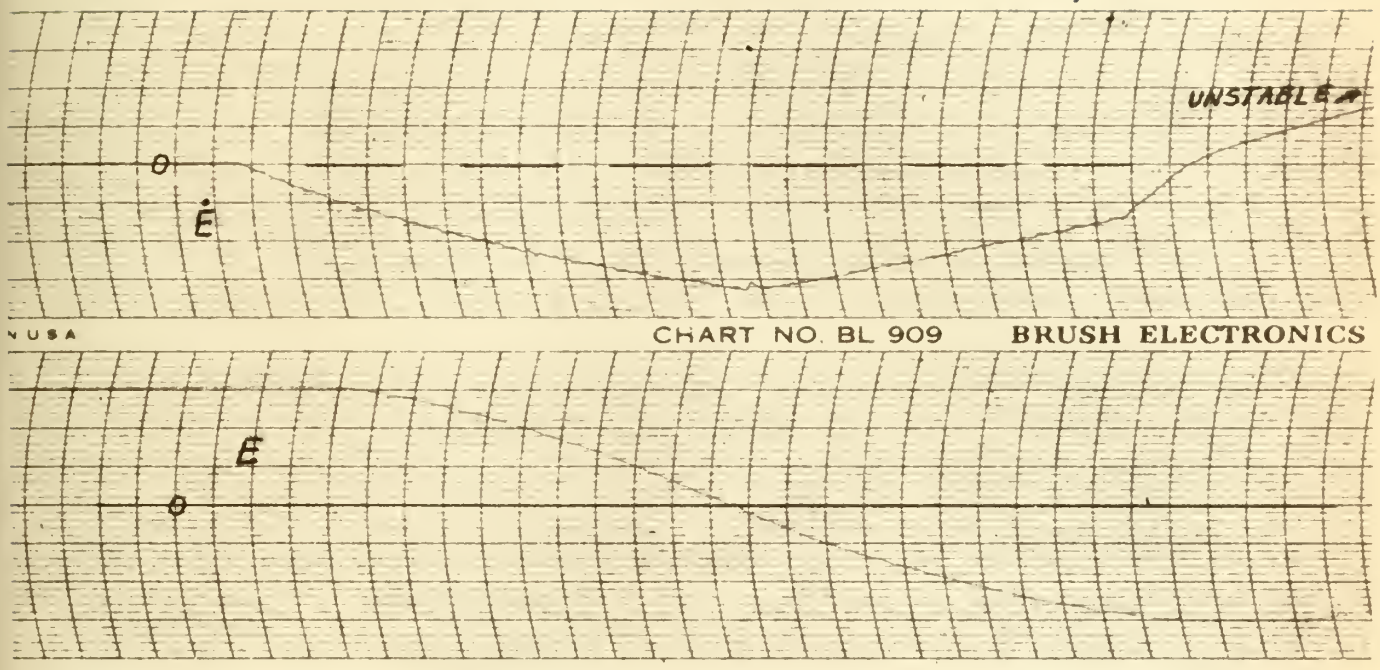

Run 40. 25° Step, No Dynamic Braking, No Tach Feedback

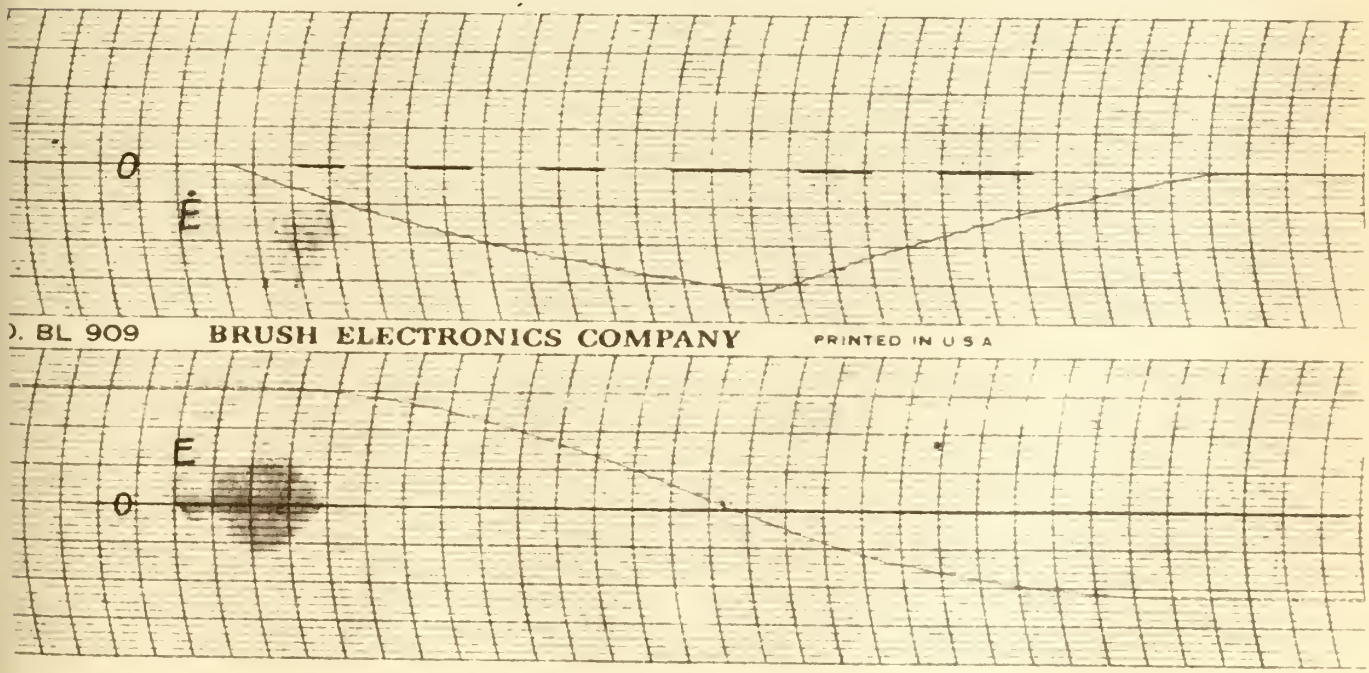

Run 41. 25° Step, R_B 70 ohms, No Tach Feedback

FIGURE 30. TRANSIENT RESPONSE, RUNS 40 AND 41 (RECORDER TAPE)

Figure 31 illustrates the response to the same two conditions imposed in Figure 29, except that a small amount of negative tach feedback is employed. In this case both test runs are deadbeat, but the dynamic braking case has less static error. Figure 32 illustrates the transient response for these two runs and shows that the dynamic braking case not only had less static error but responded 19% faster.

Figure 33 illustrates the oscillatory response to various step errors when no dynamic braking resistor is employed.

Figure 34 illustrates how the system becomes deadbeat when an R_B of 70 ohms is used. No tach feedback was used.

Figure 35 illustrates the response when the dynamic braking effect is increased by decreasing R_B. The step error is 40 degrees; no tach feedback was used.

Figure 36 illustrates how adding a small amount of tach feedback effects the conditions tested in Figure 35.

Figure 37 illustrates the response when considerable tach feedback is employed. The dynamic braking case was deadbeat, although the relay switching was too early, giving a large static error. The dynamic braking run stepped forward twice, as illustrated, ideally, in Figure 24(b).

2. Retardation Tests of the 1/8 and 1 HP Motors.

Retardation tests were run on two motors to simulate their response in the dead zone. Rated voltage was placed at the armature terminals until steady state velocity was reached and then the motors were dynamically braked to a stop using various values for R_B.

Figures 38 and 39 illustrate the retardation tests made on the 1/8 HP motor. Even when R_B was taken as low as 10 ohms (R was also

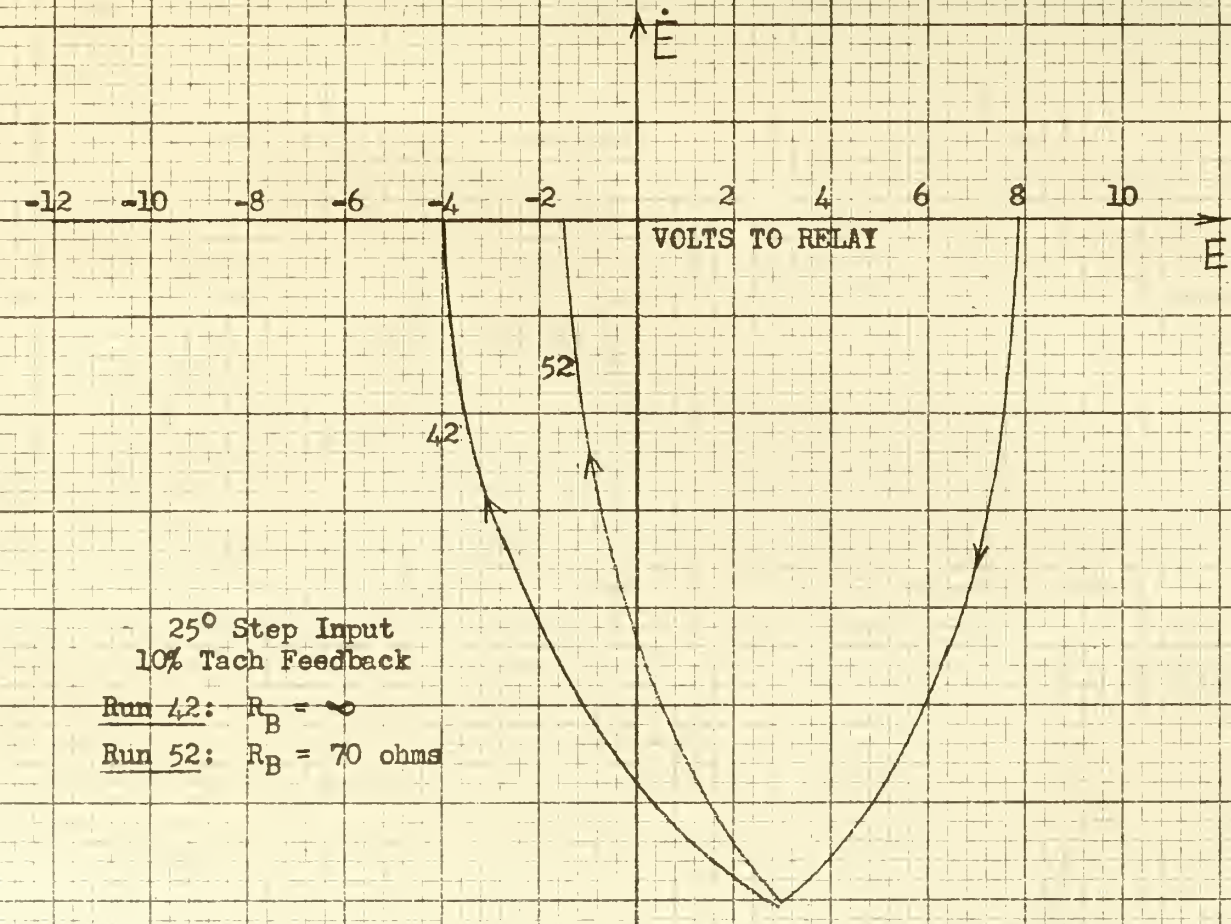

FIGURE 31. PHASE-PLANE PLOT: TEST RUNS 42 AND 52

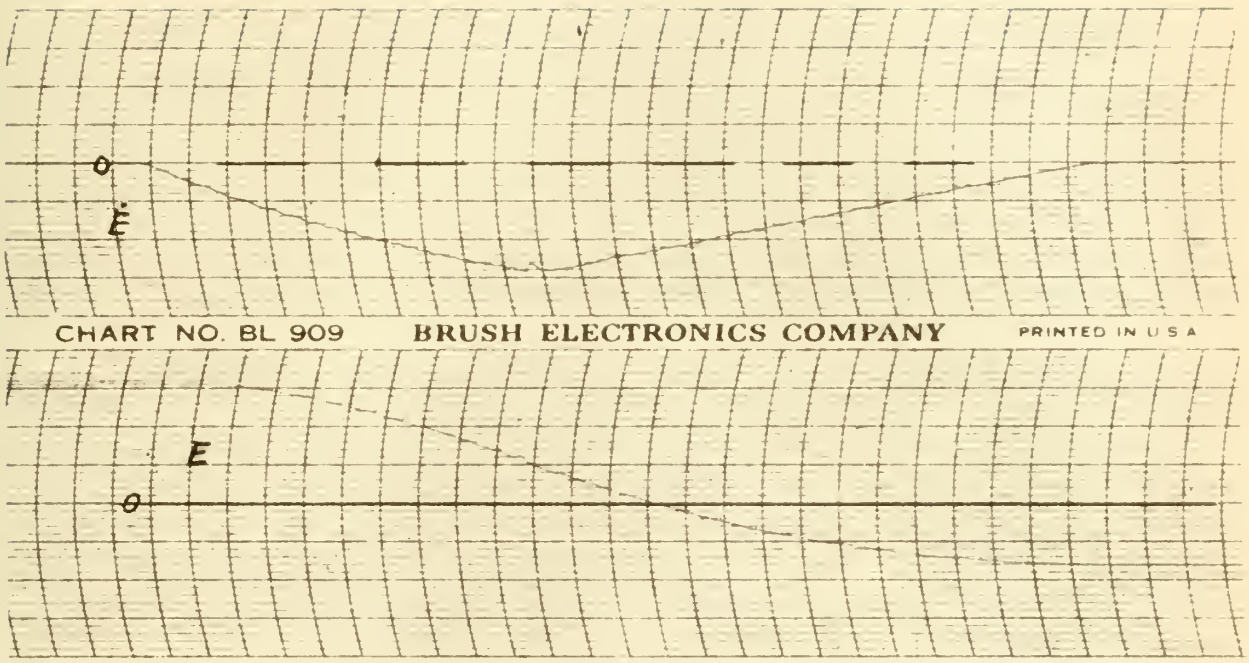

Run 42. 25° Step, No Dynamic Braking, 10% Tach Feedback

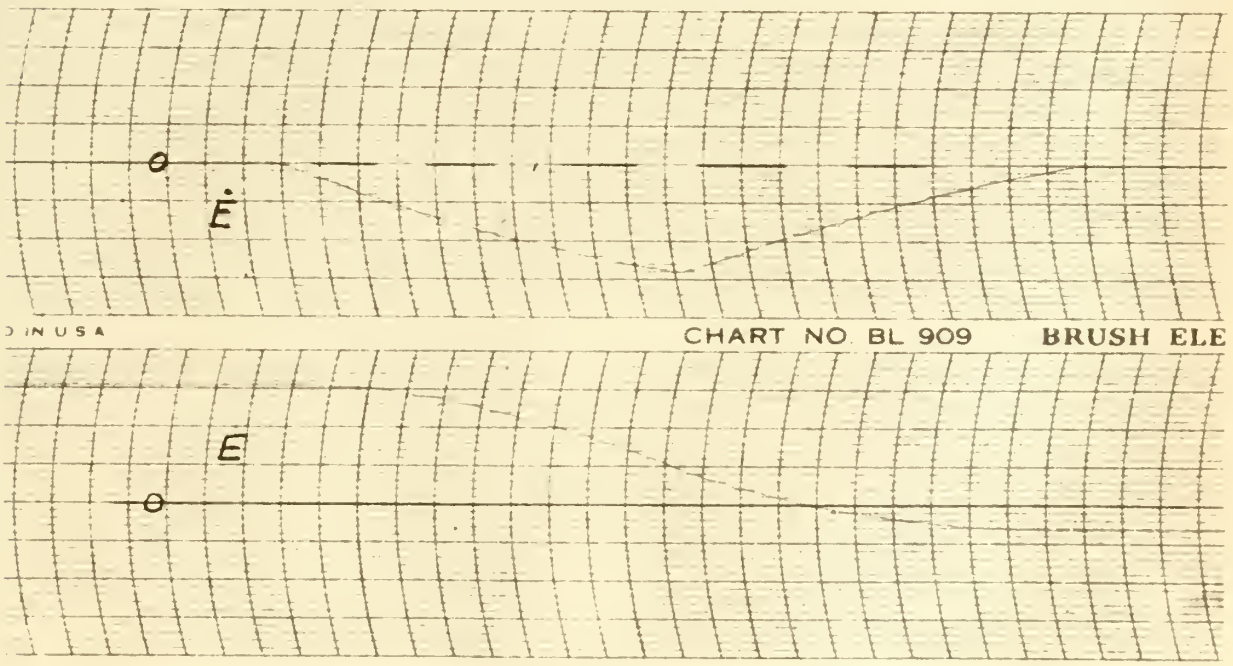

Run 52. 25° Step, R_B = 70 ohms, 10% Tach Feedback

FIGURE 32. TRANSIENT RESPONSE, RUNS 42 AND 52 (RECORDER TAPE)

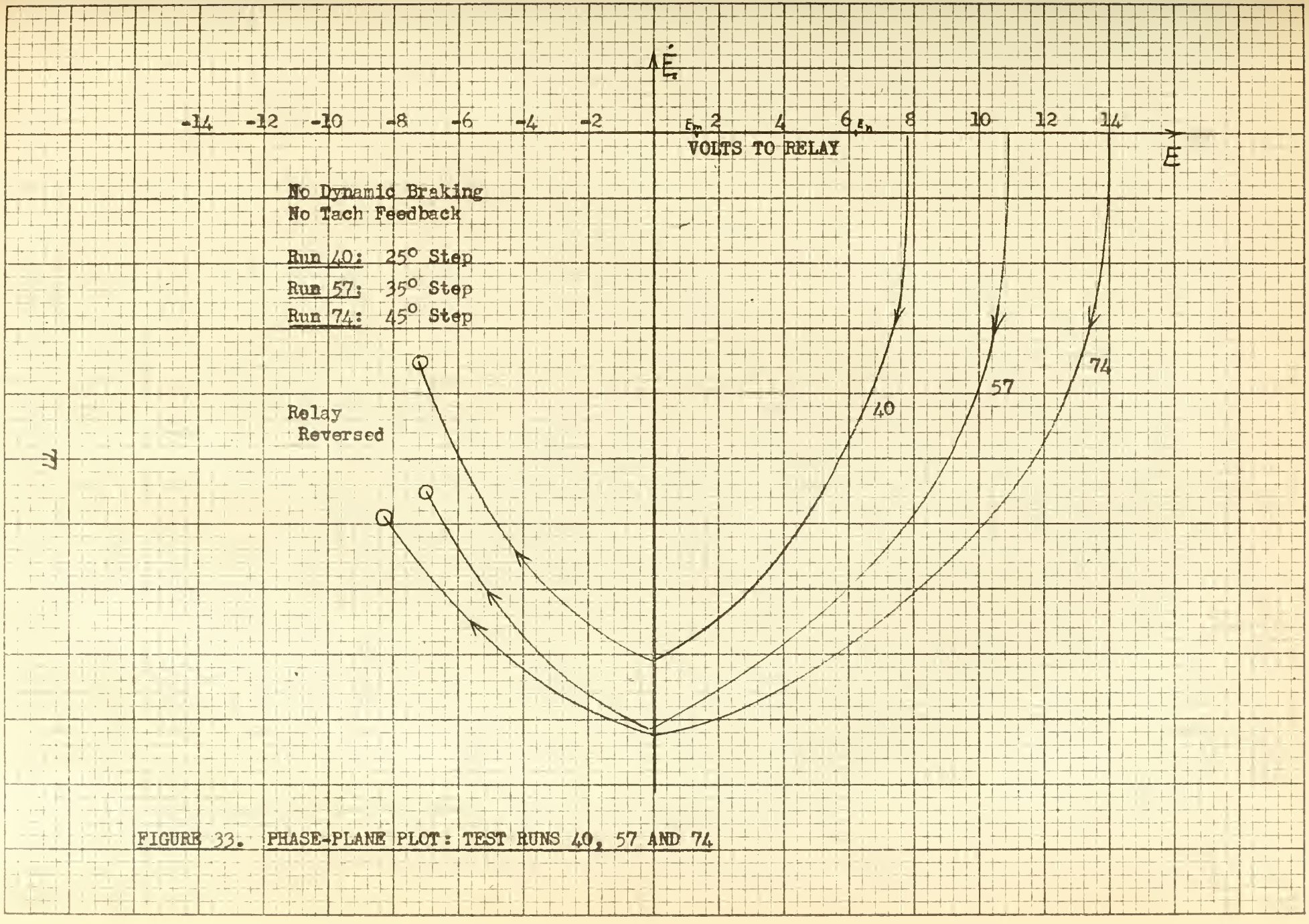

FIGURE 33. PHASE-PLANE PLOT: TEST RUNS 40, 57 AND 74

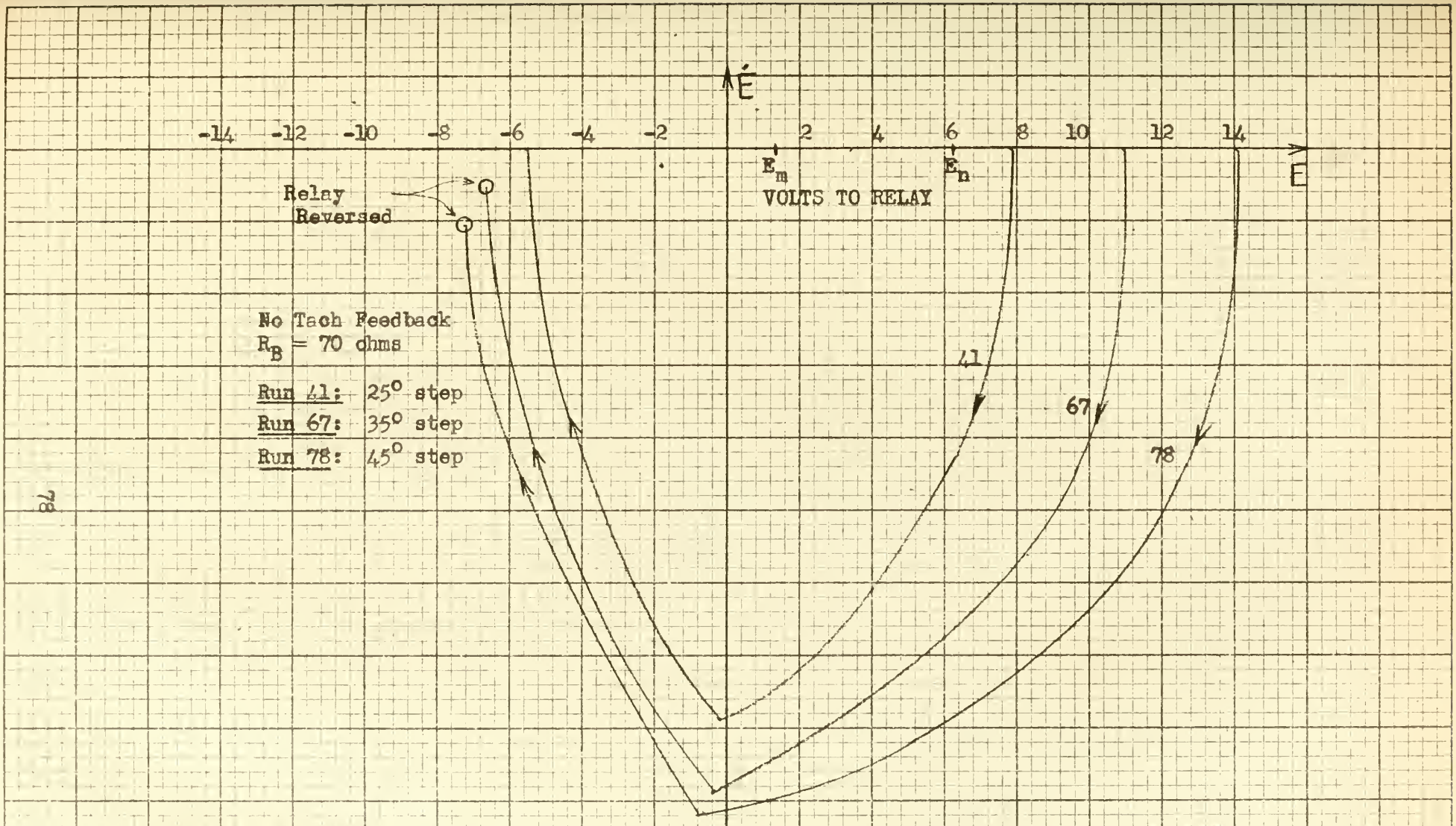

FIGURE 34. PHASE-PLANE PLOT: TEST RUNS 41, 67 AND 78

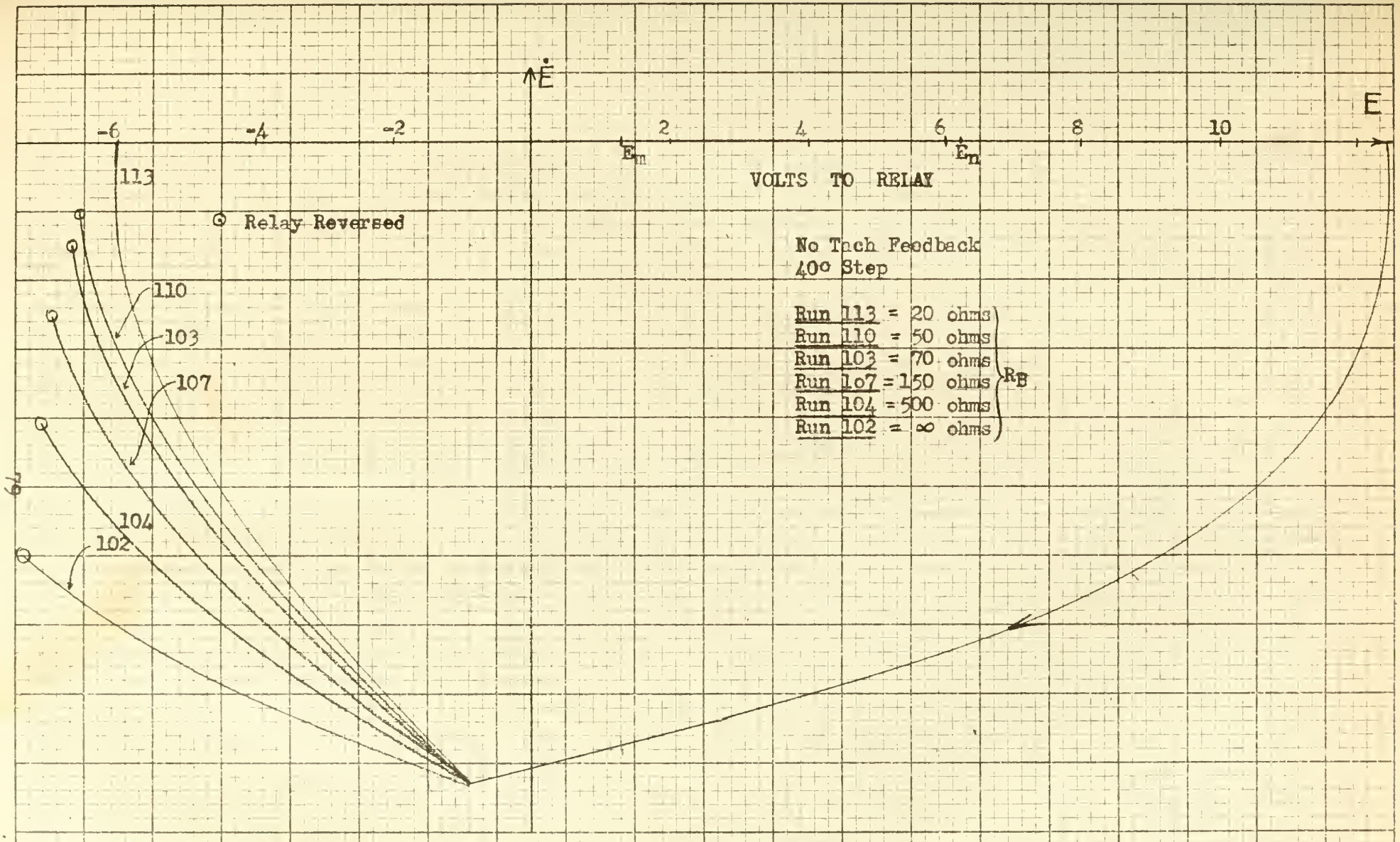

FIGURE 35. PHASE-PLANE PLOT: TEST RUNS 102, 103, 104, 107, 110 AND 113

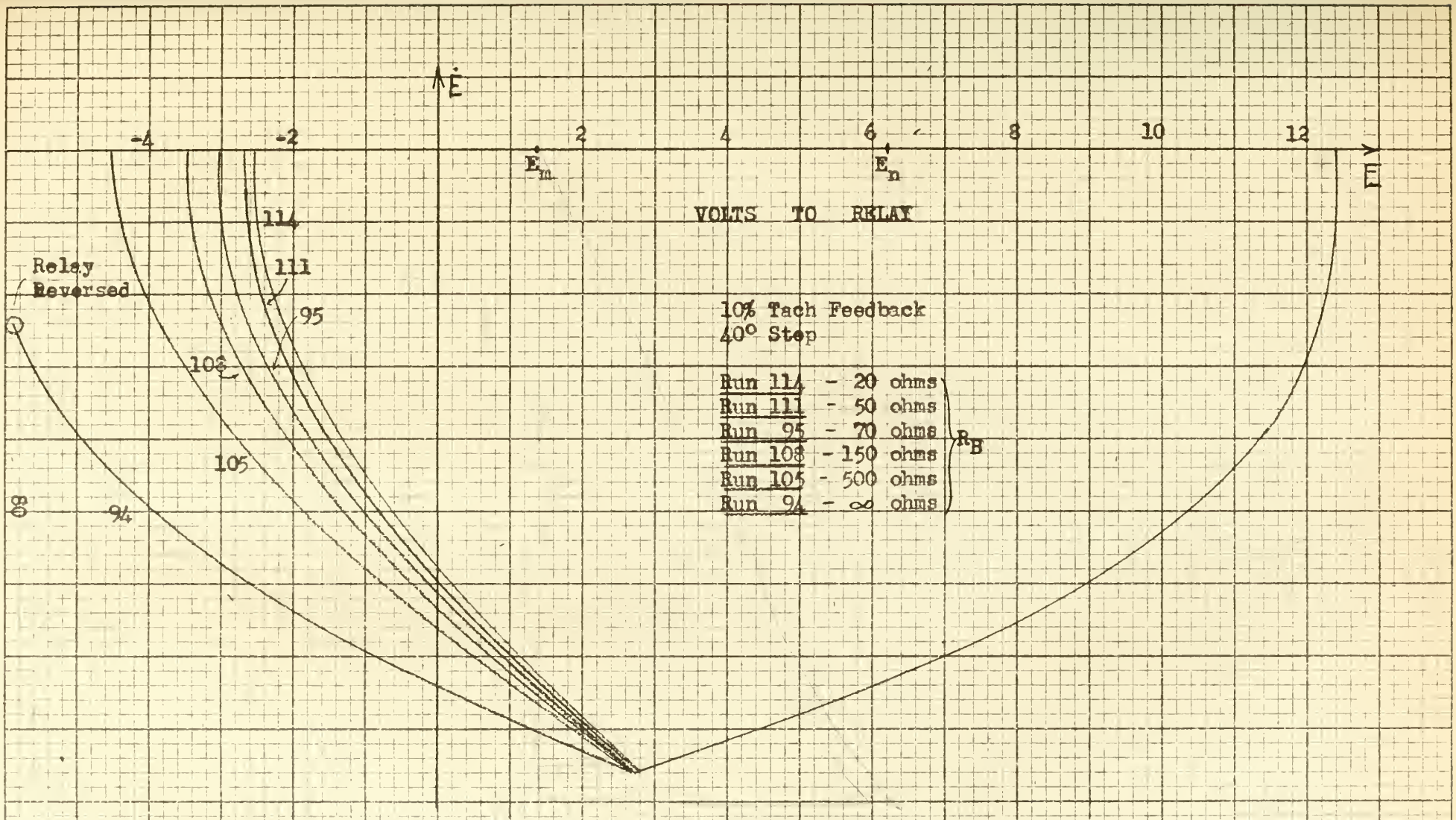

FIGURE 36. PHASE-PLANE PLOT: TEST RUNS 94, 95, 105, 108, 111 AND 114

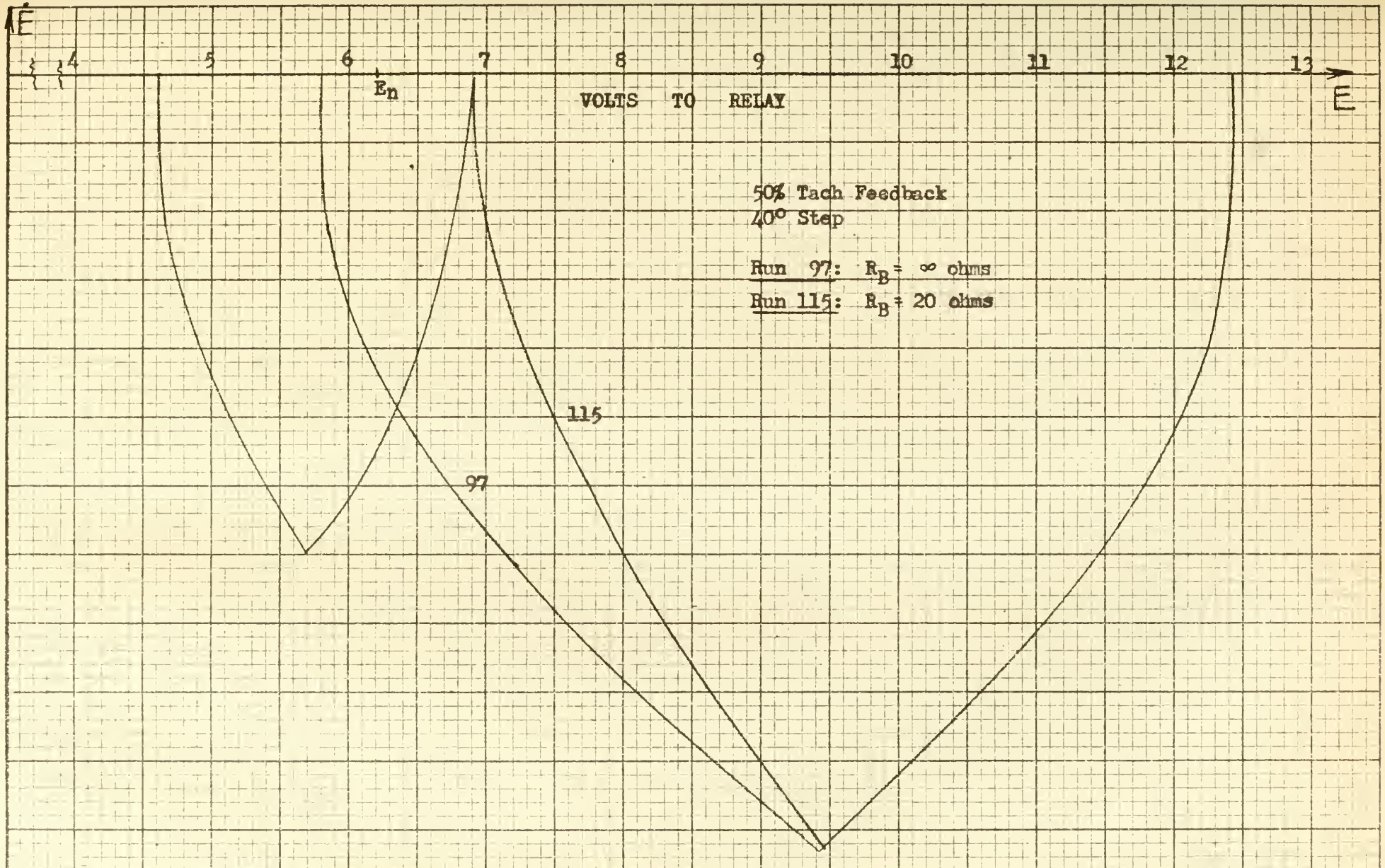

FIGURE 37. PHASE-PLANE PLOT: TEST RUNS 97 AND 115

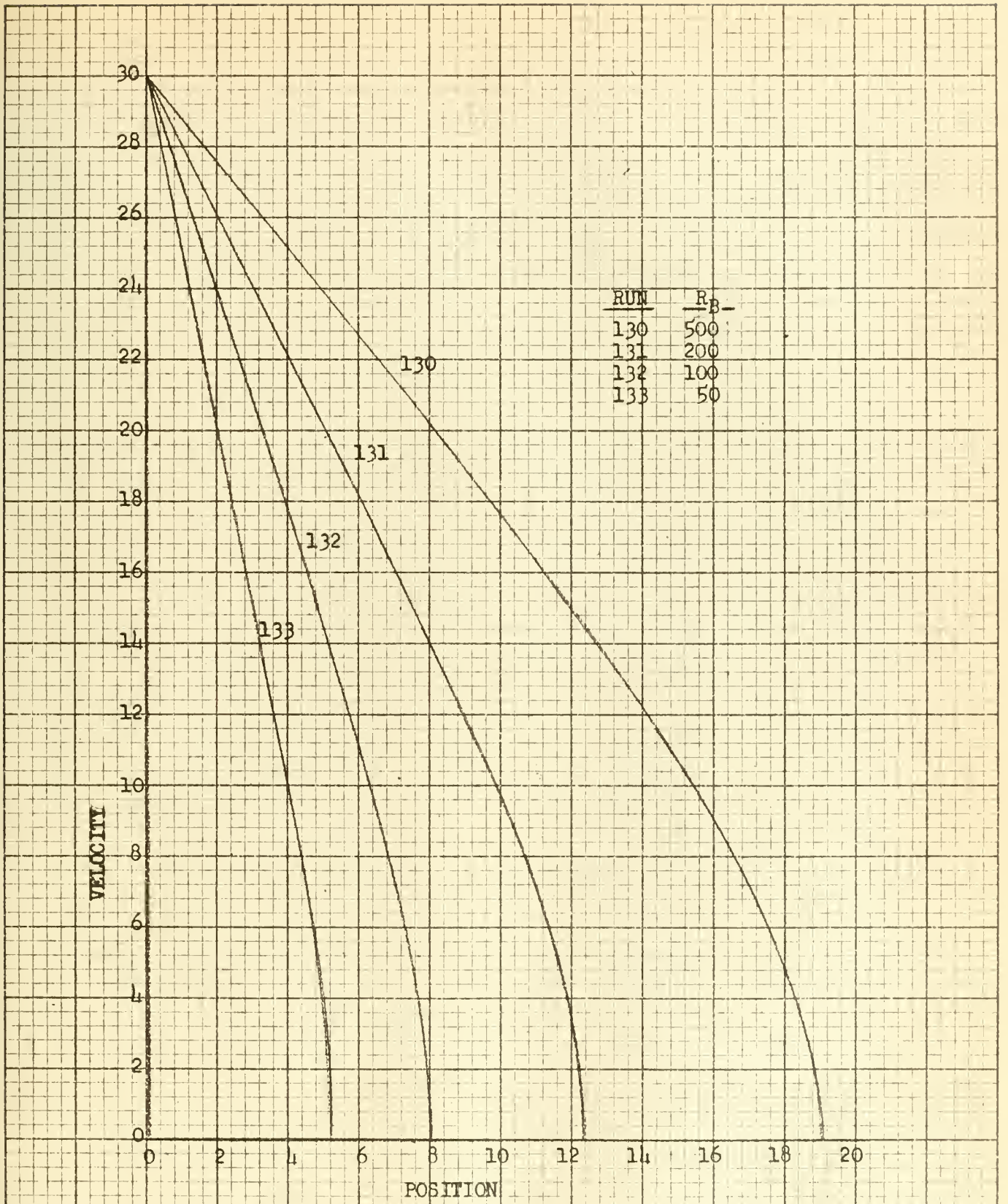

FIGURE 38. RETARDATION TESTS ON 1/8 HP MOTOR;RUNS 130-133

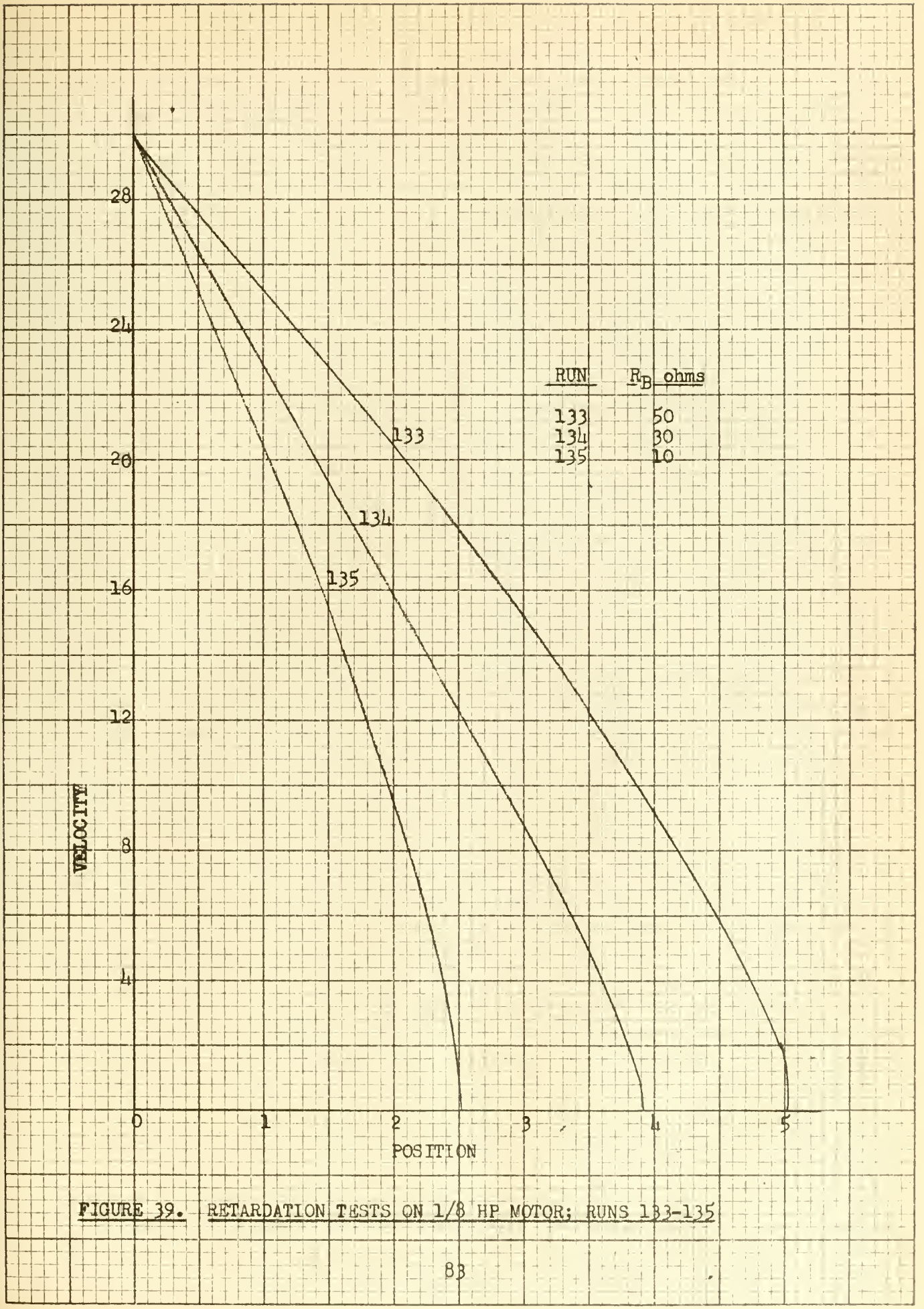

FIGURE 39. RETARDATION TESTS ON 1/8 HP MOTOR; RUNS 133-135

10 ohms) the trajectory was curved throughout a good portion of its travel. Thus the 1/8 HP motor is a good example of case 3, Figure 26, and would not give optimum performance in the proposed system.

Figures 40 and 41 illustrate the retardation tests made on the 1 HP motor. In Figure 41 it is seen that, for R_B of 23 ohms or less, the trajectory is a straight line until stiction takes over and stops the motor. The motor armature resistance was $7\frac{1}{2}$ ohms. It was decided to replace the 1/125 HP motor by the 1 HP motor in the servo set-up and run tests to corroborate the proposed theory.

3. The 1 HP Servo System.

Figure 42 is a photograph of the relay servo system employing the 1 Hp motor. Figure 43 is a schematic diagram of the system. Note that the Sigma relay is now used to close either a forward or a reverse relay. This results in additional relay time lag, but time did not permit ordering a double-pole, double-throw relay with greater current rating. Data on the components of this system appear in Appendix A.

Referring to Figure 2(c), the characteristics for relay operation were

$$E_n = \pm 6.20 \text{ volts}$$
$$E_m = \pm 1.36 \text{ volts}$$

Since the error signal gain was 10 and the reference voltage on the potentiometers was 40 volts, the dead zone (relay pull-in) was $\pm$ 5.5 degrees at the command shaft. When the relays dropped-out the error was $\pm$ 1.2 degrees at command shaft.

Data for the test runs conducted on this set-up appear in Appendix C.

With the proper amount of tach feedback deadbeat operation obtained

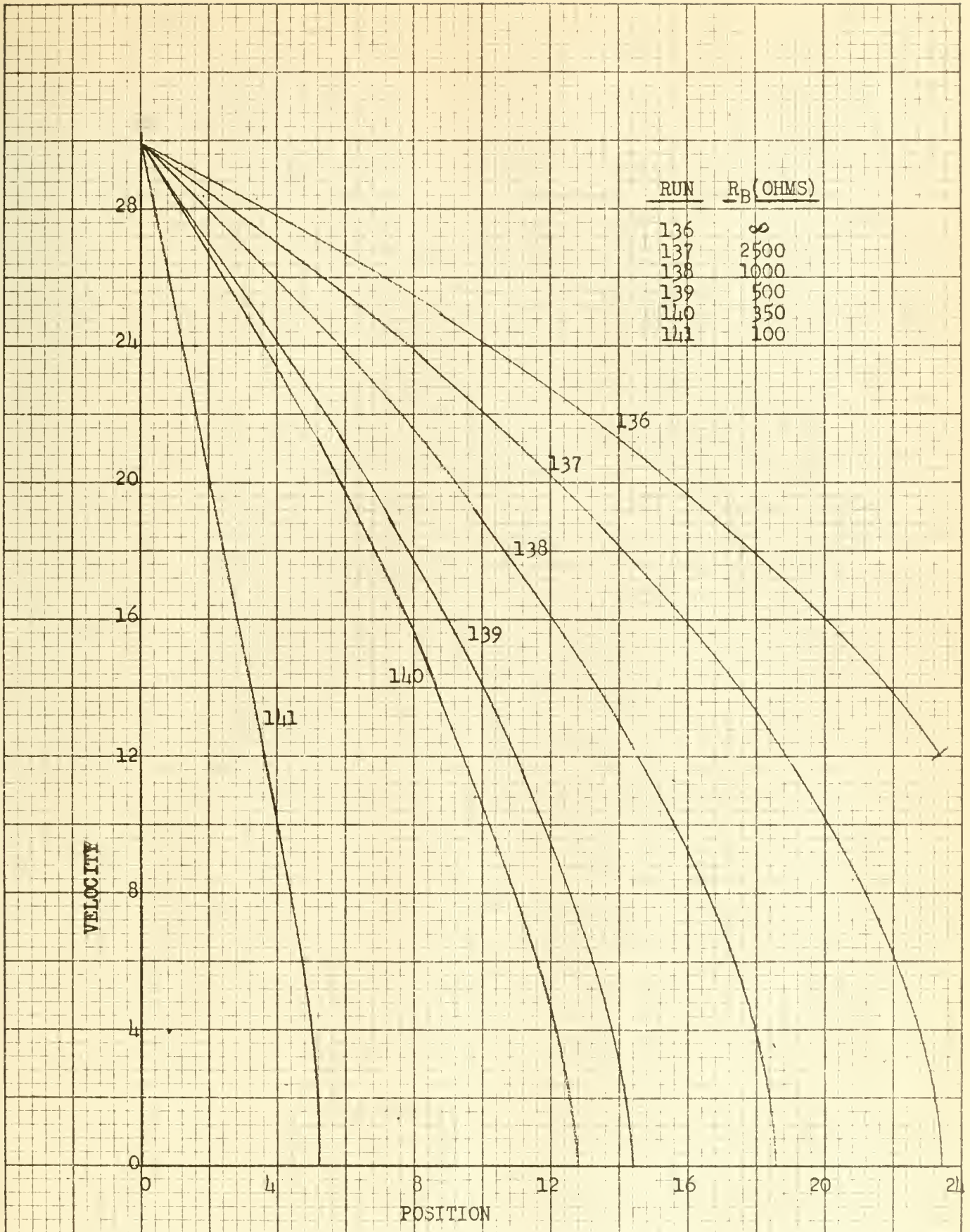

FIGURE 40. RETARDATION TESTS ON 1 HP MOTOR; RUNS 136-141

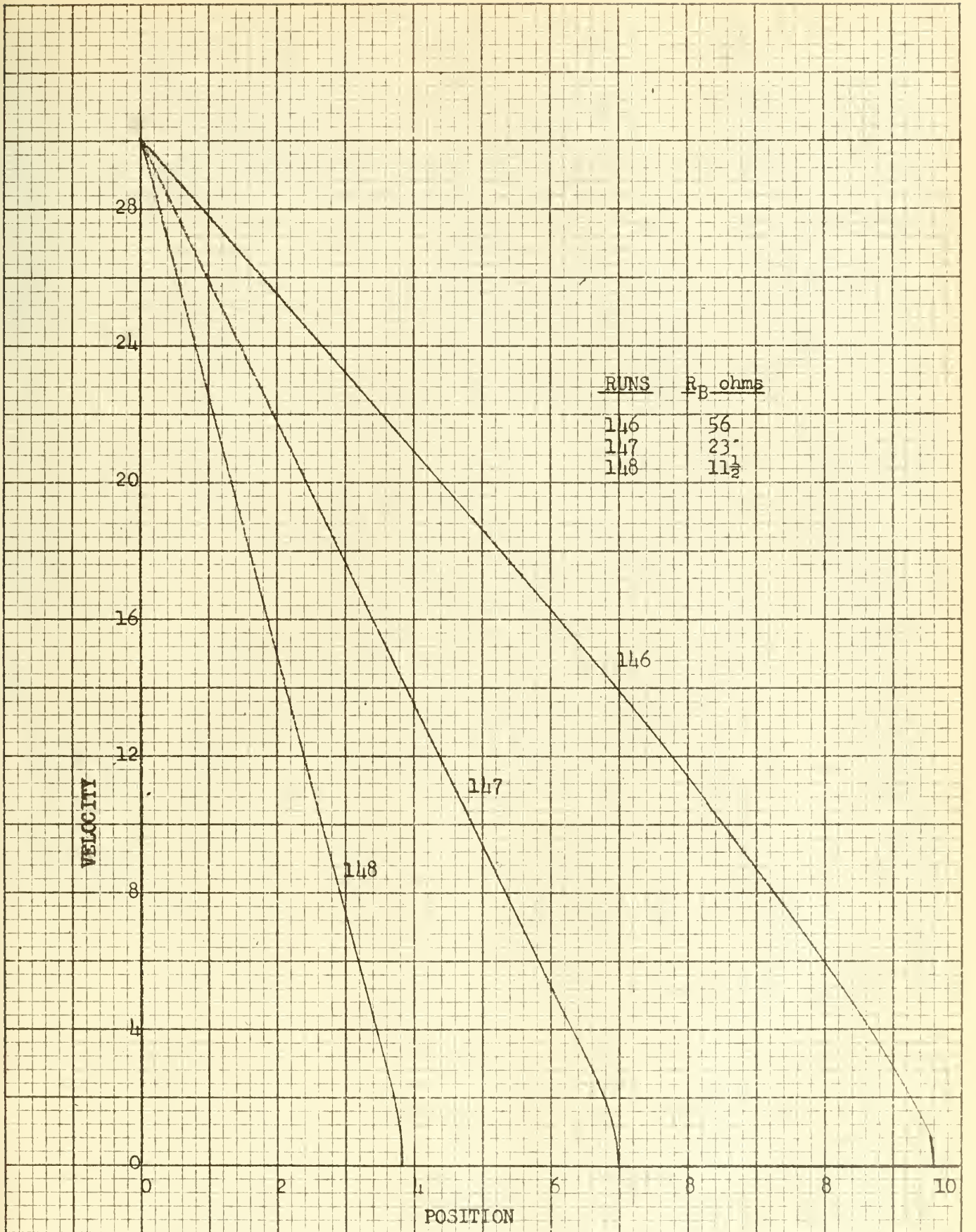

FIGURE 41. RETARDATION TESTS ON 1 HP MOTOR; RUNS 146-148

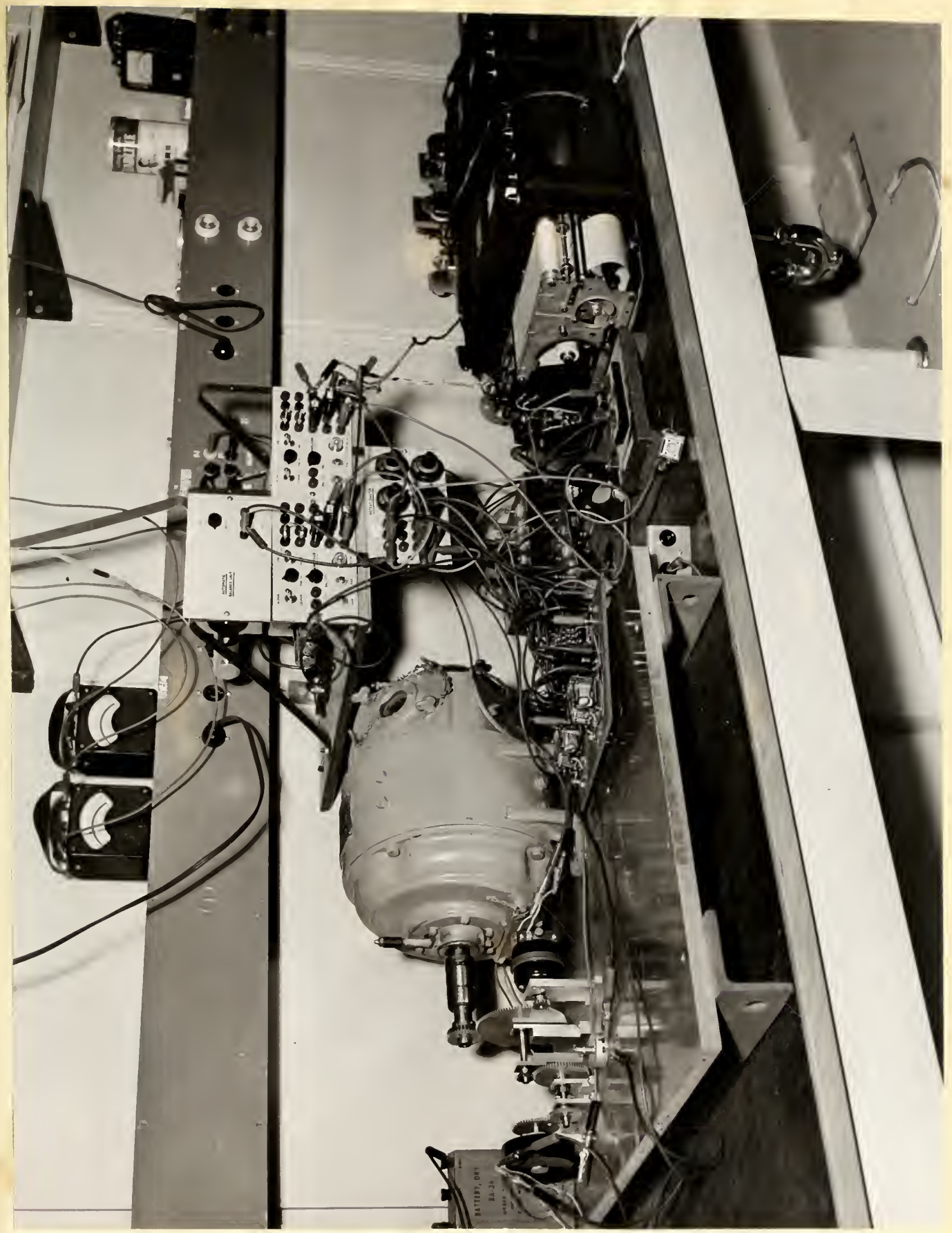

FIGURE 42. PHOTOGRAPH OF LABORATORY SET-UP OF RELAY SERVO SYSTEM EMPLOYING THE 1 HP MOTOR

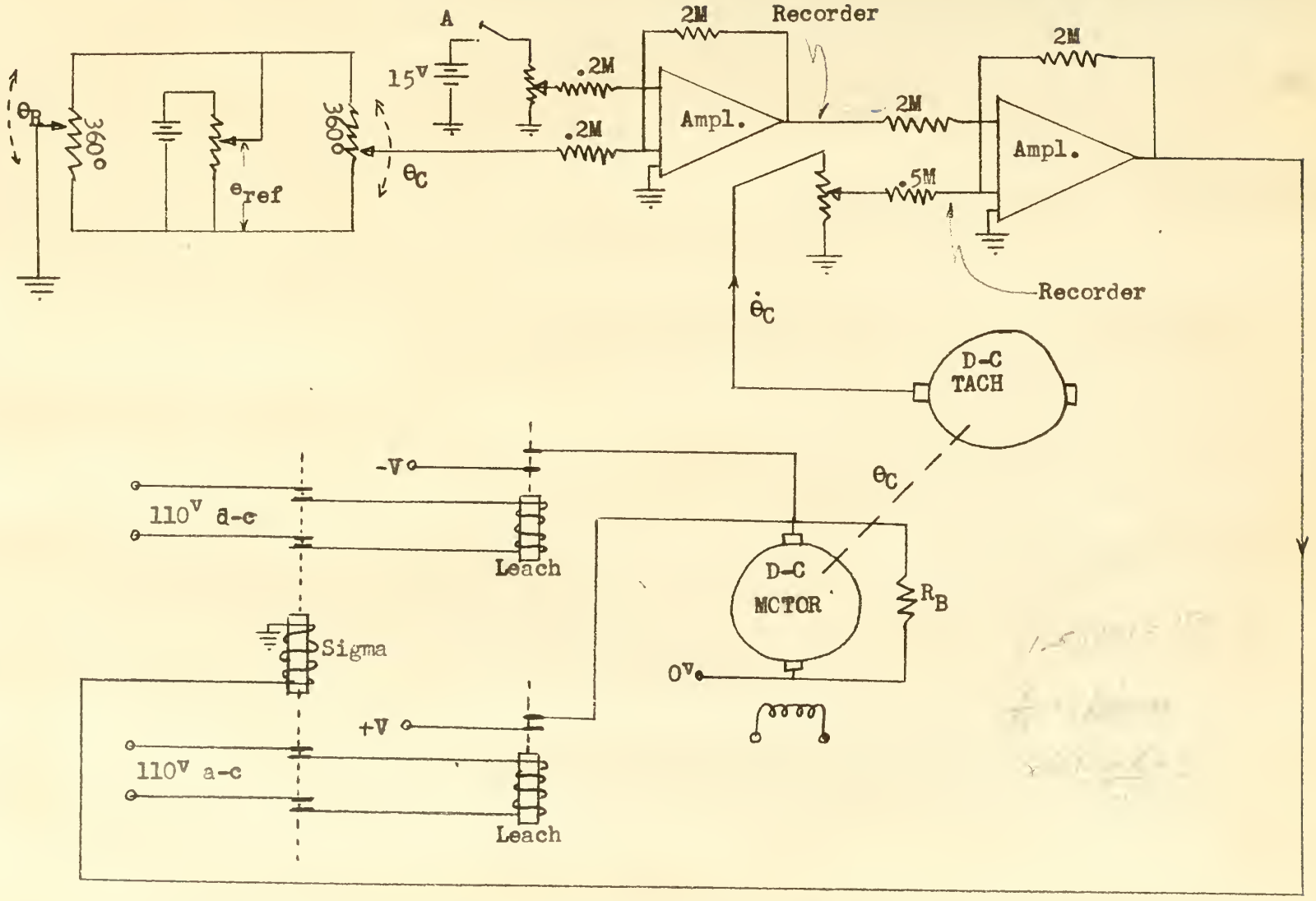

FIGURE 43. SCHEMATIC DIAGRAM OF THE 1 HP RELAY SERVO SYSTEM

for an R_B of 50 ohms or less. For the test runs illustrated R_B was 10 ohms.

Test run 202, Figure 44 illustrates deadbeat operation for a 40 degree step error. A similar response obtained for errors of 20, 80 and 100 degrees. Figure 44 also illustrates the unstable response that results when no dynamic braking resistor is employed (run 205), and when insufficient tach feedback is employed (run 206). Note that runs 202 and 205 are parallel in the dead zone. Note also that run 206, where no dynamic braking is employed, drifts across the dead zone with negligible damping.

Figure 45 illustrates E vs. t, as recorded on the Brush recorder tape, for the same runs illustrated in Figure 44.

4. Conclusions.

It is concluded that:

(a) the use of dynamic braking in the dead zone is feasible;

(b) the experimental results substantiate the theory;

(c) the dynamic braking principle improves performance in three ways:

(1) greater static accuracy,

(2) faster response,

(3) improved stability;

(d) two conditions must be met before the steady state error can be reduced to near zero:

(1) time delay in relay action must be decreased to a negligible amount, and

(2) the relay must be designed to close and open at nearly the same voltage.

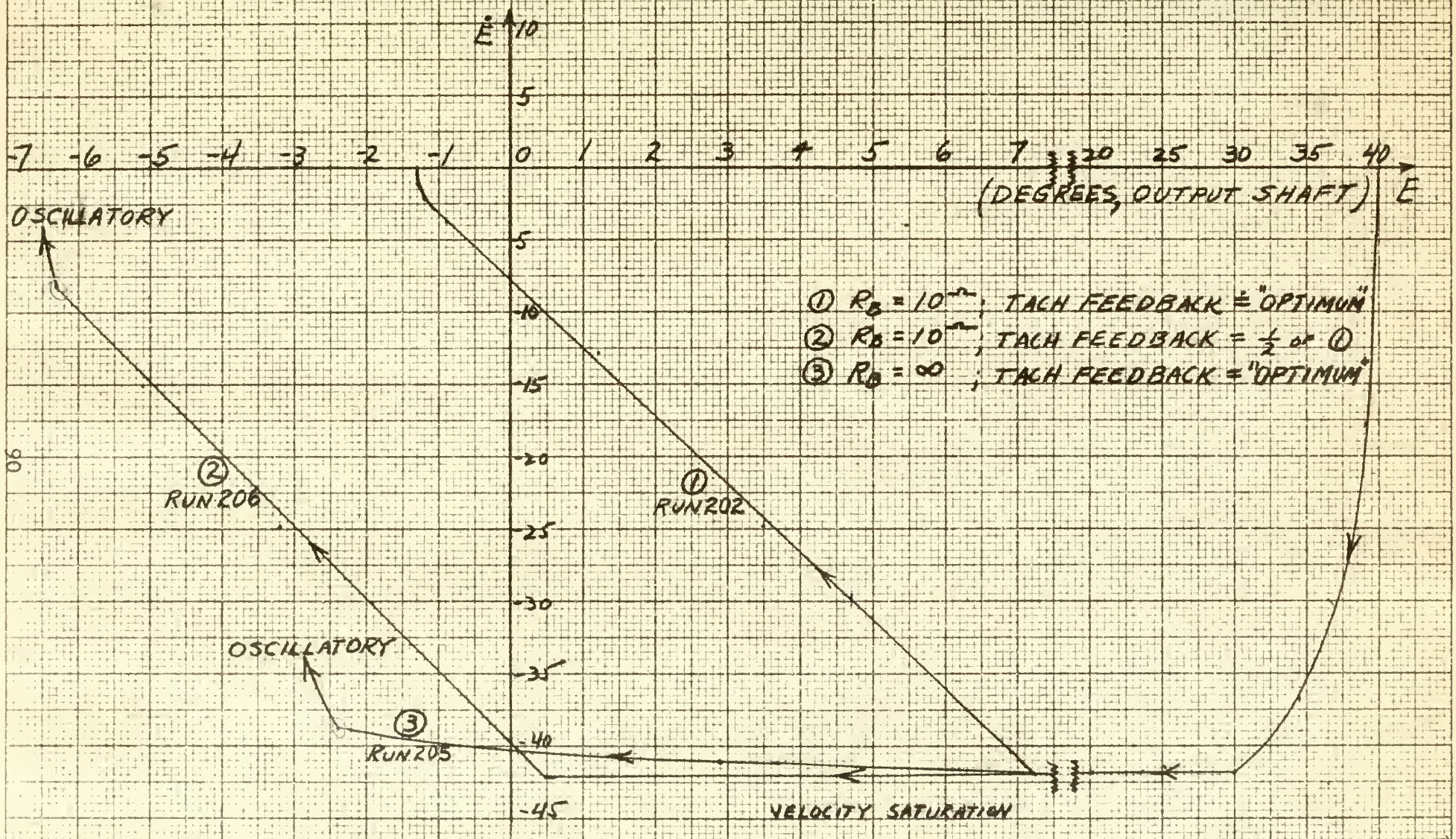

FIGURE 44. PHASE PLANE PLOT OF EXPERIMENTAL DATA ON THE ONE HP RELAY SERVO. 40° STEP.

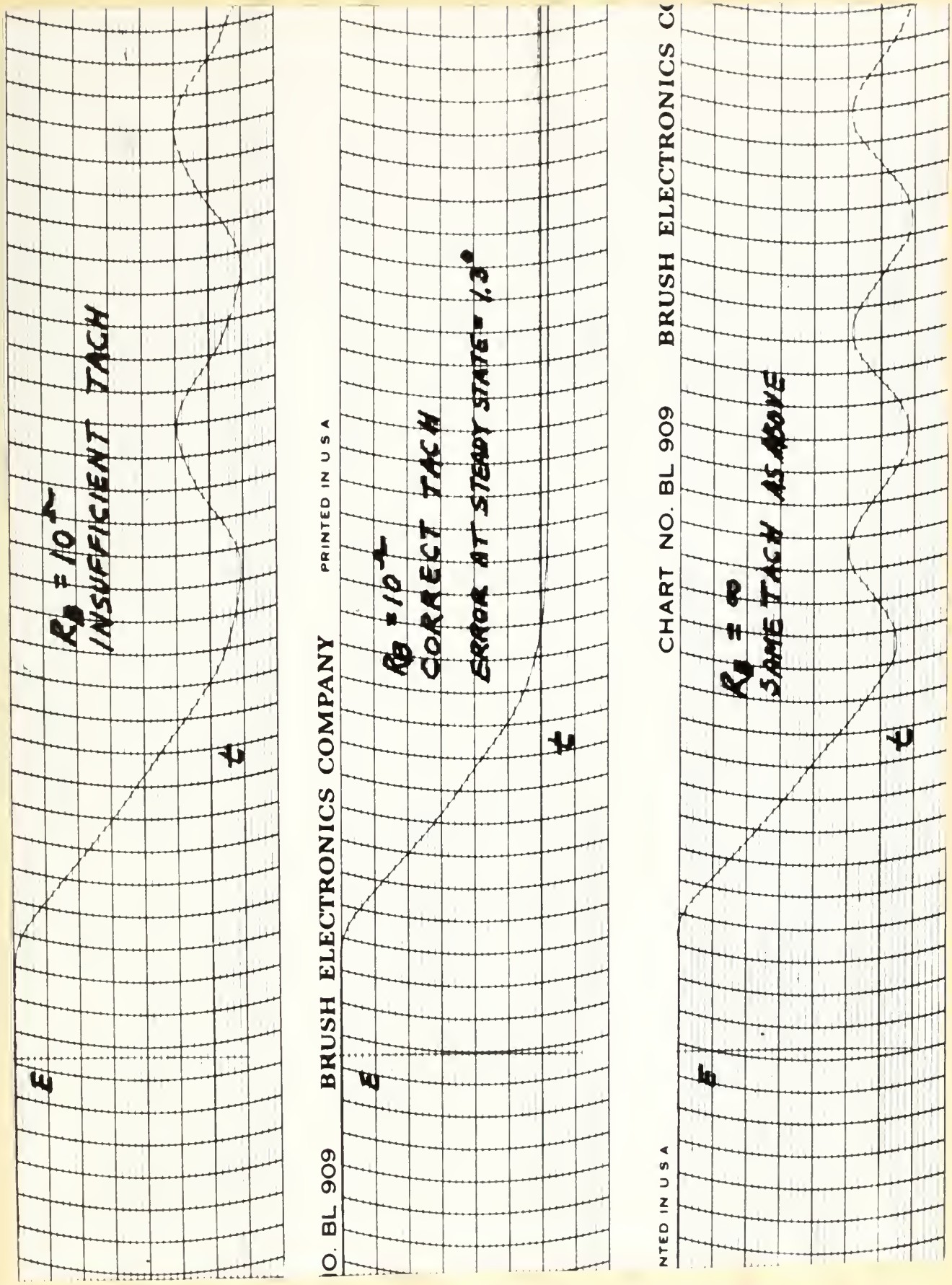

Run 206 Run 202 Run 205

FIGURE 45. TRANSIENT RESPONSE, RUNS 202, 205 AND 206

(e) the dynamic braking principle is more effective for servo systems employing larger motors, although if precautions are taken to lower the Coulomb friction smaller motors may prove feasible.

(f) design and construction of systems incorporating the dynamic braking principle should not be difficult, since the response of the system is almost exactly as predicted by theory.

5. Recommendations.

Further study is recommended in the following areas:

a. A study of methods for decreasing the Coulomb friction in small servomotors.

b. A study to determine whether the motor armature self-inductance can be considered negligible in large motors when applying the proposed dynamic braking principle.

c. Investigation of the response of a dynamically-braked relay servo to a step-velocity input.

d. Fabrication of an anticipator to work with the optimum servo with the practical d-c motor incorporated; Chapter III, section 1(b).

BIBLIOGRAPHY

1. Kahn, D. A. — AN ANALYSIS OF RELAY SERVOMECHANISMS, American Institute of Electrical Engineers Transactions, vol. 68, part II, 1949, pp. 1079-88.

2. Hazen, H. L. — THEORY OF SERVOMECHANISMS, Journal, The Franklin Institute, Philadelphia, Pa., vol. 218, Sept. 1934, pp. 279-330.

3. Thaler, G. J. — ELEMENTS OF SERVOMECHANISM THEORY (book). McGraw-Hill Book Co., New York, N.Y., 1955.

4. Kochenburger, R. J. — ANALYSIS AND SYNTHESIS OF CONTACTOR SERVOMECHANISMS. Engineering Report No. 16; 1949, Servomechanisms Laboratory, Massachusetts Institute of Technology.

5. McDonald, D. — NONLINEAR TECHNIQUES FOR IMPROVING SERVOMECHANISM PERFORMANCE. Proceedings, National Electronics Conference, Chicago, Ill., vol. 6, 1950, pp. 400-21.

6. Hopkin, M. — A PHASE-PLANE APPROACH TO THE COMPENSATION OF SATURATING SERVOMECHANISMS. American Institute of Electrical Engineers Transactions, vol. 70, part I, 1951, pp. 631-39.

7. Stout, T. M. — A STUDY OF SOME NEARLY OPTIMUM SERVOMECHANISMS. EE Department Report No. 10; 1952, University of Washington.

8. Kazda, L. F. — ERRORS IN RELAY SERVO SYSTEMS. American Institute of Electrical Engineers Transactions, vol. 72, part II, pp. 323-28.

APPENDIX A

EQUIPMENT

Motors:	1/125 HP, 115 volts d-c; Electric Indicator Co., Type FD-163; #227511.
	1/8 HP, 115 volts d-c; Marathon Electric Co., #176609.
	1 HP, 250 volts d-c, 115 volt shunt field; General Electric Co., # 1693848.
Tachometers:	1/75 HP; Electric Indicator Co., Type FD-38; #227515.
Relays:	Four-pole double-throw; Sigma Instrument Co., Type 6FX4C-5000 GD-SIL.
	Two-pole single-throw; Leach Relay Co., Type 1127.
Potentiometers:	Linear, continuous turn; Helipot Co., Series G; 10,000 ohms.
Amplifiers, d-c:	From Boeing Electronic Analog Computer, Model 7000; operational amplifier used to sum, differentiate and integrate.
Recorder:	Amplifier; Brush Co., Model BL-932. Oscilograph; Brush Co., Model BL-202.

APPENDIX B

EXAMPLE CALCULATION OF DEAD ZONE WIDTH

Relay Characteristic: Closes at $\pm$ 6.2 volts applied to coils.

Reference Battery: $e_{REF} = 1.5$ volts

Amplifier: Signal gain = 100

Dead Zone Width: Degrees error at command shaft to close relay $= \frac{(360^\circ)(\pm 6.2^V)}{(1.5^V)(100)} = \pm 15$

Step Input: 20 degrees of step error

$= \frac{20^\circ}{360^\circ} 1.5^V = 0.0833^V$ into amplifier

$= 100(.0833) = 8.33^V$ out of amplifier

APPENDIX C

DATA ON TEST RUNS

1/125 HP Servo System:

Armature voltage = 40; Field voltage = 115

Pull-in dead zone = ± 20° (e_{REF} = 1.115 volts; Gain = 100)

Run	Step Error, degrees	Tach, %	R_B, ohms
40	25	0	∞
41	25	0	70
42	25	10	∞
52	25	10	70
57	35	0	∞
67	35	0	70
74	45	0	∞
78	45	0	70
94	40	10	∞
95	40	10	70
97	40	50	∞
102	40	0	∞
103	40	0	70
104	40	0	500
105	40	50	10
107	40	0	150
108	40	10	150
110	40	50	0
111	40	50	10
113	40	0	20
114	40	10	20
115	40	50	20

1/8 HP Motor (Retardation):

Armature voltage = 80; Field voltage = 110; R = 10 ohms

Run	R_B, ohms
130	500
131	200
132	100
133	50
134	30
135	10

1 HP Motor (Retardation):

Armature voltage = 250; Field voltage = 115; R = 7 ohms

Run	R_B, ohms
136	∞
137	2500
138	1000
139	500
140	350
141	100
146	56
147	23
148	$11\frac{1}{2}$

1 HP Servo System :

Armature voltage = 56; Field voltage 117
Pull-in dead zone = $\pm 5.5^{\circ}$ (e_{REF} = 40 volts; Gain = 10)

Run	Tach, %	R_B, ohms
202	30	10
205	30	∞
206	15	10

Thesis
H293 Harris

Discontinuous damping
of relay servomechanisms.

JA 17 5-
19 APR 68
26 MAY 69
BINDERY
16886
18222
26420

32094

Thesis
H293 Harris

Discontinuous damping
of relay servomechanisms.